EFFECT OF HYDRODYNAMICS ON THE PRODUCTION OF PICKERING EMULSIONS IN UNBAFFLED STIRRED TANKS

A THESIS SUBMITTED TO
THE GRADUATE SCHOOL OF NATURAL AND APPLIED SCIENCES
OF
MIDDLE EAST TECHNICAL UNIVERSITY

BY

ÖZGE DEMİRDOĞAN

IN PARTIAL FULFILLMENT OF THE REQUIREMENTS
FOR
THE DEGREE OF MASTER OF SCIENCE
IN
CHEMICAL ENGINEERING

SEPTEMBER 2019

Approval of the thesis:

EFFECT OF HYDRODYNAMICS ON THE PRODUCTION OF PICKERING EMULSIONS IN UNBAFFLED STIRRED TANKS

submitted by **ÖZGE DEMIRDOĞAN** in partial fulfillment of the requirements for the degree of **Master of Science in Chemical Engineering Department, Middle East Technical University** by,

Prof. Dr. Halil Kalıpçılar
Dean, Graduate School of **Natural and Applied Sciences** _____

Prof. Dr. Pınar Çalık
Head of Department, **Chemical Engineering** _____

Assist. Prof. Dr. İnci Ayrancı Tansık
Supervisor, **Chemical Engineering, METU** _____

Examining Committee Members:

Prof. Dr. Görkem Külah
Chemical Engineering, METU _____

Assist. Prof. Dr. İnci Ayrancı Tansık
Chemical Engineering, METU _____

Prof. Dr. Yusuf Uludağ
Chemical Engineering, METU _____

Assist. Prof. Dr. Harun Koku
Chemical Engineering, METU _____

Assoc. Prof. Dr. Berna Topuz
Chemical Engineering, Ankara University _____

Date: 05.09.2019

I hereby declare that all information in this document has been obtained and presented in accordance with academic rules and ethical conduct. I also declare that, as required by these rules and conduct, I have fully cited and referenced all material and results that are not original to this work.

Name, Surname: Özge Demirdoğan

Signature:

ABSTRACT

EFFECT OF HYDRODYNAMICS ON THE PRODUCTION OF PICKERING EMULSIONS IN UNBAFFLED STIRRED TANKS

Demirdoğan, Özge
Master of Science, Chemical Engineering
Supervisor: Assist. Prof. Dr. İnci Ayrancı Tansık

September 2019, 135 pages

An emulsion is a fluid system obtained by dispersing one of two immiscible liquids in the other. Since this formation is thermodynamically unstable, it has to be stabilized using an emulsifier. Emulsions in which solid particles are used as emulsifiers are called Pickering emulsions.

In this study, the investigation of the effect of different hydrodynamic conditions on the production of Pickering emulsions in unbaffled stirred tanks was aimed. Oil in water Pickering emulsions were produced. Distilled water was selected as continuous phase and silicon oil was selected as dispersed phase. Hydrophilic solid glass beads were used as emulsifier. To observe the effect of different flow patterns, Rushton turbine (RT), down pumping pitched blade turbine (PBTD) and up pumping pitched blade turbine (PBTU), all at two different sizes were used. Shaft was positioned at three different locations: e/T=0, e/T=0.1 and e/T=0.2. Hydrodynamic parameters such as impeller tip speed, impeller Reynolds number, Weber number and power per mass ratio were changed to create different hydrodynamic conditions. The effect of these different hydrodynamic conditions on the production of Pickering emulsion was determined by analyzing drop size and drop size distribution with Malvern Mastersizer equipment.

It was found that an increase in the eccentricity ratio causes a decrease in the size of the vortex, an increase in the contact of the impellers with the liquid in the tank and better transfer of performances of the impellers to the system. In general, increase in eccentricity ratio causes a decrease in drop size. The amount of energy dissipated into the system has an important effect on determining drop size of the emulsions. Generally, the smallest drops and the narrowest drop size distribution were obtained with RT T/3 at e/T=0.2.

Keywords: Pickering Emulsion, Unbaffled Stirred Tank, Vortex, Eccentricity, Drop Size

ÖZ

HİDRODİNAMİK KOŞULLARIN ENGELSİZ TANKLARDA ÜRETİLEN PİCKERİNG EMÜLSİYONLARI ÜZERİNE ETKİSİ

Demirdoğan, Özge
Yüksek Lisans, Kimya Mühendisliği
Tez Danışmanı: Dr. Öğr. Üyesi İnci Ayrancı Tansık

Eylül 2019, 135 sayfa

Emülsiyon normalde birbiri içerisinde karışmayan iki sıvıdan birinin öteki içerisinde dağılmasıyla elde edilen akışkan sistemidir. Bu oluşum termodinamik açıdan kararsız olduğundan kararlı hale getirilebilmesi yüzey aktif madde kullanımı ile mümkündür. Katı taneciklerin yüzey aktif madde olarak kullanıldığı emülsiyonlara Pickering emülsiyonları adı verilmektedir.

Bu çalışmada engelsiz tanklarda üretilen Pickering emülsiyonlarına farklı hidrodinamik koşulların etkisinin belirlenmesi amaçlanmıştır. Su içerisinde yağ Pickering emülsiyonları üretilmiştir. Saf su ana faz, silikon yağı dağılan faz olarak seçilmiştir. Hidrofilik cam tozu yüzey aktif madde olarak kullanılmıştır. Farklı akış profillerinin etkilerinin gözlemlenebilmesi için ikişer farklı boyutta Rushton türbini (RT), aşağı yönlü akış sağlayan eğimli bıçaklı karıştırıcı ucu (PBTD) ve yukarı yönlü akış sağlayan eğimli bıçaklı karıştırıcı ucu (PBTU) kullanılmıştır. Şaft üç ayrı noktada konumlandırılmıştır: e/T=0, e/T=0.1 ve e/T=0.2. Karıştırıcı ucu çevresel hızı, karıştırıcı ucu Reynolds sayısı, Weber sayısı ve güç tüketimi/kütle oranı gibi hidrodinamik parametreler değiştirilerek farklı hidrodinamik koşullar oluşturulmuştur. Farklı hidrodinamik koşulların Pickering emülsiyonu üretimine etkisi Malvern Mastersizer cihazı ile damla boyutu ve boyut dağılım analizleri yapılarak belirlenmiştir.

Şaftın merkezden uzaklaşmasının girdap boyutunda azalışa, karıştırıcı uçlarının tank içerisindeki sıvı ile temasında artışa ve karıştırıcı uçlarının performanslarının sisteme iletiminde artışa neden olduğu bulunmuştur. Genel olarak, şaftın merkezden uzaklaşması damla boyutunda azalışa neden olmaktadır. Sisteme verilen enerji miktarı emülsiyonların damla boyutunun belirlenmesinde önemli bir etkiye sahiptir. Genellikle en küçük damlalar ve en dar damla boyutu dağılımı RT T/3 karıştırıcı ucu ile e/T=0.2 konumunda elde edilmiştir.

Anahtar Kelimeler: Pickering Emülsiyonları, Engelsiz Karıştırmalı Tank, Girdap, Merkez Dışı Şaft, Damla Boyutu

Dedicated to my family and my love

ACKNOWLEDGEMENTS

First, I would like to thanks to my thesis advisor İnci Ayrancı Tansık for her kind attitude and guidance. Her support, motivation and confidence in me have always increased my self-confidence. Without her, this study would not have reached its final form.

I would like to thank my family for supporting me financially and morally all the time and being there for me. First, I would like to thank my father Hüseyin Demirdoğan who provided me with all kinds of support, my mother Serpil Demirdoğan who shared my stress with me in all time and my sister Simge Demirdoğan who made me laugh even in the hardest time. I would also like to thank my love İlhan Doğan who supported me in all time for his patience and self-sacrifice.

I would like to thanks to members of Multiphase Mixing Research Laboratory, METU especially Usman Abdulrasaq, Dila Karakaya, Gökhan Gök, Ezgi Altıntaş and Başak Kütükçü for their kind cooperation and support.

I would like to thank Aslı Karausta who provided me plastic cans for carrying distilled water and not leave me alone with her conversation while working, Burak Akdeniz who helped to take microscopic images of the emulsion, Simge Gider who drew plexiglass apparatus, Gökhan Ustabaş who helped me to get plexiglass apparatus and Selin Cansu Gölboylu who helped me in case of any problems related to submission procedure of my thesis.

This study is supported by TUBITAK (The Scientific and Technological Research Council of Turkey) and METU BAP. I thank them for their financial support. TUBITAK project number is 116M304 and METU BAP project number is YLT-304-2018-3760.

TABLE OF CONTENTS

ABSTRACT v

ÖZ vii

ACKNOWLEDGEMENTS x

TABLE OF CONTENTS xi

LIST OF TABLES xiv

LIST OF FIGURES xv

LIST OF ABBREVIATIONS xix

LIST OF SYMBOLS xx

CHAPTERS

1. INTRODUCTION 1

1.1. Emulsions 1

1.2. Surfactant-based Emulsions 3

1.3. Pickering Emulsions 5

1.4. Significant Physicochemical Parameters for Pickering Emulsion Formation ... 8

1.4.1. The Effect of Particle Size 9

1.4.2. The Effect of Particle Shape 9

1.4.3. The Effect of Oil Viscosity 9

1.4.4. The Effect of pH and Salt Concentration 10

1.5. Significant Hydrodynamic Parameters for Pickering Emulsion Formation 10

1.5.1. The Effect of the Presence of Baffles 10

1.5.2. The Effect of Shaft Position in Unbaffled Tanks 12

1.5.3. The Effect of the Type of the Impeller 13

1.5.4. Significant Hydrodynamic Expressions 16

1.5.4.1. Impeller Tip Speed 16
1.5.4.2. Impeller Reynolds Number 16
1.5.4.3. Weber Number 17
1.5.4.4. Power/Mass Ratio 17
1.6. Drop Size Measurement 18
1.7. Motivation of Thesis 21
2. EXPERIMENTAL PROCEDURE 23
2.1. Materials 23
2.1.1. Determination of the Type of Particle 23
2.1.2. Determination of the Type of Oil 25
2.1.3. Determination of the Type of Water 27
2.2. Experimental Setup 28
2.3. Development of the Procedure of Emulsification Experiments 31
2.3.1. Arrangement of Experimental Setup 31
2.3.2. Determination of Oil/Water Ratio and the Amount of Particles 32
2.3.3. Determination of Agitation Speeds for Emulsification 33
2.3.4. Determination of Premixing Time 37
2.3.5. Determination of Emulsification Time 38
2.4. General Procedure of Emulsification Experiments 39
2.5. The Procedure of Mixing Time Experiments 44
2.5.1. Materials and Method for Decolorization 45
2.5.2. Method for Image Analysis 45
3. RESULTS AND DISCUSSION 49

3.1. Effect of Hydrodynamics on the Production of Pickering Emulsions in Unbaffled Stirred Tanks with Centered Shaft 49

3.1.1. Effect of Impeller Tip Speed 49

3.1.2. Effect of Impeller Reynolds Number.....56

3.1.3. Effect of Weber Number.....62

3.1.4. Effect of Power/Mass Ratio 68

3.2. Effect of Hydrodynamics on the Production of Pickering Emulsions in Unbaffled Stirred Tanks with Eccentric Shaft.....73

3.2.1. Effect of Impeller Tip Speed 77

3.2.2. Effect of Impeller Reynolds Number.....86

3.2.3. Effect of Weber Number.....93

3.2.4. Effect of Power/Mass.....99

3.3. Comparison of Performances of PBTU and PBTD Impellers at the Same V_{tip} 105

3.4. Mixing Time Analysis.....116

4. SUMMARY, OUTCOMES AND FUTURE WORK 119

4.1. Summary and Outcomes 119

4.2. Future Work.....122

REFERENCES.....123

APPENDICES

A. Mixing Time Code.....133

LIST OF TABLES

TABLES

Table 2.1. Volumetric particle size distribution 24
Table 2.2. Physical properties of glass beads 25
Table 2.3. Physical properties of silicon oil 26
Table 2.4. The speeds of oil entrainment, oil mixing and air entrainment for all impellers 35
Table 2.5. Minimum agitation speeds required for turbulent regime 36
Table 3.1. Selected Vtip values and corresponding impeller speeds..... 50
Table 3.2. Selected Reynolds numbers and corresponding impeller speeds 57
Table 3.3. Selected Weber numbers and corresponding impeller speeds..... 63
Table 3.4. Selected power/mass ratios and corresponding impeller speed..... 69

LIST OF FIGURES

FIGURES

Figure 1.1. The structure of a surfactant and micelles (a) o/w emulsion, b) w/o emulsion).....4
Figure 1.2. The contact angle and the interfacial tensions of a solid particle situated at the oil/water interface.....6
Figure 1.3. The relation between the contact angle of a solid particle and the type of an emulsion (a) Oil in water emulsion with hydrophilic solid particles b) Water in oil emulsion with hydrophobic solid particles).....7
Figure 1.4. Comparison of mixing in the baffled and the unbaffled tank.....12
Figure 1.5. The effect of eccentricity on vortex formation.....13
Figure 1.6. Flow patterns of PBT impellers in baffled tanks.....14
Figure 1.7. Flow pattern of RT impeller in baffled tanks.....15
Figure 1.8. Scattered light depending on particle size.....19
Figure 1.9. Laser diffraction configuration of Malvern Mastersizer 3000.....19
Figure 1.10. Light scattering by Mie and Fraunhofer models.....20
Figure 2.1. Particle size distribution of glass beads.....24
Figure 2.2. Microscopic image of spherical glass beads.....25
Figure 2.3. The effect of type of distilled water on drop size.....28
Figure 2.4. Tank configurations.....29
Figure 2.5. Impellers used in the experiments (from left to right respectively: RT T/2, RT T/3, PBTD T/2 and PBTD T/3).....29
Figure 2.6. PBTU T/2 and PBTU T/3 from left to right respectively.....30
Figure 2.7. Used overhead stirrers in the experiments.....31
Figure 2.8. The apparatus used for arrangement of shaft positions: e/T=0, e/T=0.1 and e/T=0.2 from left to right respectively.....32
Figure 2.9. Arrangement of shafts using plexiglass apparatus.....32

Figure 2.10. The effect of premix time on drop size 37
Figure 2.11. The effect of emulsification time on drops size for large impellers..... 38
Figure 2.12. The effect of emulsification time on drops size for small impellers..... 39
Figure 2.13. Malvern Mastersizer 3000..... 40
Figure 2.14. Sample in wet dispersion unit 42
Figure 2.15. Emulsion drop size distribution..... 43
Figure 2.16. Microscopic image of Pickering emulsion drops..... 44
Figure 2.17. Frames of color change 46
Figure 2.18. Mixing time graph..... 47
Figure 3.1. The effect of impeller tip speed on drop size 51
Figure 3.2. Formed vortices at the same impeller tip speed (132 m/min) for the large impellers 54
Figure 3.3. Formed vortices at the same impeller tip speed (132 m/min) for the small impellers 55
Figure 3.4. Drop size distribution of all impellers at the same impeller tip speed: 132 m/min..... 56
Figure 3.5. The effect of Reynolds number on drop size 58
Figure 3.6. Drop size distribution of all impellers at Reynolds number 22 000..... 61
Figure 3.7. Drop size distribution of all impellers at Reynolds number 30000..... 62
Figure 3.8. The effect of Weber number on drop size..... 66
Figure 3.9. Drop size distribution of all impellers at Weber number 350 67
Figure 3.10. Drop size distribution of all impellers at Weber number 450 68
Figure 3.11. The effect of power/mass on drop size..... 71
Figure 3.12. Drop size distribution of all impellers at the same power/mass ratio: 350 73
Figure 3.13. Vortex formations at different eccentricity ratios with PBTD T/3 74
Figure 3.14. Vortex formations with RT impellers at e/T=0.2 75
Figure 3.15. Vortex formations with PBTD impellers at e/T=0.2..... 76
Figure 3.16. Vortex formations with RT impellers at e/T=0.1 76
Figure 3.17. Vortex formations with PBTD impellers at e/T=0.1 77

Figure 3.18. The effect of impeller tip speed on drop size at e/T=0.1 78
Figure 3.19. Formed vortices at the same impeller tip speed (132 m/min) for the small impellers at e/T=0.1 79
Figure 3.20. Formed vortices at the same impeller tip speed (132 m/min) for the large impellers at e/T=0.1 80
Figure 3.21. Drop size distribution of all impellers at the same impeller tip speed: 132 m/min at e/T=0.1 81
Figure 3.22. The effect of impeller tip speed on drop size at e/T=0.2 82
Figure 3.23. Formed vortices at the same impeller tip speed (132 m/min) for the large impellers at e/T=0.2 83
Figure 3.24. Formed vortices at the same impeller tip speed (132 m/min) for the small impellers at e/T=0.2 84
Figure 3.25. Drop size distribution of all impellers at the same impeller tip speed: 132 m/min at e/T=0.2 85
Figure 3.26. Effect of eccentricity on drop size at the same impeller tip speed (V_{tip}= 132 m/min) 86
Figure 3.27. The effect of Reynolds number on drop size for all impellers located at e/T=0.1 88
Figure 3.28. Drop size distribution of all impellers at the same Reynolds number: 30 000 at e/T=0.1 89
Figure 3.29. The effect of Reynolds number on drop size for all impellers located at e/T=0.2 91
Figure 3.30. Drop size distribution of all impellers at the same Reynolds number: 30 000 at e/T=0.2 92
Figure 3.31. Effect of eccentricity on drop size (Re=30 000).....93
Figure 3.32. The effect of Weber number on drop size for all impellers located at e/T=0.1 94
Figure 3.33. Drop size distribution at Weber number 450 at e/T=0.1 96
Figure 3.34. The effect of Weber number on drop size for all impellers located at e/T=0.2 97

Figure 3.35. Drop size distribution at Weber number 450 at e/T=0.2 98
Figure 3.36. Effect of eccentricity on drop size (Weber=450) 99
Figure 3.37. The effect of power/mass on drop size at e/T=0.1 101
Figure 3.38. Drop size distribution of all impellers at the same power/mass ratio: 400 at e/T=0.1 102
Figure 3.39. The effect of power/mass on drop size at e/T=0.2 103
Figure 3.40. Drop size distribution of all impellers at the same power/mass ratio: 400 at e/T=0.2 104
Figure 3.41. Effect of eccentricity on drop size (power/mass=400)..... 105
Figure 3.42. Formed vortices at the same impeller tip speed (132 m/min at e/T=0) 106
Figure 3.43. The effect of impeller tip speed on drop size at e/T=0..... 108
Figure 3.44. Drop size distribution of all impellers at the same V_{tip} (at e/T=0)..... 109
Figure 3.45. Formed vortices at the same impeller tip speed (132 m/min at e/T=0.1) 110
Figure 3.46. The effect of impeller tip speed on drop size at e/T=0.1..... 111
Figure 3.47. Drop size distribution of all impellers at the same V_{tip} (at e/T=0.1)... 112
Figure 3.48. Formed vortices at the same impeller tip speed (132 m/min at e/T=0.2) 113
Figure 3.49. The effect of impeller tip speed on drop size at e/T=0.2..... 114
Figure 3.50. Drop size distribution of all impellers at the same V_{tip} (at e/T=0.2)... 115
Figure 3.51. Effect of eccentricity on the impellers at the same V_{tip}..... 116
Figure 3.52. Mixing time analysis for all impellers at the same impeller speed (865 rpm)..... 117

LIST OF ABBREVIATIONS

ABBREVIATIONS

o/w	-	Oil in water
PBTD	-	Down Pumping Pitched Blade Turbine
PBTU	-	Up Pumping Pitched Blade Turbine
ppm	-	Power per mass (W/kg)
Re	-	Impeller Reynolds number
RGB	-	Red-blue-green
RO	-	Reverse osmosis
RT	-	Rushton Turbine
UP	-	Ultra-pure
w/o	-	Water in oil
We	-	Weber number

LIST OF SYMBOLS

SYMBOLS

Roman characters

c	-	The volume fraction of the dispersed phase
C	-	Off-bottom clearance (m)
D	-	Impeller diameter (m)
d_{32}	-	Sauter mean diameter (μm)
d_{50}	-	Number mean diameter (μm)
e	-	The distance between the center of the tank and the center of the shaft (m)
e/T	-	Eccentricity ratio
H	-	Liquid height (m)
H_{imp}	-	Impeller height (m)
m_p	-	Particle mass (kg)
m_w	-	Particle mass (kg)
N	-	Impeller rotational speed (rpm)
N_E	-	Air entrainment speed (rpm)
N_{JD1}	-	Oil entrainment speed (rpm)
N_{JD2}	-	Oil mixing speed (rpm)
N_{mixed}	-	The number of mixed pixels

N_p	-	Impeller power number
N_q	-	Impeller flow number
N_{total}	-	The total of pixels
P	-	Power (W)
T	-	Inner tank diameter (m)
t_{circ}	-	The mean circulation time (s)
V_{imp}	-	Impeller swept volume (m^3)
V_{tank}	-	Tank volume (m^3)
V_{tip}	-	Impeller tip speed (m/min)
w/w	-	Weight fraction

Greek characters

γ_{ow}	-	Interfacial tension between oil/water phases (N/m)
γ_{so}	-	Interfacial tension between solid particle/oil phase (N/m)
γ_{sw}	-	Interfacial tension between solid particle/water phase (N/m)
ε	-	Power/mass
η_r	-	Relative viscosity
μ	-	Emulsion viscosity (kg/m s)
μ_c	-	Continuous phase viscosity (kg/m s)
μ_s	-	Emulsion viscosity (kg/m s)
ρ	-	Emulsion density(kg/m^3)

ρ_c	-	Continuous phase density (kg/m^3)
ρ_p	-	Particle density (kg/m^3)
ρ_w	-	Water density (kg/m^3)
σ	-	Interfacial tension (N/m)

CHAPTER 1

INTRODUCTION

1.1. Emulsions

An emulsion is a fluid system obtained by dispersing one of two immiscible liquids into the other. Emulsification processes are used in many different industries including cosmetics (lotions and lipsticks), food processing (creams, milk, mayonnaise, salad dressings, ice creams and margarine etc.), paint (water-based emulsions), petroleum (crude oil emulsions) and pharmaceutical industries (drugs and creams) (Rigg and York, 1985; Comstock, 1992; Choplin et al., 1998; Khan et al., 2012). Research on emulsions include interdisciplinary studies among interfacial chemistry, fluid mechanics, colloid and polymer chemistry (McClements, 2016).

Emulsions are generally composed of oil and water. When these two phases come together, since the density of oil phase is lower than the density of water phase, the oil phase is positioned above the water phase. When emulsification process is applied, spherical drops form. The interfacial force that keeps the drops spherical is defined as Laplace pressure (ΔP_L) and expressed by Young-Laplace equation (Adamson and Gast, 1997):

$$\Delta P_L = \frac{4\gamma}{d} \tag{1.1}$$

Here, γ is the interfacial tension between the phases and d is the drop diameter. At equilibrium, the pressure inside of the drop is larger than the pressure outside of the drop. Increase in the interfacial tension between the phases or decrease in the size of drops results in increase in Laplace pressure. For drop breakup, an external stress to be applied must be greater than the Laplace pressure. Since the Laplace pressure of smaller drops are higher, the energy required to disrupt the drops is larger (Walstra, 1993).

The reason of the thermodynamic unstability of emulsions can be explained by Gibbs free energy concept (Tadros, 2013; McClements, 2016). According to the second law of thermodynamics, Gibbs energy of emulsion formation is expressed by:

$$\Delta G_{formation} = \gamma \Delta A - T\Delta S_{configuration} \quad (1.2)$$

where γ is the interfacial tension between the phases, ΔA is the contact area between oil and water phases, T is the absolute temperature and S is the configurational entropy. When one of two phases is dispersed into the other phase to form an emulsion, the contact area between the phases increases. This means that ΔA term is always positive during emulsion formation. Entropy term is also positive because the number of emulsion drops increases during emulsion formation. In general, $\gamma\Delta A$ term is greater than $-T\Delta S_{configuration}$ and this makes the $\Delta G_{formation}$ positive. However, it is known that $\Delta G_{formation}$ should be negative for the system to be spontaneous. Therefore, emulsion formation is thermodynamically unfavorable, so phases separate after a while and return to their initial stage.

Apart from thermodynamic stability, kinetic stability of an emulsion is also important. Kinetic stability is related to long-term stability of an emulsion. After emulsification process is applied, an emulsion is formed at metastable state. When some physicochemical processes such as sedimentation or creaming due to gravity, flocculation and coalescence take place, stability of an emulsion disappears, and phase separation occurs (McClements and Gumus, 2016). For an emulsion to be kinetically stable, the activation energy of the system must be larger than the thermal energy of the system (kT). An emulsion that has greater kinetic stability has longer shelf life. The smaller the emulsion drops the higher the kinetic stability and the lower the thermodynamic stability (McClements, 2016).

To provide thermodynamic and kinetic stability of emulsions, emulsifiers have to be used (Wu and Ma, 2016; McClements, 2016). With the adsorption of emulsifiers at the oil-water interface, the interfacial area between the phases (ΔA) decreases and this provides thermodynamic stability (Wu and Ma, 2016). Also, emulsifiers form a

protective shield around the emulsion drops to prevent them becoming very close and coalesce (Tang et al., 2015; McClements, 2016). This results in an increase in kinetic stability of emulsions.

There are mainly two types of emulsion: oil-in-water (o/w) and water-in-oil (w/o). If the oil phase is dispersed in the water phase, oil drops are formed in the water and this type of emulsion is called as oil in water (o/w) emulsion. In that type of emulsion, oil is referred to as dispersed phase and water is referred to as continuous phase. On the other hand, if the water phase is dispersed into the oil phase, water drops are formed in the oil and this type of emulsion is called as water in oil (w/o) emulsion. In that type of emulsion, water is referred to as dispersed phase and oil is referred to as continuous phase.

Without emulsifiers, the type of an emulsion is based on the volume fractions of the phases. If the volumetric amount of oil phase is lower than the volumetric amount of water phase, the oil phase is dispersed into the water phase and oil in water emulsion is formed (McClements, 2016). However, when emulsifiers are added to the mixture of these phases, the type of emulsifier used for stabilization determines the type of an emulsion.

1.2. Surfactant-based Emulsions

To stabilize emulsions, various types of emulsifier can be used. In the conventional emulsification processes, chemical surfactants are used for stabilization (Wu and Ma, 2016; Binks, 2002). Chemical surfactants are asymmetric molecules. A surfactant consists of hydrophilic head and hydrophobic tail parts. This means they have amphiphilic structure. Surfactants are surface active agents, so they decrease the interfacial tension. When they are adsorbed at the interface, water and oil molecules are replaced by surfactants. While hydrophilic head of the surfactant is placed in the water phase, hydrophobic tail of the surfactant is placed at the oil phase. Therefore, increase in molecular interactions causes decrease in interfacial tension (Rosen, 2004). Adsorbing of surfactants at the fluid-fluid interface provides emulsion stabilization by

decreasing interfacial area between the phases and preventing coalescence of newly formed drops. Thus, the system becomes thermodynamically and kinetically stable. According to Bancroft rule, the phase in which the solubility of a surfactant is high becomes continuous phase (Bancroft, 1913). Which type of surfactant should be used for the desired type of emulsion is determined by HLB method developed by Griffin (1949). This method depends on the balance between the hydrophilic and hydrophobic parts of a surfactant. A surfactant molecule has a hydrophile - lipophile balance (HLB) number and the type of an emulsion is determined by this number (Binks, 2002). While when HLB number has a range between 4 and 6, w/o emulsion is formed, when HLB number has a range between 8 and 18+, o/w emulsion is formed (Griffin, 1949). When surfactants are used for emulsion stabilization, they form micelles in the system. The structure of a micelle varies with the type of an emulsion. The structure of a surfactant and formed micelles can be seen in Figure 1.1.

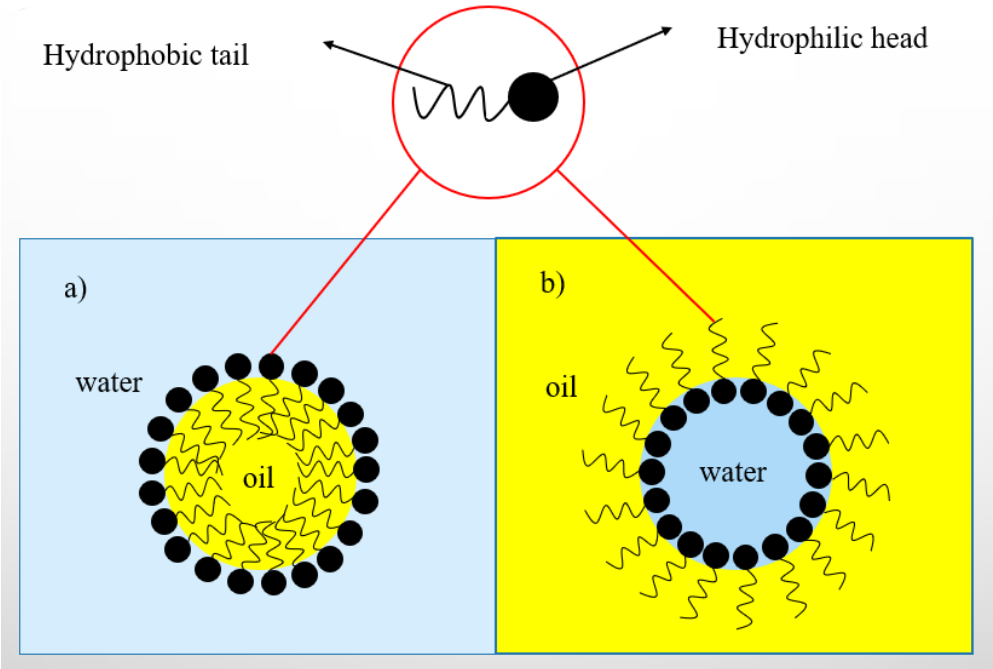

Figure 1.1. The structure of a surfactant and micelles (a) o/w emulsion, b) w/o emulsion)

1.3. Pickering Emulsions

Surfactants used as emulsifier in the conventional emulsions have some disadvantages. They are expensive materials. They can cause tissue irritation and cell damage due to their chemical contents. When these drawbacks are taken into consideration, their applications especially in cosmetics, biomedical, food and pharmaceutical industries are challenging (Schrade et al., 2013; Chevalier and Bolzinger, 2013; Tang et al., 2015). Therefore, alternative ways to stabilize emulsions have been searched. Studies conducted by W. Ramsden and S. U. Pickering have been pioneered in finding alternative emulsifiers. Ramsden (1903) observed that solid particles which are placed at the interface of the two phases decrease the surface energy of the free surface. Pickering (1907) realized that when solid particles which adsorb at the oil/water interface were used as emulsifier, stable emulsions were obtained. Emulsions stabilized using solid particles are called Pickering emulsions.

Solid particles have superior properties than surfactants. Since they contain low toxicity, they are less harmful to human health and the environment. Solid particles work like surfactants during emulsification process. Both are adsorbed at the oil/water interface and decrease the interfacial area between the phases. Thus, surface free energy is also reduced, and the system becomes thermodynamically favorable. There are two main steps for stabilization of an emulsion with solid particles. In the first step, solid particles form a steric and electrostatic protective shield around the dispersed drops in the system by adsorbing at the oil/water interface. Therefore, coalescence of newly formed drops is prevented. In the second step, a three dimensional network is formed by particle-particle interactions to provide stabilization (Binks, 2002).

Solid particles do not have sides with different properties unlike surfactants that have amphiphilic structure (Binks, 2002). Therefore, in determination of the type of an emulsion, different property of a solid particle is utilized. While the type of an emulsion is determined by HLB number when surfactants are used for stabilization,

when solid particles are used as emulsifier, the type of an emulsion depends on the particle wettability. Particle wettability is stated by three-phase contact angle of a solid particle (θ) shown in Figure 1.2. The contact angle of a solid particle is measured in the water phase and expressed by the Young equation given in the following (Binks and Clint, 2002).

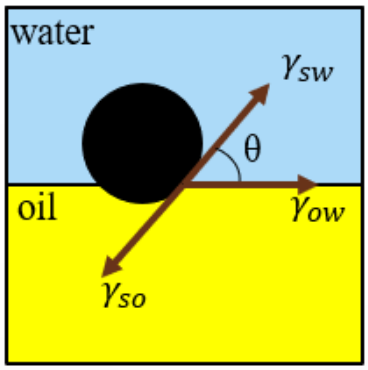

Figure 1.2. The contact angle and the interfacial tensions of a solid particle situated at the oil/water interface

$$\cos\theta = \frac{\gamma_{so} - \gamma_{sw}}{\gamma_{ow}} \tag{1.3}$$

Here, γ_{so} is the interfacial tension between the solid particle and the oil phase, γ_{sw} is the interfacial tension between the solid particle and the water phase and γ_{ow} is the interfacial tension between the oil phase and the water phase. Surfactants decrease the interfacial tension between the phases because they are surface active materials. However, the effect of the solid particles on the interfacial tension between the phases is complicated since studies about this topic have contradictions. Levine et al. (1989) observed that interfacial tension was decreased by hydrophilic silica particles in carbon tetrachloride-water emulsion. However, Drelich et al. (2010) observed that interfacial tension was not affected in paraffin oil-water emulsion stabilized with hydrophobic silica particles.

A solid particle that has a contact angle lower than 90° shows hydrophilic property and most part of the particle is wetted by the water phase. Thus, this type of particle is used to stabilize oil in water emulsions. On the other hand, a solid particle has a contact angle higher than 90° shows hydrophobic property and most part of the particle is wetted by the oil phase. Therefore, this type of particle is used to stabilize water in oil emulsions. The relation between the contact angle of a solid particle and the type of an emulsion is shown in Figure 1.3.

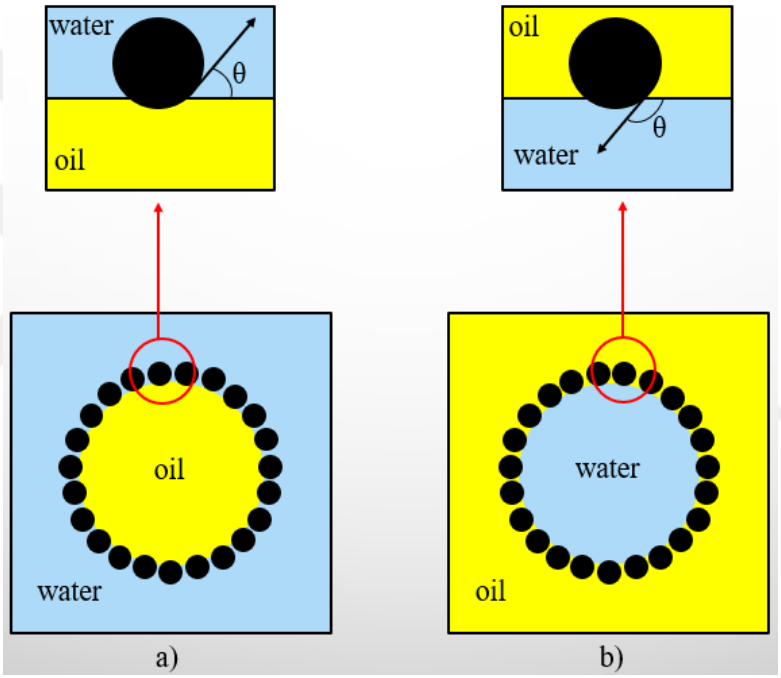

Figure 1.3. The relation between the contact angle of a solid particle and the type of an emulsion (a) Oil in water emulsion with hydrophilic solid particles b) Water in oil emulsion with hydrophobic solid particles)

The contact angle of a solid particle plays an important role on emulsion stabilization. If the contact angle of a solid particle is too low or too high, in other words, the particle is very hydrophilic or very hydrophobic, the emulsion cannot be stabilized because particles are located in one phase instead of being at the interface between the phases

(Binks, 2002). More stable emulsions are obtained with the solid particles which have a contact angle close to 90° (Kaptay, 2006).

According to Binks (2002), energy is required to detach a particle from the interface. Detachment energy (ΔE) depends on particle radius (r), oil/water interfacial tension (γ_{ow}) and particle contact angle (θ). The relation between them is expressed by the following formula:

$$\Delta E = \pi r^2 \gamma_{ow} (1 \pm \cos\theta)^2 \quad (1.4)$$

Detachment energy of a particle is greater than its thermal energy (kT). Therefore, it can be said that solid particles are adsorbed at the interface almost irreversibly. In terms of this aspect, solid particles provide better stability than surfactants because surfactant can be adsorbed and desorbed more easily (Binks, 2002).

Apart from solid particles with homogeneous surface, there are also solid particles with heterogeneous surface. They show amphiphilic property like surfactants. These particles have been prepared from glass spheres by Casagrande et al. (1989) and they are named as Janus particles. Since particle detachment energy of Janus particles is higher than ordinary solid particles, an emulsion stabilized with Janus particles has better stability compared to an emulsion stabilized with homogeneous solid particles (Binks and Fletcher, 2001).

1.4. Significant Physicochemical Parameters for Pickering Emulsion Formation

There are some significant physicochemical parameters that affect drop size and drop size distribution of Pickering emulsions. These parameters can be classified as the type, size, amount and shape of the solid particles, the type and viscosity of oil, the oil/water ratio, water pH and salt concentration in the system. The effect of these physicochemical parameters on the production of Pickering emulsions have been searched previously in detail. The results of some studies related to these parameters are summarized in the following.

1.4.1. The Effect of Particle Size

The size of particles has an important effect on the emulsion stabilization. The surface coverage of newly formed drops is affected by the size of the particles. Binks and Lumsdon (2001) performed a study with polystyrene latex particles and they observed that increase in particle size leads to increase in drop size. The same result was also obtained with the study conducted by Tsabet and Fradette (2015b) with glass microspheres. The smaller the particles, the more stable the emulsion drops.

1.4.2. The Effect of Particle Shape

Madivala et al. (2009) showed that when ellipsoid particles are used instead of spherical particles, more stable emulsions are produced. They observed that ellipsoid polystyrene latex particles provide higher stability compared to spherical ones. This is an indication that emulsion stability is affected by the aspect ratio of the particles. According to their study, ellipsoid particles cover the surface of the drops more effectively because they have stronger capillary forces. Also, since they form elastic shield around the drops, coalescence of drops is prevented.

1.4.3. The Effect of Oil Viscosity

According to studies conducted by Tsabet and Fradette (2015a, b), increase in oil viscosity adversely affects emulsion stabilization. Increase in oil viscosity makes drop movement difficult and the contact of drops with the particles becomes less (Chesters, 1991). Tsabet (2014) showed in his study that increase in oil viscosity causes increase in particle adsorption time. An increase in oil viscosity may also result in decreased levels of shear in the tank. As a result, larger drops are formed. However, decrease in oil viscosity leads to increase in shear in the tank and this cause drop breakup. Since mobility of drops and particles increases, their contact also increases, and particle adsorption becomes easy. Therefore, more stable drops are produced with low viscosity oils.

1.4.4. The Effect of pH and Salt Concentration

Addition of a salt or an acid into an emulsion increases ionic species in the system. The interactions between the ionic species and the particles gives rise to particle flocculation and this situation creates the similar effect of stabilizing of an emulsion with large particles (Tsabet and Fradette, 2015b). Therefore, increase in salt concentration in the system leads to formation of larger and less stable drops. Binks et al. (2006) also observed that increase in ionic species in the system leads to drop coalescence.

1.5. Significant Hydrodynamic Parameters for Pickering Emulsion Formation

Apart from physicochemical parameters, hydrodynamic conditions in the system play also an important role for mixing of immiscible liquids. Hydrodynamics of a system are influenced by many factors: the geometry of the tank, flow regime, the type and the size of the impellers, the thickness and the number of impeller blades, the off-bottom clearance of the impeller, the presence of baffles and the position of the shaft. Also, different hydrodynamic conditions are created by changing hydrodynamic parameters such as impeller tip speed, impeller Reynolds number, Weber number and power per mass ratio. Some of these parameters are mentioned in detail in the following.

1.5.1. The Effect of the Presence of Baffles

Mechanically agitated stirred tanks are used for many purposes including blending, suspending, dispersing, homogenizing and transferring. The shape of a conventional stirred tank is vertical cylindric and the fluid in tank is agitated by top-entering rotating motor (Hemrajani and Tatterson, 2004). Mixing can be done in a baffled or an unbaffled stirred tank depending on process requirements. The presence or absence of baffles influences the flow pattern in a stirred tank. Wall baffles transform tangential flows to vertical flows, provide top-to-bottom mixing without swirl, and minimize air entrainment (Hemrajani and Tatterson, 2004). Despite these advantages, there are some drawbacks of the presences of baffles also. Dead zones where mixing is slower

and more difficult to become homogeneous are formed behind the baffles. This accumulation also makes tank cleaning difficult. Therefore, in food, pharmaceutical and cosmetic industries where cleaning is one of the most important criteria, the usage of baffled stirred tanks for mixing process is challenging (Assirelli et al., 2008). Also, when precipitation processes are done in baffled tanks, incrustations are formed on the baffles (Rousseaux et al., 2001). Hekmat et al. (2007) observed from their studies that performing of crystallization process which is an alternative way for purification of biomolecules in a baffled tank causes formation of smaller crystal particles compared to unbaffled tank because the presence of baffles results in damaging of growing particles. Also, in biotechnological applications, working with baffled tanks can cause death of shear sensitive cells (Aloi and Cherry, 1996).

Due to drawbacks of working with baffled tanks, in the recent years, mixing in unbaffled tanks has drawn attention. When baffles are removed, a central vortex begins to form at the free surface. The depth of the central vortex gets larger when the impeller speed is increased. Formed vortex on the surface begins to reach the impeller as the impeller speed increases (Devi and Kumar, 2017). The impeller speed that the vortex reaches the impeller is defined as critical speed (N_{cr}). After critical impeller speed, air entrainments occur. When the impeller speed continues to increase, vortex enlarges below the impeller and an air cavity is formed below the impeller (Assirelli et al., 2008; Scargiali et al., 2013). The formed vortex is not steady but moves slightly and oscillates in the system (Busciglio et al., 2016).

Unbaffled tanks are used in many industrial applications. When unbaffled tank is used as bioreactor that contains shear sensitive cells, required oxygen for the cells can be taken into the system without any cell damage. It should be noticed that for the application of the oxygen feeding for the cells, reaching of the vortex to the impeller blades should be avoided. Since air entrainment occurs when the vortex reaches to impeller blade, air bubbles are formed in the system and this can affect the cells negatively also (Scargiali et al., 2012).

However, without baffles fluid in the tank performs solid body rotation. This causes poorer mixing in the unbaffled tanks rather than baffled tanks. The comparison of mixing in the baffled and the unbaffled tank can be seen in Figure 1.4. The central vortex formation due the absence of baffles can be seen clearly.

a) Baffled tank b) Unbaffled tank

Figure 1.4. Comparison of mixing in the baffled and the unbaffled tank

1.5.2. The Effect of Shaft Position in Unbaffled Tanks

To eliminate of negative effects of unbaffled stirred tank on mixing, the position of the shaft can be changed. When the shaft is located at away from the tank center instead of at the tank center, the vortex formation is affected. Eccentricity is the distance between the center of the tank and the center of the tank. The ratio of this distance to tank diameter is defined as eccentricity ratio. Depending on the eccentricity ratio, the depth of the vortex changes. The vortex even begins to disappear as the eccentricity ratio increases. When the shaft is located at away from the center of the tank, the formed vortex gains an inclination with respect to the vertical axis. As the eccentricity ratio increases, the size of the vortex becomes smaller and inclination with respect to the vertical axis becomes larger (Galletti and Brunazzi, 2008; Musik and Talaga, 2016) . After a certain impeller speed, a lower vortex is formed below the impeller (Montante et al., 2006). However, the system is affected mostly by the upper

vortex and the effect of the lower vortex on the system is weak compared to the upper vortex (Galletti et al., 2008). The effect of eccentricity ratio on the vortex formation can be seen in Figure 1.5.

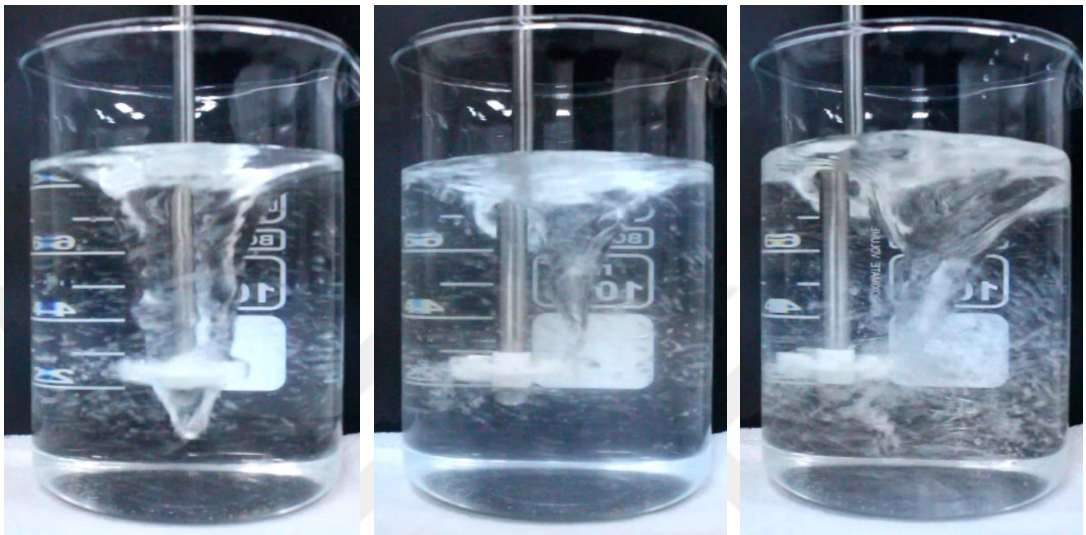

a) e/T=0 **b)** e/T=0.1 **c)** e/T=0.2

Figure 1.5. The effect of eccentricity on vortex formation

1.5.3. The Effect of the Type of the Impeller

The flow pattern created in a tank varies with the type of the impeller. Impellers can be classified as axial flow, radial flow, mixed flow and high shear. In selection of an impeller, the purpose of mixing should be taken into consideration. While solid suspension is provided more efficiently with axial flow impellers, fluid-fluid dispersion occurs better with radial flow impellers (Hemrajani and Tatterson, 2004).

The pitched blade turbine (PBT) is built by mounting an even number of angled blades to a hub. In general, pitched blade turbines that contain 4 blades with 45° blade angle are used. A pitched blade turbine is a mixed flow impeller that means it creates both axial and radial flow patterns. It can be designed to provide two different flow directions: down pumping pitched blade turbine (PBTD) and up pumping pitched

blade turbine (PBTU). When PBTD is used in a stirred tank, the impeller discharge is first sent to the bottom of the tank. Then it moves up, circulates in the tank and comes back to the impeller. On the other hand, when PBTU is used, the impeller discharge is first sent to the top of the tank. Then it moves down and circulates in the tank and comes back to the impeller. Created flow patterns with PBT impellers in baffled stirred tanks are seen in Figure 1.6. PBT impellers are good in solid suspension and blending processes.

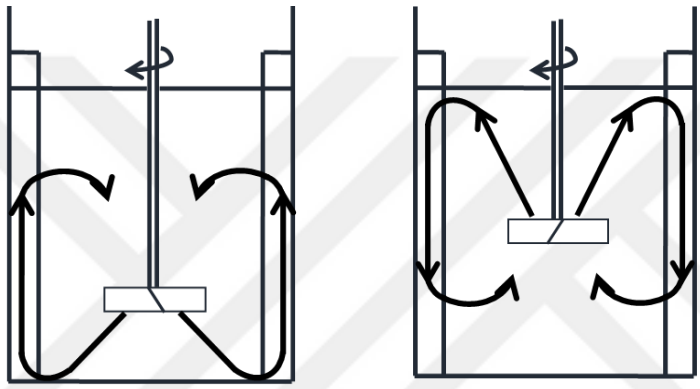

a) PBTD b) PBTU

Figure 1.6. Flow patterns of PBT impellers in baffled tanks

Rushton turbine (RT) impellers are built by mounting 6 vertical blades to a disc. It creates radial flow pattern in the system. The impeller discharge firstly impinges to the tank wall and then circulates in the tank as two parts: one is above the impeller and the other one is below the impeller and come back to the impeller. Created flow pattern in a baffled stirred tank can be seen in Figure 1.7. RT impellers are good in fluid-fluid dispersion.

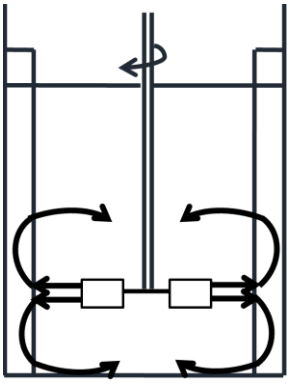

Figure 1.7. Flow pattern of RT impeller in baffled tanks

Since Pickering emulsion formation includes solid suspension and liquid-liquid dispersion, to investigate which type of impeller will give better performance, PBT and RT impellers were used in this thesis.

While RT impellers create higher shear than PBT impellers, PBT impellers have higher pumping capacity compared to RT impellers (Hemrajani and Tatterson, 2004). PBT impellers have greater flow number, so their pumping capacity is higher compared to RT impellers. Impeller power number is similar to drag coefficient. Just as the drag coefficient depends on the shape of the object, the power number depends on the type of the impeller. The power number of RT impeller is higher than PBTD impeller (Chapple et al., 2002). Therefore, RT impeller gives more energy into the system.

When baffles are removed, created flow patterns by the impellers in the tank are affected. When the shaft is at the center, the flow patterns created in unbaffled tanks by the small impellers are the same with the flow patterns created in baffled tanks. However, for the large impellers, there is a difference between the flow patterns created in baffled and unbaffled tanks. In the unbaffled tanks, radial component of the flow pattern formed with centrically located PBTD T/2 is more dominant. Also, the impeller discharge is sent with a downward inclination when RT T/2 is centrically

located in an unbaffled tank. Therefore, it can be said that the flow patterns created with the large impellers are almost the same.

The flow patterns are also affected by the shaft position. When the shaft is located away from the center, different flow patterns are created for all sizes of the impellers compared to baffled and centrically located unbaffled cases. Similar flow patterns are created with RT, PBTU and PBTD impellers at the region where the shaft is close to the tank wall. The impeller discharge impinges to the tank wall and due to interaction between the fluid and the tank wall, fluid separates into two loops at that region. On the other hand, at the region where the shaft is away from the tank wall, fluid circulates the tank by following an elliptic path.

1.5.4. Significant Hydrodynamic Expressions

1.5.4.1. Impeller Tip Speed

Impeller tip speed (V_{tip}) is the maximum speed that can be obtained at the end of the impeller blade. In this section, the effect of change in impeller tip speed on the emulsion drop size was investigated in unbaffled tanks with centered shaft. The formula of impeller tip speed is given below:

$$V_{tip} = \pi ND \tag{1.5}$$

1.5.4.2. Impeller Reynolds Number

Impeller Reynolds number (Re) represents the ratio of the inertial forces to viscous forces and it is expressed by the following:

$$Re = \frac{ND^2\rho}{\mu} \tag{1.6}$$

The flow regime in the tank is adjusted by changing impeller Reynolds number. When Re < 10, the flow regime in the tanks becomes laminar. When Re > 20 000, the flow regime in the tank becomes turbulent. The flow regime between these two is defined as transitional (Hemrajani and Tatterson, 2004). The fluid flows by following the streamlines when the flow regime is laminar. However, when the flow regime is

turbulent, eddies are formed in the system and they cause turbulent fluctuations. They provide better mixing compared to laminar regime. The presence of turbulent fluctuations contributes to drop breakup and formation of smaller drops.

1.5.4.3. Weber Number

Weber number (We) represents the ratio of inertial forces to surface forces and it is expressed by the following:

$$We = \frac{\rho_c N^2 D^3}{\sigma} \tag{1.7}$$

While inertial forces cause formation of smaller drops, surface forces try to keep a drop in original shape. Also, since the interfacial tension between the phases affects the drop size and Weber number is a parameter associated with the interfacial tension, investigation of the effect of varying Weber number on the system can be a guiding for understanding of drop breakup mechanism of the system. As Weber number increases, inertial forces become dominant in the system and it is expected that drop breakup occurs mostly.

1.5.4.4. Power/Mass Ratio

Power/mass is an indication of breakup potential of an emulsion system in a stirred tank. Mass includes volume. When the impeller swept volume is used, the power/mass is known as the maximum energy dissipation in the tank. At the same power/mass ratio with different impellers, the same amount of energy is dissipated into the system. In this thesis, the effect of varying power/mass ratios on drop sizes was investigated. This ratio is expressed with the following relation:

$$\varepsilon = \frac{P}{\rho V_{imp}} = \frac{\rho N^3 D^5 N_p}{\rho V_{imp}} = \frac{N^3 D^5 N_p}{V_{imp}} \tag{1.8}$$

1.6. Drop Size Measurement

The final drop size of an emulsion depends on the balance between drop breakup and coalescence and the final value is affected from the conditions created in the system. Therefore, measurements of drop size and drop size distribution are necessary to investigate how hydrodynamics affect the system. There are many techniques for determination of drop size and drop size distribution such as direct imaging, laser systems and sound systems (Niknafs, 2011). In this thesis, Malvern Mastersizer 3000 equipment was utilized for the measurements. Particle size range between 0.01 μm and 3500 μm can be analyzed using this equipment. It works with laser diffraction principle. A certain amount of particle is put into the wet dispersion unit of the equipment. Whether the added amount is sufficient is controlled by the obscuration range. Particle addition is continued until the amount is within the desired obscuration range. This range can be arranged by the user. During addition of particles, the equipment applies mixing for better dispersion. If particles agglomerate, adding more energy can be required to disperse the particles. In that case, the speed of stirrer can be increased, or ultrasound can be activated. After sufficient dispersion is achieved, particles are vacuumed and sent to the optical unit. In the optical unit, a laser beam is directed to the particles. There are two different types of laser beams that can be utilized during measurements: red light and blue light. Red light source is 4 mW He-Ne and has 632.8 nm wavelength. Blue light source is 10mW LED and has 470 nm wavelength (Mastersizer 3000). Once light hits the particles, it scatters. While large particles create small scattering angle, small particles create large scattering angle as shown in Figure 1.8.

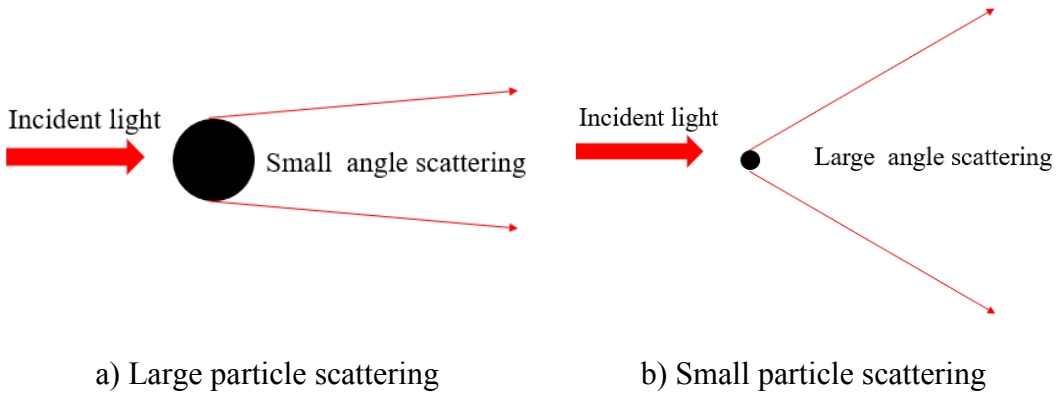

Figure 1.8. Scattered light depending on particle size

While red light is suitable for the measurement of small angle scattering, blue light is suitable for the measurement of large angle scattering. When the size of the particles is smaller than 1 µm, the usage of blue light gives more accurate result. The usage of blue light for the particles above this size reduces the accuracy of the measurements. Also, wrong results can be obtained when blue light is used to measure drop size of the particles which contain red and yellow color because of blue light absorption (Malvern, 2017). In Figure 1.9, diffraction configuration for red light and blue light is shown.

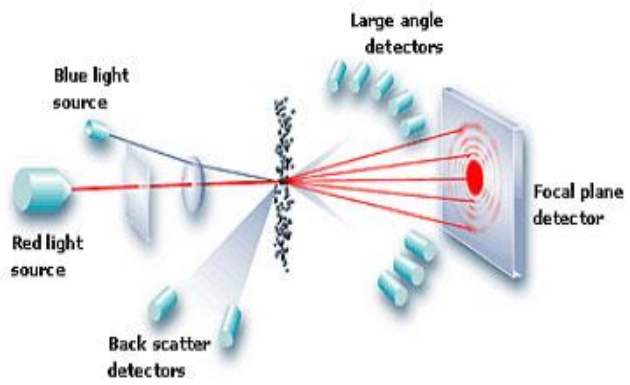

Figure 1.9. Laser diffraction configuration of Malvern Mastersizer 3000

The angular scattered light intensity data collected by detectors is used to create scattering pattern. Scattering pattern created by the particles can be obtain using two different optical methods which are Mie theory and Fraunhofer approximation. After scattering pattern is obtained, particle size and particle size distribution are represented as volume equivalent sphere diameter (*A Basic Guide to Particle Characterization,* 2015).

Mie theory requires the information related to optical properties of the particles and the dispersant. In this theory, incident light is not only scattered but also refracted and absorbed (Aydın, 2015; Virden, 2017; *A Basic Guide to Particle Characterization*, 2015). Therefore, refractive and absorption index of both particle and dispersant should be known. However, according to ISO 13320 standard, if optical properties of the particles are not known and the size of particles is larger than 50 µm, the usage of Fraunhofer approximation can be used for particle size and size distribution analysis. Particles are assumed completely opaque in this approximation and the incident light is just scattered, so the information of refractive and absorption indices is not required (*A Basic Guide to Particle Characterization*, 2015; Rawle, 2003; Ye et al., 2012). If the size of particles is smaller than 50 µm, Fraunhofer approximation can cause multiple scattering and wrong results, so for size analysis of the particles below that size, Mie theory should be used. In Figure 1.10, the difference between Mie and Fraunhofer model is shown.

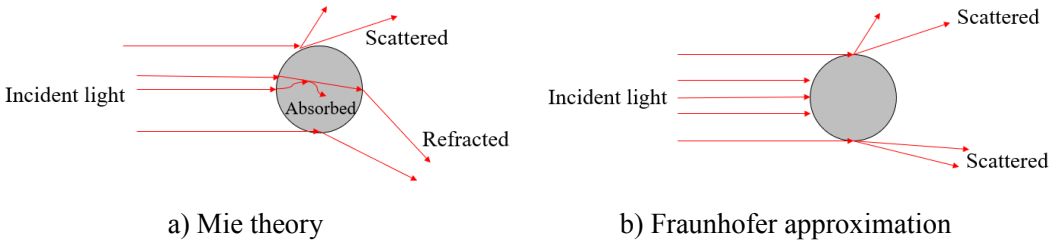

Figure 1.10. Light scattering by Mie and Fraunhofer models

Drop size can be expressed by various different mean diameter values (Leng and Calabrese 2004) and all can be obtained by Malvern Mastersizer 3000 equipment:

- **The Sauter mean diameter (d_{32}):** It is also known as surface-volume mean diameter and represents the ratio of the third to second moments of the drop size distribution.

$$d_{32} = \frac{\sum_{i=1}^{i=m} n_i d_i^3}{\sum_{i=1}^{i=m} n_i d_i^2} \tag{1.9}$$

- **Mass mean diameter (d_{43}):** It represents the ratio of the fourth to third moments of the drop size distribution.

$$d_{43} = \frac{\sum_{i=1}^{i=m} n_i d_i^4}{\sum_{i=1}^{i=m} n_i d_i^3} \tag{1.10}$$

- **Arithmetic mean diameter (d_{10}, d_{50}, d_{90}):** d_{10} means 10% by volume of all drops smaller than d_{10}, d_{50} means 50% by volume of all drops smaller than d_{50} and d_{90} means 90% by volume of all drops smaller than d_{90} (Leng and Calabrese 2004)

$$d_n = \frac{\sum_{i=1}^{i=m} n_i d_i}{\sum_{i=1}^{i=m} n_i} \tag{1.11}$$

In these relations, the number of drops is represented by n_i and the diameter of drops is represented by d_i.

1.7. Motivation of Thesis

There are many studies in the literature about the effect of physicochemical parameters on the production and the stability of Pickering emulsions. However, studies about the effect of hydrodynamic conditions on Pickering emulsion formation are still scant.

Also, experiments related to Pickering emulsions were done in vials and the production were performed by handshaking method. In food industries, on the other hand, homogenizers were utilized to produce Pickering emulsions. There are some studies carried out by Tsabet and Fradette (2015a, b) that the productions were done in the stirred tanks. They have mainly focused on the effect of physicochemical parameters on Pickering emulsions in their studies. They did not compare types of impeller and different hydrodynamic conditions. They have performed the experiments in unbaffled stirred tanks with eccentrically located shaft but did not provide any information about the eccentricity ratio. Therefore, the effect of eccentricity ratio on the production of Pickering emulsions are unknown. Abdulrasaq and Ayranci, (2019) investigated the effect of hydrodynamics on the drop size of Pickering emulsions, but they used a baffled stirred tank.

In this thesis, it was aimed to investigate the effect of hydrodynamics on the production of Pickering emulsions in unbaffled stirred tanks by analyzing drop size. For this purpose, productions were performed with three different types of impeller which are PBTD, PBTU and RT at two different sizes: T/2 and T/3. Also, experiments were done when the shaft was located at three different positions: e/T=0, e/T=0.1 and e/T=0.2. To observe only the effects of hydrodynamic conditions, physicochemical properties were kept constant throughout the experiments. The emulsions were produced with the listed impellers at given eccentricity ratios at varying tip speed, impeller Reynolds number, Weber number and power per mass. Their performances were compared at the same value of each hydrodynamic parameter.

In Chapter 2, experimental procedure of the experiments performed in this study is given in detail. In Chapter 3, the effect of different types of impellers and the effect of different hydrodynamic conditions on the production of Pickering emulsions are given as drop size and drop size distribution. Impeller performances and the effect of shaft position are compared by measuring drop size of the emulsions. In Chapter 4, results of this study are summarized, and suggestions are done to improve this study.

CHAPTER 2

EXPERIMENTAL PROCEDURE

2.1. Materials

The aim of this study was to investigate the effect of hydrodynamic conditions on the production of Pickering emulsions in unbaffled stirred tanks. To perform this aim oil in water Pickering emulsions were prepared. Hydrophilic solid particles were used for stabilization. Details of the materials are given below.

2.1.1. Determination of the Type of Particle

The selection of a set of solid particles that were appropriate for the production of o/w Pickering emulsions was based on a literature survey. The studies carried out by Tang et al. (2015) and Tsabet and Fradette (2015a, b) reported a range of possible particle types. Several types of particles were selected: micronized calcite, micronized silica, micronized zinc powder, titanium dioxide, glass beads, micronized zinc oxide and micronized copper oxide. To test their suitability for this study, the particle size and particle size distribution of these particles were analyzed with Malvern Mastersizer 3000. O/w Pickering emulsions were formed with each of the particles in vials. The most appropriate particle type was selected as Sovitec brand glass beads from Omnis Kompozit considering the particle size distribution and stability and size distribution of the formed emulsion drops. These glass beads had a narrow particle size distribution and yielded stable drops with narrow drop size distribution without any visible agglomeration. The particle size and particle size distribution analysis done with Malvern Mastersizer 3000, are given in Figure 2.1 and volumetric particle size distribution is given in Table 2.1. The average particle diameter, d_{50} 18.3 μm and 99% of the particles are smaller than 60 μm according to this analysis.

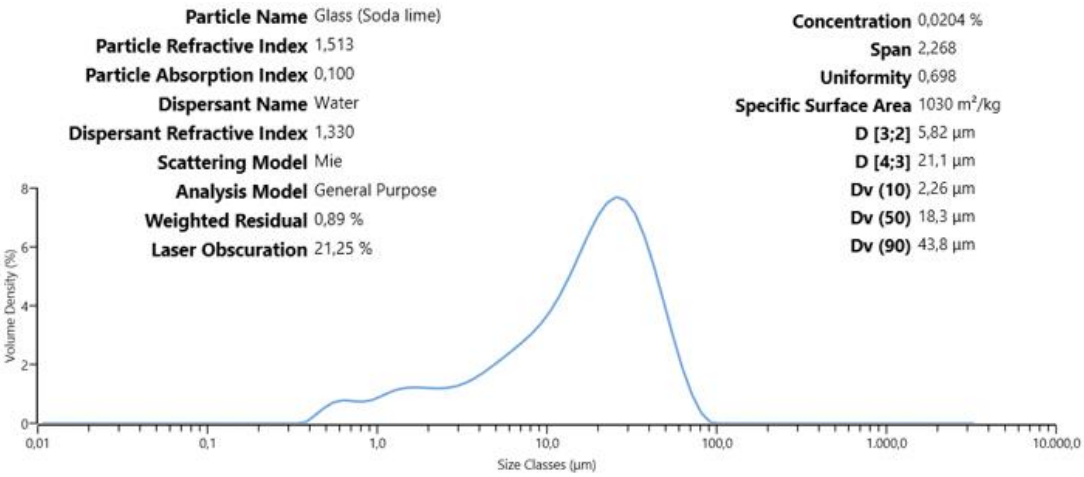

Figure 2.1. Particle size distribution of glass beads

Table 2.1. *Volumetric particle size distribution*

Size (µm)	% Volume In	Size (µm)	% Volume In	Size (µm)	% Volume In	Size (µm)	% Volume In	Size (µm)	% Volume In	Size (µm)	% Volume In	Size (µm)	% Volume In
1,65	1,02	3,12	1,14	5,92	2,08	11,2	3,63	21,2	6,27	40,1	4,44	76,0	0,27
1,88	1,00	3,55	1,28	6,72	2,30	12,7	4,16	24,1	6,44	45,6	3,47	86,4	0,00
2,13	0,99	4,03	1,46	7,64	2,54	14,5	4,75	27,4	6,34	51,8	2,47	98,1	0,00
2,42	1,00	4,58	1,66	8,68	2,83	16,4	5,35	31,1	5,95	58,9	1,56	111	0,00
2,75	1,05	5,21	1,87	9,86	3,19	18,7	5,88	35,3	5,30	66,9	0,81	127	0,00

As shown in Figure 2.2 the particle shape was determined to be spherical based on microscopic image taken with Olympus BX53 Upright Microscope. Physical properties of glass beads can be seen in Table 2.2.

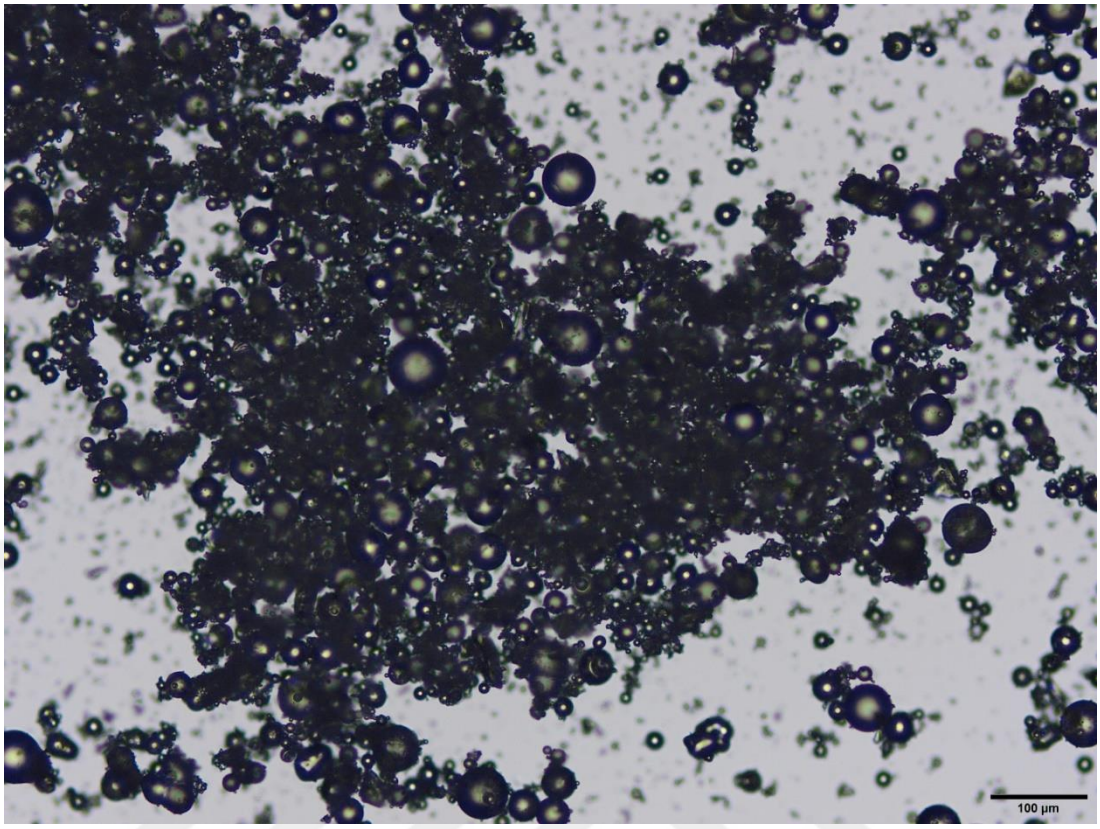

Figure 2.2. Microscopic image of spherical glass beads

Table 2.2. *Physical properties of glass beads*

The name of the product	Microperl® (Sovitec)
Chemical Composition	Soda lime glass
Particle Size (μm)	18.3
Density (g/cm^3)	2.52

2.1.2. Determination of the Type of Oil

The selection of a set of possible types of oil was also based on literature survey. Sunflower oil, corn oil, castor oil and silicon oil were used for production of Pickering emulsions within the vials and their performance were compared to each other. Based

on these tests, silicon oil was chosen as dispersed phase because smaller emulsion drops were obtained with this oil. Another point taken into consideration during the selection of silicon oil as dispersed phase is the production technique of the oil. Cooking oils could have had varying properties between batches due to their different fatty acid contents. This situation could have affected the results of the experiments in an undesirable way. Silicon oil, however, was produced based on a standard procedure that would keep the properties almost the same and could be purchased in large batches. Tsabet and Fradette (2015a, b) who worked on the production of Pickering emulsions in stirred tanks also used silicon oil. They investigated the effect of viscosity of silicon oil on the production of Pickering emulsions in stirred tanks with off-centered shaft. According to the results of their experiments performed with using silicone oils with different viscosities, smaller drops can be obtained when low viscosity of silicon oil is used. When the viscosity of oil decreases, oil/particle affinity increases and thanks to this, the interface is covered in a more effective way. Also, they found that the size of formed emulsion drops is close when silicon oil viscosity is between 10 cst and 500 cst. In the light of these studies, 100 cst Dow Corning silicon oil was selected as the dispersed phase. It was purchased from Pistol Kimya. Using pendant drop technique, the oil in water interfacial tension was determined as 59.748 mN/m. The physical properties of silicon oil used in this study is given in Table 2.3.

Table 2.3. *Physical properties of silicon oil*

The name of the product	XIAMETER® PMX-200 Silicone Fluid
Viscosity (cst)	100
Density (25°C) (g/cm^3)	0.964
Refractive index	1.4030
Surface tension (25°C) (mN/m)	20.9
Interfacial tension (25°C) (mN/m)	59.748
Solubility in some solvents	
Pure alcohol	Poor
Water	Poor

2.1.3. Determination of the Type of Water

Based on previous studies, it was decided that distilled water would be used as continuous phase. However, there was no information about which type of distilled water was used in those studies. Distilled water can be classified as RO (reverse osmosis) and UP (ultra-pure). To observe the effect of type of water on the production of Pickering emulsions, two experiments were done (4 experiments with repetitions in total) with RT T/3 impeller at 1443 rpm when the shaft was 2 cm away from the tank center. One of them was done using RO water and the other one was done using UP water. After every hour, a sample was taken. Then the size of formed emulsion drops was compared by analysis done with Malvern Mastersizer 3000. According to the results of these analysis, the size of produced emulsion drops is very close to each other and there is almost no difference between the UP and RO water for the production of Pickering emulsions. This can be seen in Figure 2.3. Since RO water can be obtained more easily compared with UP water, RO water was chosen as the continuous phase for this study.

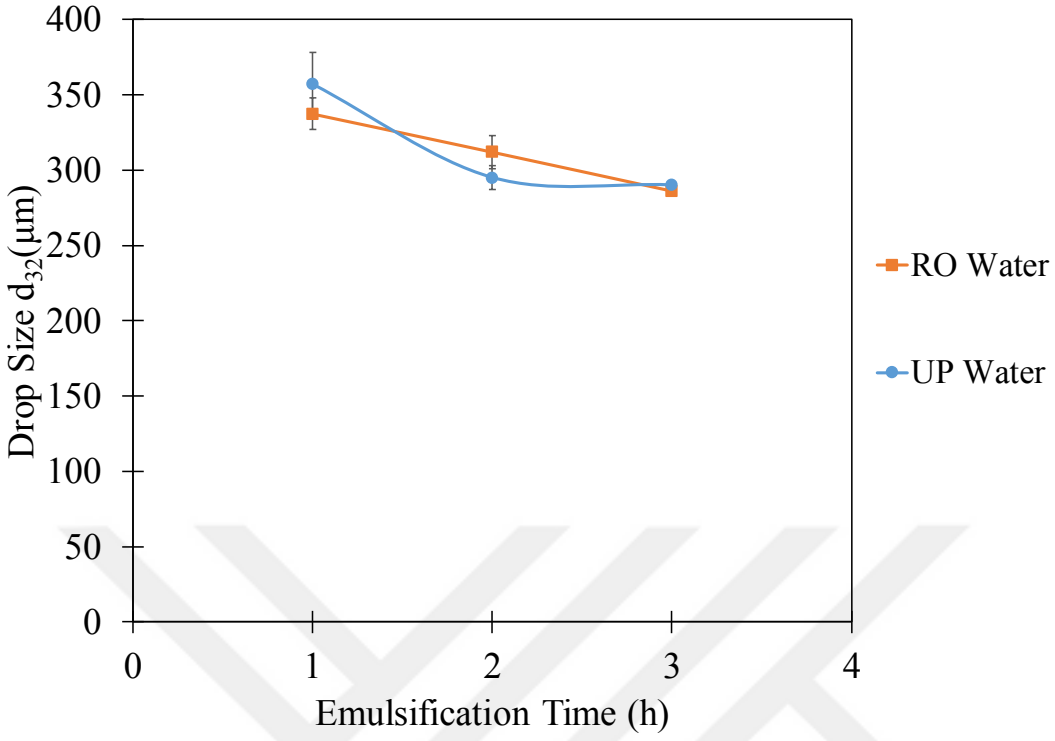

Figure 2.3. The effect of type of distilled water on drop size

2.2. Experimental Setup

Experiments were performed in unbaffled tanks. 1 L glass cylindrical beaker with inner diameter T=9.9 cm was used as tank. Shaft was positioned at three different locations: e/T=0, e/T=0.1 and e/T=0.2 where e is the distance between the center of the tank and the center of the shaft. The tank configurations can be seen in Figure 2.4.

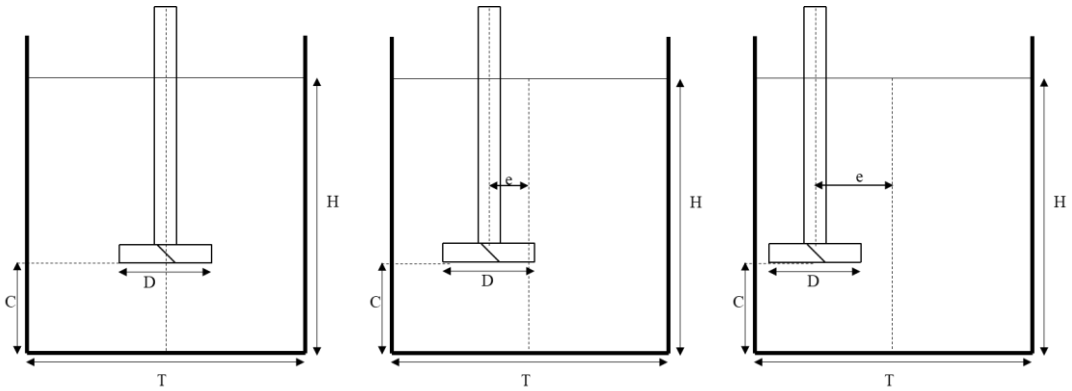

a) e/T=0 b) e/T=0.1 c) e/T=0.2

Figure 2.4. Tank configurations

To observe the effect of different flow patterns on the emulsion formation, Rushton Turbine (RT) and 45° down pumping Pitched Blade Turbine (PBTD) at two sizes were used: T/2 and T/3 where T is the inner tank diameter. Same size impellers also have the same blade thickness and blade width. All impellers were made up of polyamide and they were produced with 3D printer. Used impellers are shown in Figure 2.5.

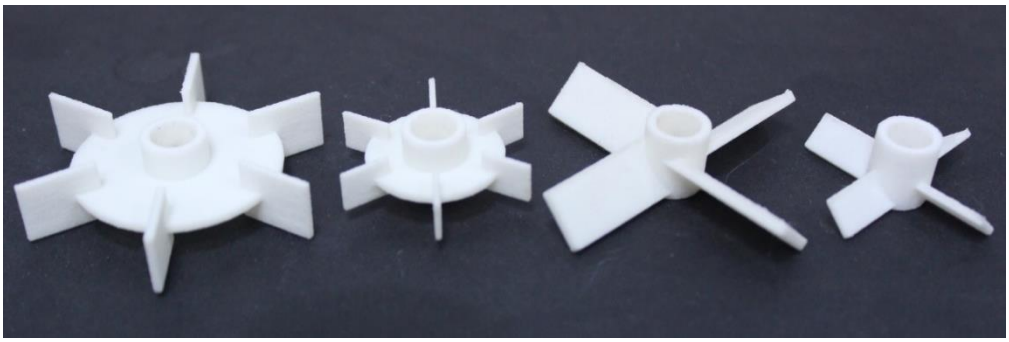

Figure 2.5. Impellers used in the experiments (from left to right respectively: RT T/2, RT T/3, PBTD T/2 and PBTD T/3)

To see the difference of performance between 45° down pumping Pitched Blade Turbine (PBTD) and 45° up pumping Pitched Blade Turbine (PBTU), PBTU at two different sizes was used: T/2 and T/3. They were used just in the experiments which were done to investigate of the effect of impeller tip speed on the production of Pickering emulsions. They were not used in the other experiments because they produced undesired emulsion drops and their performance was not good. Used PBTU impellers are shown in Figure 2.6.

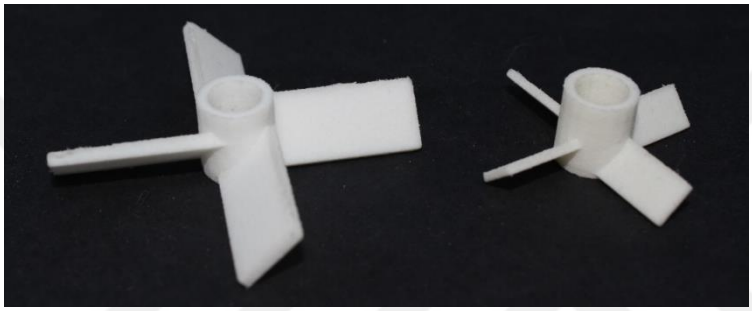

Figure 2.6. PBTU T/2 and PBTU T/3 from left to right respectively

All impellers were adjusted to have off-bottom clearance as C=T/3 in all experiments. The liquid height (H) within the tank was equal to the inner tank diameter (H=T) for effective mixing. The agitation was done with three different types of overhead stirrer motors all of which provide constant impeller speed during operation: IKA® Microstar 7.5 control, Daihan Scientific® HS-30D and Heidolph® Hei-TORQUE Precision 100. They can be seen in Figure 2.7.

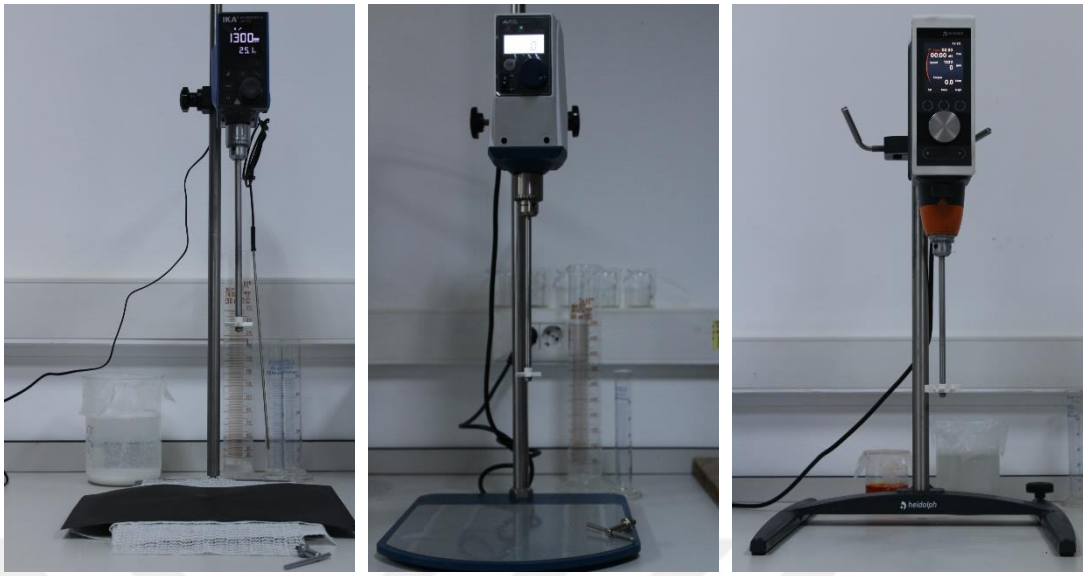

a) IKA® Microstar 7.5 control b) Daihan Scientific® HS-30D c) Heidolph® Hei-TORQUE Precision 100

Figure 2.7. Used overhead stirrers in the experiments

2.3. Development of the Procedure of Emulsification Experiments

2.3.1. Arrangement of Experimental Setup

Different hydrodynamic conditions were created with different shaft positions as well as the use of different type of impellers. The effect of all hydrodynamic parameters on the production of Pickering emulsions, were tested at three different shaft positions: e/T=0, e/T=0.1 and e/T=0.2. To arrange the shaft position correctly, three apparatus were designed as seen in Figure 2.8. They were made up of plexiglass material. After impellers were set according to off bottom clearance (C=T/3), shaft was positioned using these apparatus as seen in Figure 2.9.

Figure 2.8. The apparatus used for arrangement of shaft positions: e/T=0, e/T=0.1 and e/T=0.2 from left to right respectively

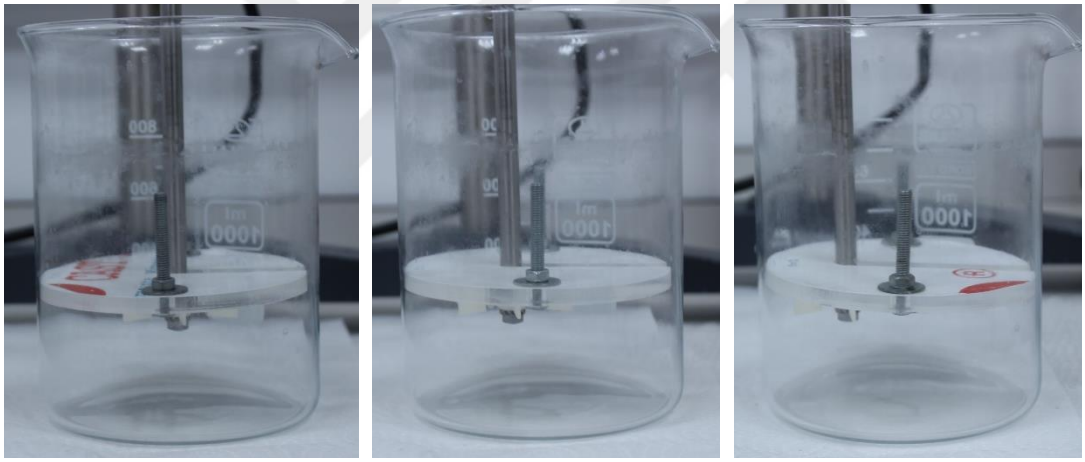

a) e/T=0 b) e/T=0.1 c) e/T=0.2

Figure 2.9. Arrangement of shafts using plexiglass apparatus

2.3.2. Determination of Oil/Water Ratio and the Amount of Particles

In the determination of oil to water ratio, it was paid attention to conduct experiments without phase inversion. Therefore, experiments were carried out so that the oil content was 10% and 30% of the total volume in the tank. Stable emulsion drops were

produced when the oil content was 30%, so it was decided that 30% oil to water ratio would be used in all experiments in this study. After determination of the oil to water ratio, the next step was the determination of the amount of solid glass beads used for emulsification. Various amounts -10, 15, 17, 20, 25, 30, 50, 60, 70, 80, 90, 100 and 200 g- of particles were tested to find needed amount. The amount of particles used below 100 g was insufficient and some amount of oil remained on the surface without emulsifying. In order to eliminate the effect of coverage potential of the particles on the final drop size and to highlight just the impact of hydrodynamic conditions on the production of Pickering emulsions, excess amount of particle needed to be used. 100 g solid glass beads were found to be sufficient as a result of the experiments carried out considering this information. In the experiments performed using 200 g particles, it became difficult to disperse the solid particles in the continuous phase and too many particles settled to the bottom of the tank. This situation can be explained by the result of the work of Tsabet and Fradette (2015a). According to their study, too much particle causes decrease in turbulent energy dissipation and this situation makes dispersion difficult.

2.3.3. Determination of Agitation Speeds for Emulsification

Determination of the speeds required for emulsification process is one the most important steps of emulsion production procedure. Some conditions should be considered for appropriate speed selection for the system. Movement of oil in the system should be observed for determination the speed limit at which mixing can be performed. When oil and water begin to be mixed, the speed at which the first oil drop enters the water phase is called oil entrainment speed (N_{JD1}) and the speed at which the oil phase can completely mix with the water phase is called oil mixing speed (N_{JD2}). For emulsion formation, the oil phase must be completely dispersed in the water phase. This means that the oil mixing speed determines the lower speed limit at which emulsification is to be carried out. Therefore, agitation speeds should be higher than N_{JD2}.

Another important factor that should be considered in order to determine emulsification speeds is the air entrainment to the system. The lowest speed at which air bubbles enter and remain in the system is called air entrainment speed (N_E) (Bhattacharya et al., 2007). Air entrainment causes foam formation and the inclusion of a new phase in the system may affect the results; therefore, agitation should be performed below this speed.

To determine agitation speed limits, experiments were carried out in the previously specified experimental set-up using all determined impellers. 30% silicon oil and 70% distilled water were placed into the tank at a height equal to the inner tank diameter. The agitation speed was gradually increased to determine N_{JD1}. After determination the oil entrainment speed, agitation speed was increased with smaller increments. Ten minutes after each increment, the system was observed to determine N_{JD2}. The agitation speed was continued to be increased and to determine the air entrainment speed.

Table 2.4 shows N_{JD1}, N_{JD2} and N_E for all configurations. When small impellers are used for emulsification, higher agitation speeds are required for complete dispersion of oil phase within the water phase compared to the large impellers. Since air entrainment also occurs at higher agitation speeds with small impellers, it is possible to produce emulsions at higher speeds. By this way, turbulence intensity within the system can be increased. When RT and PBTD impellers are compared, it was found that the required agitation speeds for PBTD T/3 are higher than RT T/3; however, required agitation speeds for RT T/2 are higher than PBTD T/2 impellers for complete oil dispersion within the water phase. Therefore, the highest agitation speeds are needed when PBTD T/3 impeller is used. These results are valid both when the shaft is positioned at the center and away from the center. In the experiments conducted with RT impellers in unbaffled tanks with centered shaft, as the agitation speed was increased, the oil phase began to disperse into the water phase by the angular rotation due to absence of axial flow, so the oil entrainment speed could not be observed. This speed could be determined when the shaft was at eccentric position. As the eccentricity

increased, air entrainment speed decreased when the large impellers were used. On the other hand, increase in eccentricity affected air entrainment speed differently when the small impellers were used. In the usage of small impellers, the lowest air entrainment speeds occurred at e/T=0.1 compared with e/T=0 and e/T=0.2. These results were caused by different hydrodynamic conditions within the tanks and their effect on the formed emulsion drops was discussed in detail in the Results and Discussions Part.

Table 2.4. *The speeds of oil entrainment, oil mixing and air entrainment for all impellers*

	e/T	N_{JD1} (rpm)	N_{JD2} (rpm)	N_E (rpm)
PBTD T/3	0	220	850	920
	0.1	190	430	780
	0.2	230	570	870
PBTD T/2	0	90	200	550
	0.1	110	160	430
	0.2	110	180	360
RT T/3	0	-	440	830
	0.1	180	340	670
	0.2	260	360	810
RT T/2	0	-	300	500
	0.1	90	260	380
	0.2	100	220	340

Apart from N_{JD1}, N_{JD2} and N_E, flow regime is also important to determine the emulsification speeds of the experiments. Turbulent regime is more effective for emulsification procedure in this study since the viscosity of the oil is low. The speeds required for emulsification for each impeller to provide emulsification in the turbulent regime were determined by impeller Reynolds number:

$$Re = \frac{\rho N D^2}{\mu} \tag{2.1}$$

In this equation, ρ represents the density of the liquid in the tank (kg/m^3), N is the agitation speed (rps), D is the impeller diameter (m), μ is the viscosity of the liquid (kg/m s). For the calculation of the emulsion viscosity, an equation modelled by Roscoe (1952) was utilized:

$$\eta_r = {}^{\mu_s}/_{\mu_c} = (1 - 1.35 * c)^{-2.5} \tag{2.2}$$

In this equation, η_r is the relative viscosity, μ_s is the viscosity of emulsion, μ_c is the viscosity of continuous phase and c is the volume fraction of the dispersed phase. This equation was modified from Einstein's viscosity equation to be valid for the dispersion of uniform spheres with high volume fraction. In this study the oil volume fraction is high at 30%, and formed emulsion drops are spherical; therefore, equation can be used in this study for calculation of emulsion viscosity. In this equation, the system is assumed as a unimodal suspension. According to this formula, glass beads and water are assumed as the continuous phase and oil drops are assumed as the dispersed phase. After calculation of emulsion viscosity, speed limits required for emulsion production in the turbulent regime were calculated using Equation 1. Reynolds number should be greater than 20 000 for the agitation to be carried out in the turbulent regime. Based on this, minimum speeds required for he agitation in the turbulent regime are given in Table 2.5.

Table 2.5. *Minimum agitation speeds required for turbulent regime*

Type of impeller	**N (rpm)**
PBTD (T/3)	1238
PBTD (T/2)	549
RT (T/3)	1238
RT (T/2)	549

To produce emulsions in turbulent regime, some air entrainment occurred due to vortex formation. However, this amount was neglected since it was more important to produce emulsions in turbulent regime. Premixing speeds were much lower than the emulsification speeds because there would be much more air entrainment if the premixing speeds were the same with emulsification speeds.

2.3.4. Determination of Premixing Time

After particles and water are added into the tank, the mixture should be stirred to break up particle aggregation and disperse particles to entire tank volume. An experiment was carried out to determine the time required for dispersion of particles. According to the drop size of the produced emulsions with premixing time of 10 min and 30 min, increase in premixing time causes increase in drop size as can be seen in Figure 2.10. Therefore, it was decided that premixing would be done for 10 min.

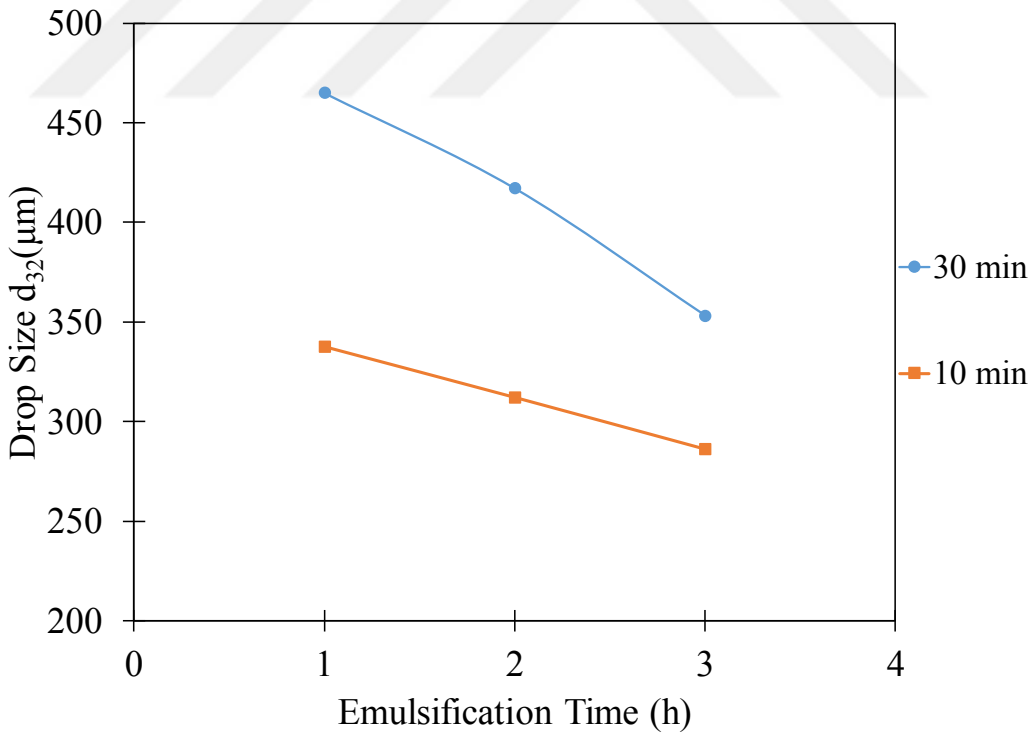

Figure 2.10. The effect of premix time on drop size

2.3.5. Determination of Emulsification Time

To determine required time for emulsification, some experiments were performed. The time required for emulsion drops to reach an equilibrium size for all configurations was determined and general emulsification procedure was obtained. The experiments were performed at 755 rpm for T/2 impellers and at 1393 for T/3 impellers. After every hour samples were taken from the tanks for 6 hours and analyzed with Malvern Mastersizer 3000. Figure 2.11 and Figure 2.12 shows the effect of emulsification time on drop size of Pickering emulsions. According to these two graphs, it can be said that at end of 3 hours, emulsion drops almost reached equilibrium size. Therefore, emulsification time was decided as 3 hours for all experiments.

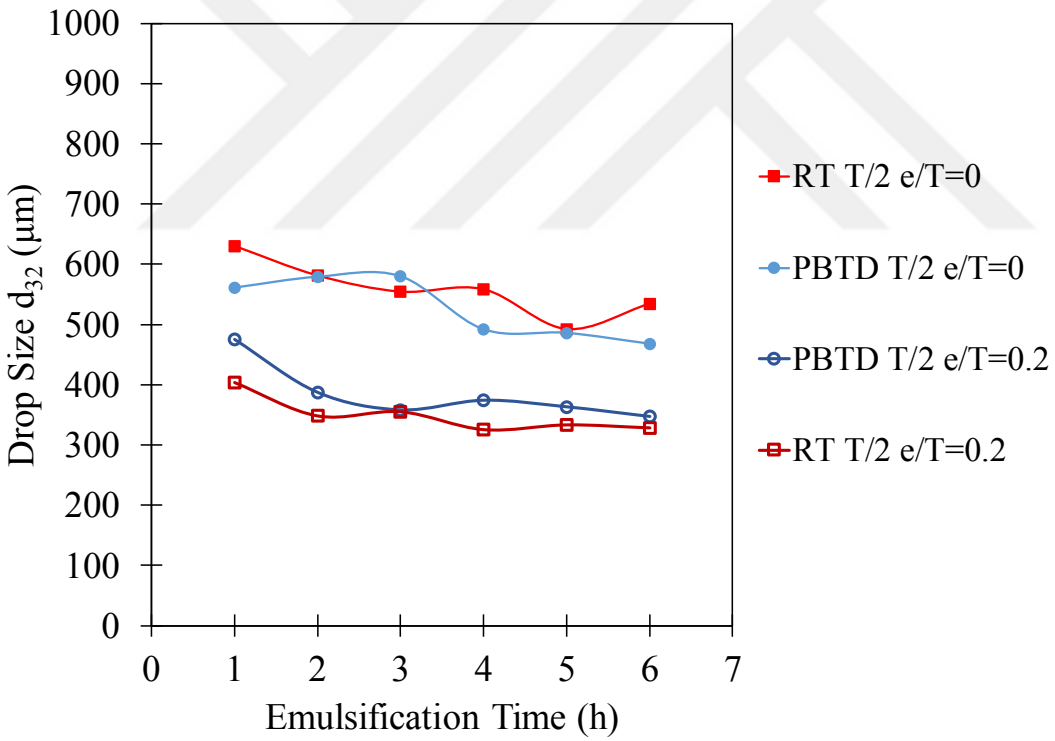

Figure 2.11. The effect of emulsification time on drops size for large impellers

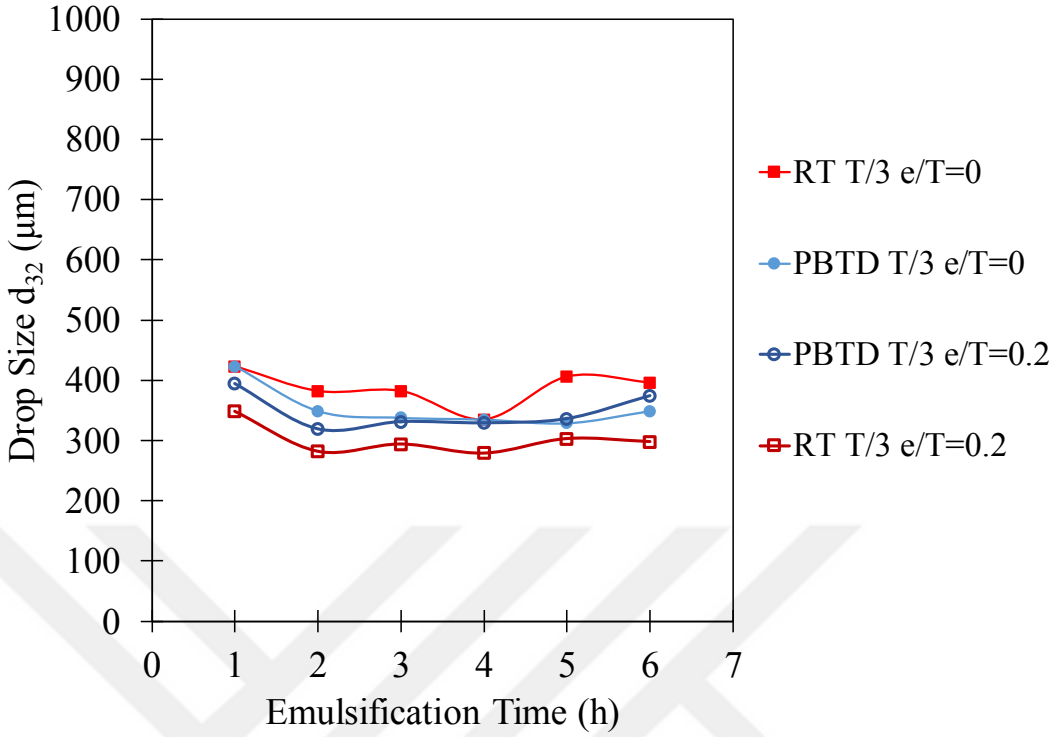

Figure 2.12. The effect of emulsification time on drops size for small impellers

2.4. General Procedure of Emulsification Experiments

In all experiments, firstly, 100 g solid glass beads (48% (w/w) particle/oil ratio) were put into the tank. After particle adding, impeller and shaft were positioned. Appropriate amount of distilled water was added to the tank so that the oil to water ratio was 30%. Based on this ratio, 532 ml distilled water and 230 ml silicon oil were used in every experiment. Particle-water mixture was stirred for 10 min for premixing process. For the large impellers, premixing speed was 350 rpm and for the small impellers, premixing speed was 800 rpm. After premixing completed, while motor was still on, silicon oil was added quickly to particle-water mixture and the agitation speed was increased to desired emulsification speed. At the end of 3 hours mixing, samples were taken into 2 vials by pipette from the tank while motor was still on in order to better representation of the emulsion in the tank. By this way, the smallest

and the largest drops could be taken from the tank. Samples were taken at the same point in the tank for all experiments: from just above the impellers in the vertical direction and from the middle distance between the left side of the shaft and the tank wall in the horizontal direction. Taken samples were waited for a while until the excess glass beads had settled to the bottom of the tank to prevent misleading of analysis. Analysis of emulsions was done on the same day. In this study, drop size and drop size distribution of the emulsions were analyzed with Malvern Mastersizer 3000 shown in Figure 2.13.

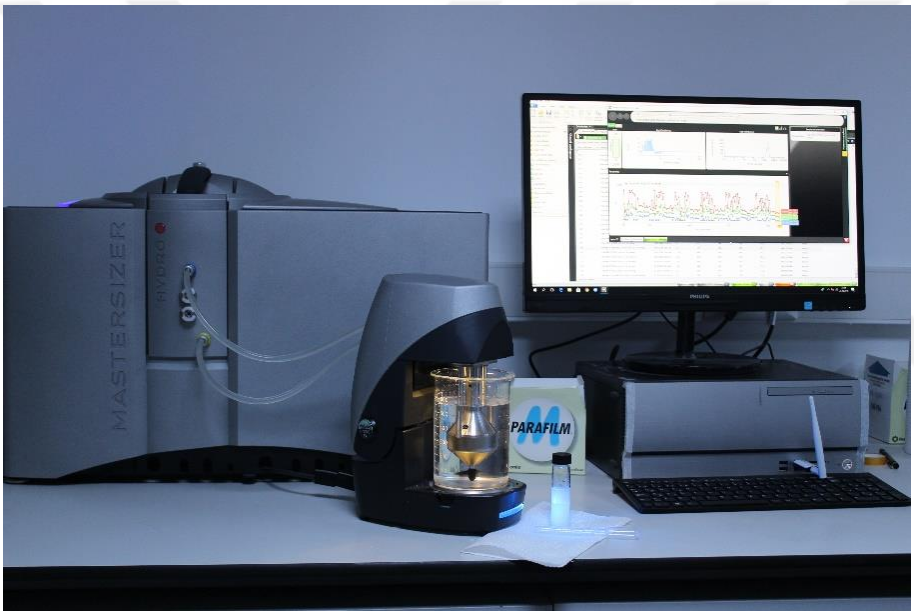

Figure 2.13. Malvern Mastersizer 3000

In the analysis of the sample, firstly, the name of sample was recorded in Malvern software. During analysis of the size and size distribution of glass beads, the type of particle was chosen as spherical and Mie scattering model was utilized. The average size of the glass beads was determined approximately 22 μm by the company. If the size of the particle is smaller than 50 μm and refractive and absorption indices of the

material and the dispersant are known, Mie scattering should be used to obtain true result. After the type of material and the type of dispersant were determined, their refractive and absorption indices were chosen from materials database included in the software. Glass (soda lime) was selected as material type and water was selected as dispersant type. The refractive index of glass beads is 1,513 and absorption index of glass beads is 0,1. The refractive index of water is 1,33. As a result of the analysis, average size of glass beads was found as 18.3 μm.

In the analysis of emulsion drops, the type of particle was chosen as opaque and Fraunhofer approximation was utilized. Therefore, optical properties of materials were not taken into consideration. Measurements were done with red light. Since the size of materials in this study was larger than 1 μm, the usage of only red light was sufficient, and the usage of blue light was not required. Measurement durations were arranged as 10 seconds for background measurement and 6 seconds for sample measurement. Ultrasound was not used to avoid possible drop breakup which would have mislead the results. The number of measurements was selected as 5. This means five measurements were performed per sample. One vial was analyzed two times, so 20 results were obtained for one tank. Obscuration range was arranged between 0.5% and 20% and sample was put into the wet dispersion unit via pipette until the amount was between in this range like in Figure 2.14.

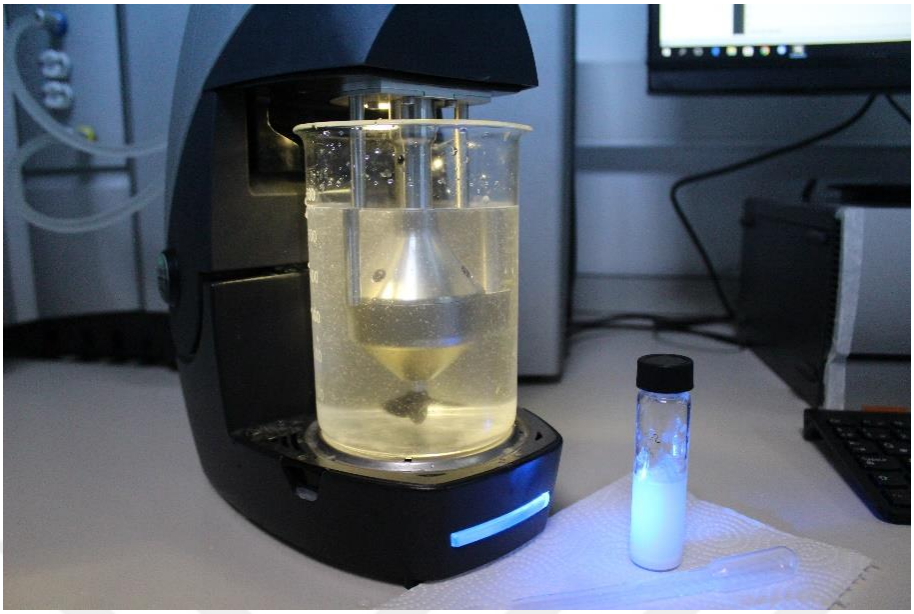

Figure 2.14. Sample in wet dispersion unit

The stirrer speed of the dispersion unit was arranged as 1050 rpm for all measurements from the accessory control settings. During determination of this speed, the case of drop breakup and adequate amount of sample vacuuming by the equipment were taken into consideration. For example, if higher stirrer speed was used, drop breakup would occur. On the other hand, if lower stirrer speed was used, sufficient amount of the sample would not be sent to inside of the equipment. Moreover, general purpose was selected for analysis model from the analysis settings. After all these settings, analysis was performed, and 20 results were obtained for one tank. Than average of these 20 results were calculated by Malvern program to obtain mean drop size of the sample. Mean drop size was represented as d_{32} called as Sauter mean diameter. All experiments were performed in twice to ensure repeatability of the experiments. As a result of the analysis of the samples, it was realized that samples contained excess glass beads although they were waited at least 2 hours. By particle size analysis of the glass beads it is known that the size of 99% glass beads is less than 60 microns. Based on this knowledge, a second analysis was carried out by assuming that drops smaller

than 60 microns actually represents glass beads and those were not taken into account. Emulsion drop size distribution is given in Figure 2.15. Moreover, microscopic image of formed emulsion drops is given in Figure 2.16. The graphs are plotted by averaging of particle eliminated 20 data of the main experiment and particle eliminated 20 data of the repeated experiment. Error bars are also given for each data on the graphs and they represent standard deviations. Top of the error bar and bottom of the error bar show the largest and the smallest drop size respectively. Drop size distribution graphs are also plotted using averaged data and the information of span that represents width of the distribution is also added as another graph into distribution graphs.

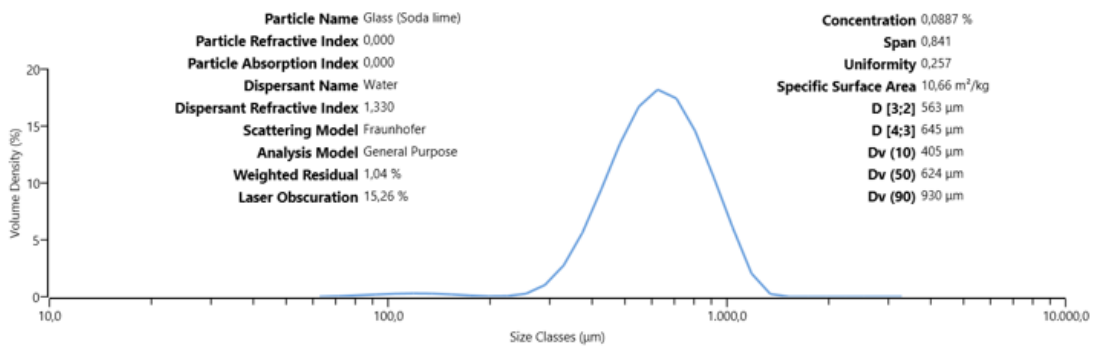

Figure 2.15. Emulsion drop size distribution

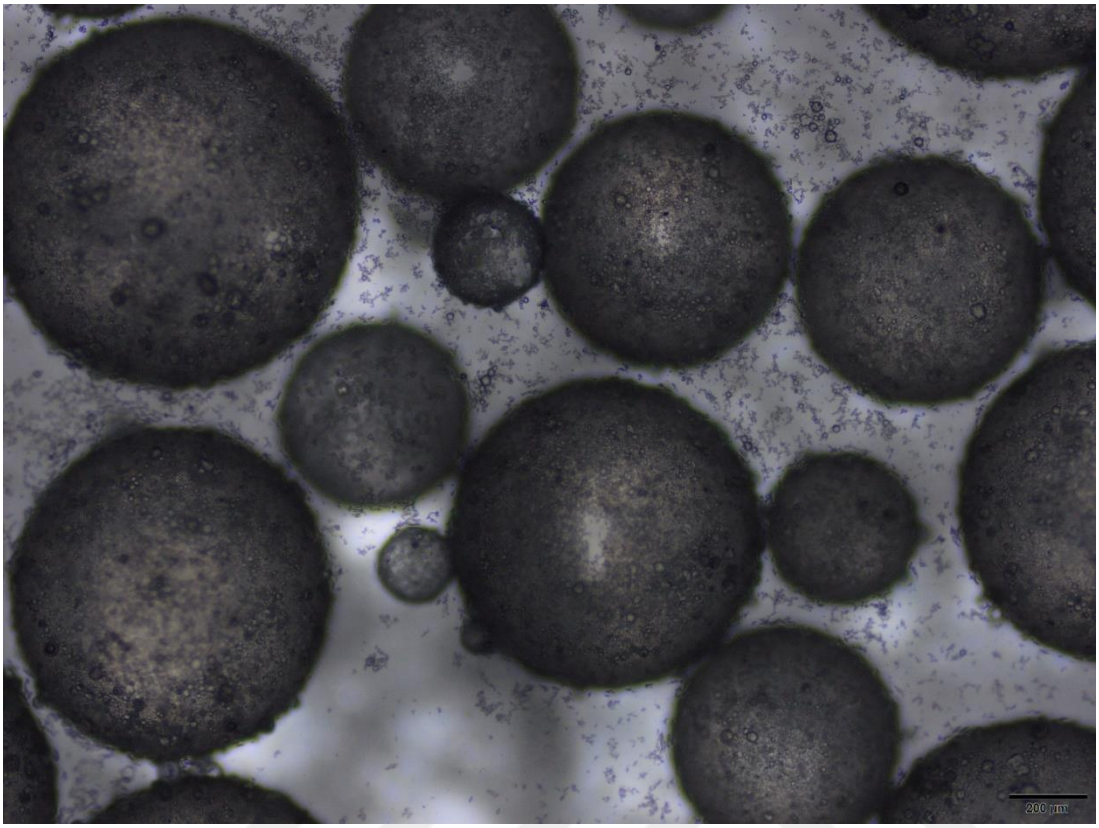

Figure 2.16. Microscopic image of Pickering emulsion drops

2.5. The Procedure of Mixing Time Experiments

The mixing time is the time taken to achieve a certain degree of homogeneity. This is an important parameter to understand mixing efficiency of different mixing geometries. By measuring mixing time, performance of different impellers in stirred tanks can be characterized. For determination of mixing time, various techniques can be used and decolorization technique was preferred in this study. In this method, mixing time was determined by chemical color change using two acid-base indicators and colorimetric diagnosis of digital images (Cabaret et al., 2007; Delaplace et al., 2004).

2.5.1. Materials and Method for Decolorization

For decolorization technique, fast acid-base reaction was performed. 10M hydrochloric acid (Merck) as acid and 10M sodium hydroxide (Merck) as base were selected to carry out the reaction. The bromocresol purple (Sigma Aldrich) (0.08% (w/w) bromocresol purple/water ratio) was used as indicator. This indicator gives yellow color when pH is lower than 5.2 (acid) and gives purple color when pH is higher than 6.8 (base).

The experiments were carried out by following the similar procedure of the study conducted by Cabaret et al. (2007). Based on this study, acid-base ratio should be higher than 2 in order to observe macromixing time within the tank correctly. Therefore, 1 ml of NaOH and 2 ml of HCI were used in the experiments. The change from purple color to yellow color was observed since analysis of change in dark color to light color is much easier. Firstly, 1 ml of NaOH was added to the tank and then 20 ml of bromocresol purple indicator was added. The mixture was agitated for some time to ensure that the dispersion of them was done homogenously within the tank. After homogenous dispersion, the color within the tank turns to purple. Later, the mixture of 2 ml of HCI and 3 ml of sample were added to the tank. The addition of the HCI and sample mixture was done due to the fact that the density difference between the emulsion within the tank and added sample would be small as much as possible. The addition point was same in all experiments to provide repeatability. It was done quickly over the liquid surface between the shaft and the tank wall. Color change from purple to yellow during the addition of the HCI and sample mixture to the tank was recorded with Canon EOS 100 D camera.

2.5.2. Method for Image Analysis

The videos were recorded 640*480 in size at 25 frames per second. Later they were split into the frames and converted to bitmap (bmp) format using VLC software shown in Figure 2.17.

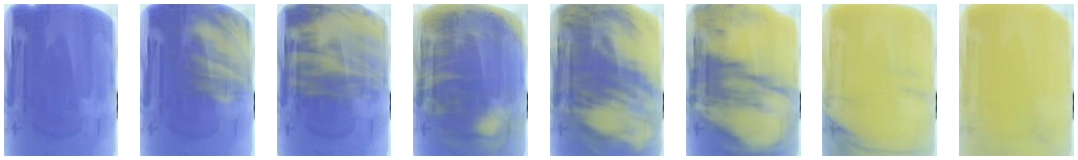

Figure 2.17. Frames of color change

For comparison of color change between the frames, RGB (red-green-blue) model was used. In the RGB model, a color can be represented by pure red, green and blue colors at levels ranging from 0 to 255. The RBG components of a pixel can be determined by converting the bmp images to the portable pixel map (ppm) format. A threshold value can be defined for RGB components to separate unmixed pixel from mixed pixel. From the literature, it is known that green component of RGB model and threshold value of 50% should be used for bromocresol purple (Cabaret et al., 2007). A pixel is accepted as mixed at a point where the green component of it exceeds the threshold value. A mixing graph is obtained by plotting time versus division of the number of mixed pixels (N_{mixed}) to the total number of pixels (N_{total}). In the study conducted by Cabaret et al. (2007), it was accepted that homogeneity within the tank is sufficient when the ratio of N_{mixed} to N_{total} called as mixedness is reached to 90%. In the experiments conducted with the light of this study, it was decided to take this value as 95%. Mixing time can be calculated by mixing graph. The difference between the time corresponding to the point at which 95% is reached and the time corresponding to the point at which the mixing started gives the mixing time as shown in Figure 2.18. A code was written to conduct this analysis automatically given in Appendix A.

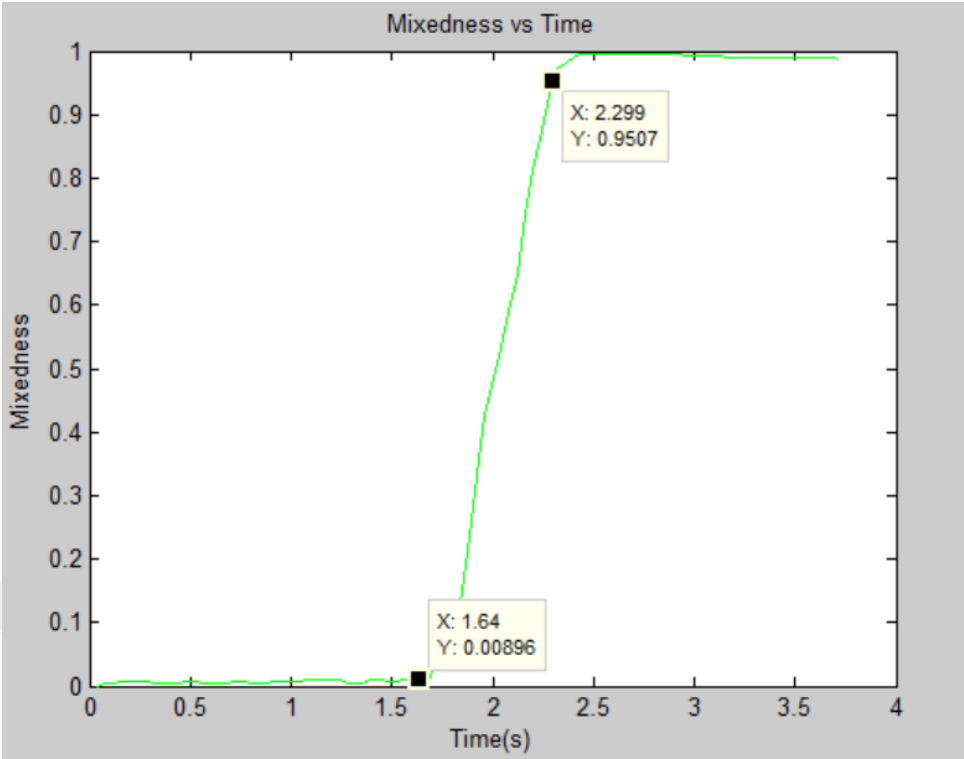

Figure 2.18. Mixing time graph

CHAPTER 3

RESULTS AND DISCUSSION

In this study, investigation of the effect of different hydrodynamic conditions on the production of Pickering emulsions in unbaffled stirred tanks was aimed. Physicochemical properties of the emulsions were kept constant. Hydrodynamic parameters such as impeller tip speed (V_{tip}), Reynolds number (Re), Weber number (We) and power per mass were changed to create different hydrodynamic conditions. Performances of two different types of impellers were compared: 45° down pumping Pitched Blade Turbine (PBTD) and Rushton Turbine (RT) at two different sizes to find optimum mixing geometry. Shaft position was also varied. Drop sizes of Pickering emulsions were analyzed to determine which type of impeller in which shaft position gives better performance. In this chapter, drop sizes and drop size distributions are given in terms of Sauter mean diameter (d_{32}).

3.1. Effect of Hydrodynamics on the Production of Pickering Emulsions in Unbaffled Stirred Tanks with Centered Shaft

3.1.1. Effect of Impeller Tip Speed

Impeller tip speed (V_{tip}) is the maximum speed that can be obtained at the end of the impeller blade. In this section, the effect of change in impeller tip speed on the emulsion drop size was investigated in unbaffled tanks with centered shaft. The formula of impeller tip speed is given below:

$$V_{tip} = \pi N D \tag{3.1}$$

Impeller tip speed depends on impeller diameter (D) and impeller speed (N), but not on the type of the impeller. In this study, impeller speeds were selected to ensure that

the flow regime was turbulent. At the same impeller tip speed, impeller speeds are the same for the impellers which have the same diameter. For the large impellers when the agitation was done above a certain impeller tip speed the liquid within the tank exceeded the tank height and overflowed. For the small impellers, on the other hand, when the agitation was performed below a certain impeller tip speed, mixing could not be done in turbulent regime. The impeller tip speeds were selected considering all these limitations. The selected impeller tip speeds and corresponding impeller speeds are given in Table 3.1. Only one common impeller tip speed could be determined for T/2 and T/3 impellers: 132 m/min. The values in Table 3.1 were also used when the shaft is off-centered.

Table 3.1. *Selected Vtip values and corresponding impeller speeds*

V_{tip} (m/min)	**N (rpm) T/2 impellers**	**N (rpm) T/3 impellers**
98	645	
115	755	
132	865	1300
141		1393
151		1496

Figure 3.1 shows the results. Increase in impeller tip speed leads to a continuous decrease in drop size for the large impellers. This is expected because increase in impeller tip speed means increase in impeller speed and this results in increase in the amount of energy dissipated into the system. When more energy is dissipated into the system, drop breakup becomes easier and smaller drops are formed. Among the large impellers it is seen that PBTD gives smaller drops than RT. When the small impellers are used, with RT the drop size decreases with increasing tip speed. With PBTD T/3,

the drop size increases for the middle V_{tip}, but decreases after that. When the small impellers are compared, it can be seen that RT T/3 produces smaller drops than PBTD T/3.

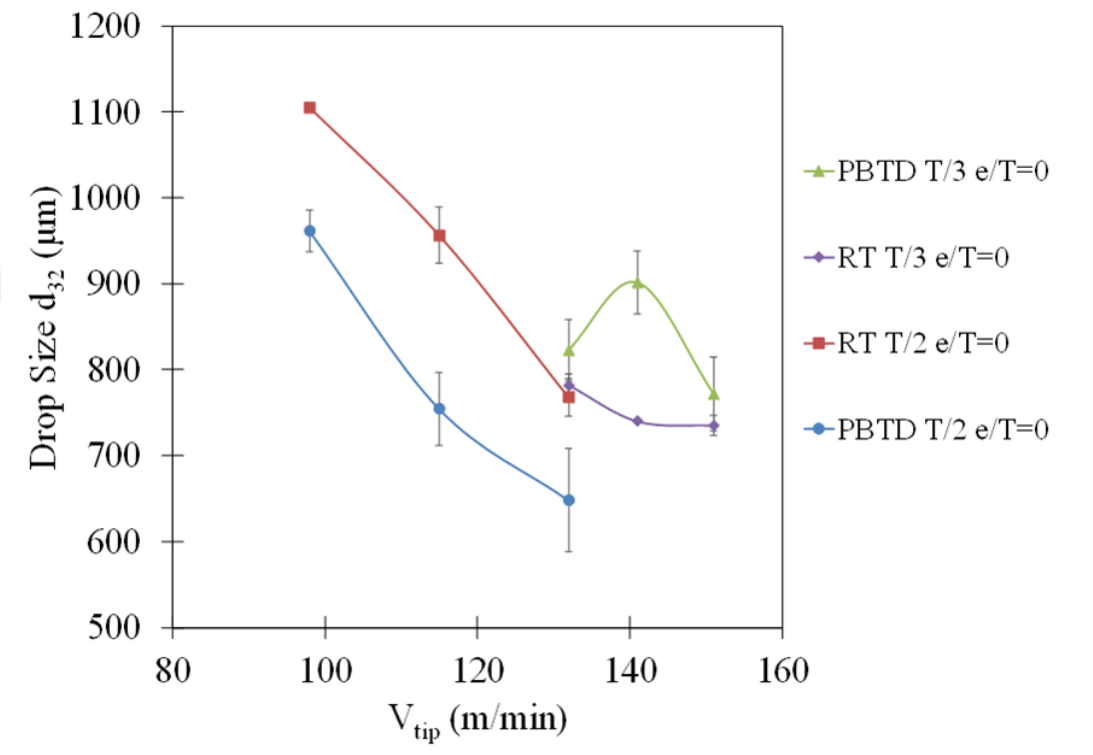

Figure 3.1. The effect of impeller tip speed on drop size

For better understanding of differences in performances of different impellers, comparison should be done at the same impeller tip speed. Experiments could be performed at only one common impeller tip speed for all impellers: 132 m/min. As shown in Figure 3.1, the smallest drop size is obtained with PBTD T/2 impeller. RT T/2 and T/3 impellers give similar drop sizes. PBTD T/3 impeller yields slightly larger drops. The difference between the large and the small PBTD is based on the sizes of the impeller and coalescence zones.

The data for RT T/3 seems almost like a continuation of the data for RT T/2. At 132 m/min the data for the two impellers overlap nicely. This indicates that tip speed is the determining factor for drop size for this impeller. RT is known as a high shear impeller. The drops are sheared and broken into smaller drops, until reaching equilibrium, around the impeller. While the energy dissipations are different for the two sizes of this impeller at the same V_{tip}, similar drop sizes indicate that the hydrodynamics in the absence of baffles and presence of a large central vortex removes the energy dissipation as a factor for final drop size. PBTD, on the other hand, is a flow impeller. The larger impeller creates better flow, allowing for a better circulation throughout the tank compared to the PBTD T/3. Therefore, the drops formed with PBTD T/2 do not necessarily spend extensive time in the coalescence zone.

Drop breakup occurs mostly in the regions close to the impeller because shear and dissipated energy are higher in the impeller zone. Drop coalescence takes place near the tank wall or the liquid surface (Tsabet and Fradette, 2015a, b). With the large impeller the impeller zone is larger and coalescence zone is smaller; therefore, smaller drops are formed with the large impeller. However, coalescence zone is larger for the small impellers, so bigger drops are produced.

In a baffled tank with no vortex, it would be expected to have smaller drops with the shear intensive impeller, RT T/2, compared to PBTD T/2 (Abdulrasaq and Ayranci, 2019). However, as seen in Figure 3.1, at the same impeller tip speed, PBTD T/2 gives smaller drops than RT T/2. This can be attributed to the shape of vortex. In unbaffled stirred tanks with centered shaft, vortex is formed on the free surface at the center of the tank and gets larger as the impeller tip speed increases. Similar observation has been also obtained from the study performed in a unbaffled stirred tank with concave type impeller. According to this study, vortex depth increases with the increase in impeller speed (Devi and Kumar, 2017). Formed vortices for the large impellers at the same impeller tip speed are shown in Figure 3.2. Vortex formation in water filled tanks are photographed for a better view of the vortices. As seen in these photographs,

vortices reach the impeller blades and air entrainment occurs because experiments are performed in the turbulent regime and required impeller speeds exceeded the air entrainment speed limits. An air cavity is formed under the impeller. Similar observations have been also found in studies conducted by Assirelli et al. (2008) and Scargiali et al. (2013). They have studied the flow with RT T/3 impeller in an unbaffled, only water filled stirred tank and observed that increase in impeller speed causes increase in the depth of vortex and formation of air cavity below the impeller. The amount of air entrainment is smaller in Pickering emulsions than in these photographs because the presence of oil and glass beads within the tanks affects the flow regime and air entrainment occurs at higher impeller speeds. Therefore, the size of formed vortex and air cavity under the impeller are much smaller compared with water filled tank at the same impeller speed. When impeller tip speed is 132 m/min, most part of the impeller remains in the vortex. Decrease in contact of impeller blades with the liquid reduces the effect of shear (Francesca Scargiali et al., 2013). The size of the formed vortex is much larger when RT T/2 impeller is used. Formed air cavity under the impeller is also much bigger for the RT T/2. Hemrajani and Tatterson (2004) reported that as the size of the PBTD impeller increases, the radial component of PBTD becomes dominant and the flow patterns of RT and PBTD impellers become similar. Even if they have similar flow patterns, PBTD impeller is in contact with the liquid more. Therefore, at the same impeller tip speed, formed drops with PBTD T/2 are smaller than formed drops with RT T/2 when they are at the center of the tank.

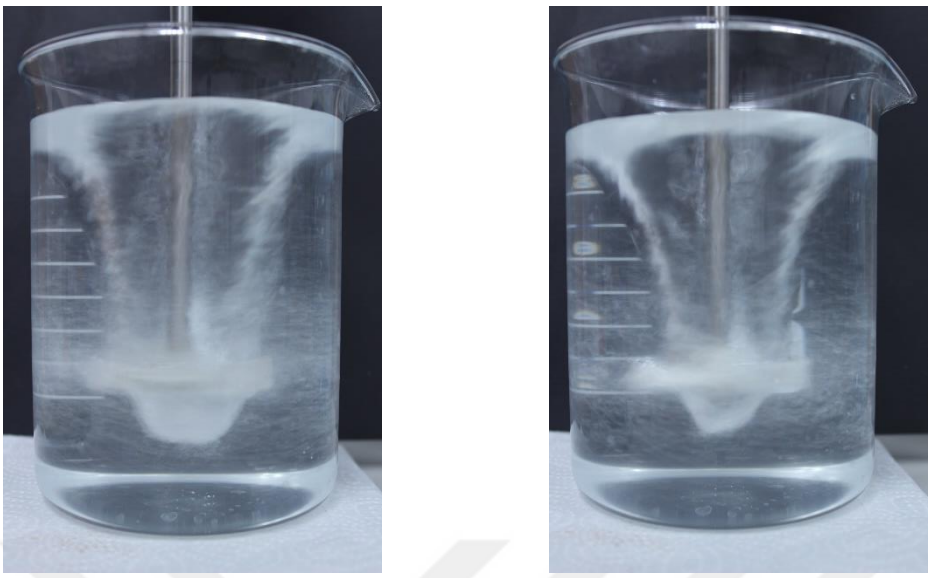

a) RT T/2 b) PBTD T/2

Figure 3.2. Formed vortices at the same impeller tip speed (132 m/min) for the large impellers

At the same impeller tip speed, RT T/3 gives smaller drops than PBTD T/3. Formed vortices for the small impellers at the same impeller tip speed are shown in Figure 3.3. Even if the formed vortex size is larger with RT T/3 impeller and contact of impeller blades with liquid decreases, smaller drops are produced because the system is exposed to more shear. RT impeller is known as a high shear impeller, so more shear is created within the system. Since there is more space in the tank for coalescence compared to large impellers, shear capacity of an impeller has more effect on drop size when small impellers are used. Also, at the same impeller speed, RT impeller gives more energy to the system compared to the PBTD impeller due to having higher power number. The PBTD does not create much shear at this small size, it cannot form sufficient flow like it did at the larger size, and it does not provide large energy to the system. As a result, at the smaller impeller size, the advantage of produced flow with the large PBTD disappears, and smaller drops are produced with the RT impeller.

a) RT T/3 b) PBTD T/3

Figure 3.3. Formed vortices at the same impeller tip speed (132 m/min) for the small impellers

Figure 3.4 shows drop size distribution of all impellers at the same impeller tip speed, 132 m/min. When obtained drop size decreases, drop size distribution becomes narrower. The impeller that produces the smallest drop size, PBTD T/2, has also the narrowest drop size distribution. Even though the average drop sizes obtained with RT T/2 and RT T/3 are very close, RT T/2 has narrower drop size distribution than RT T/3. Based on these results, it can be concluded that larger impellers produce not only smaller drops but also narrower drop size distribution than small impellers at the same impeller tip speed.

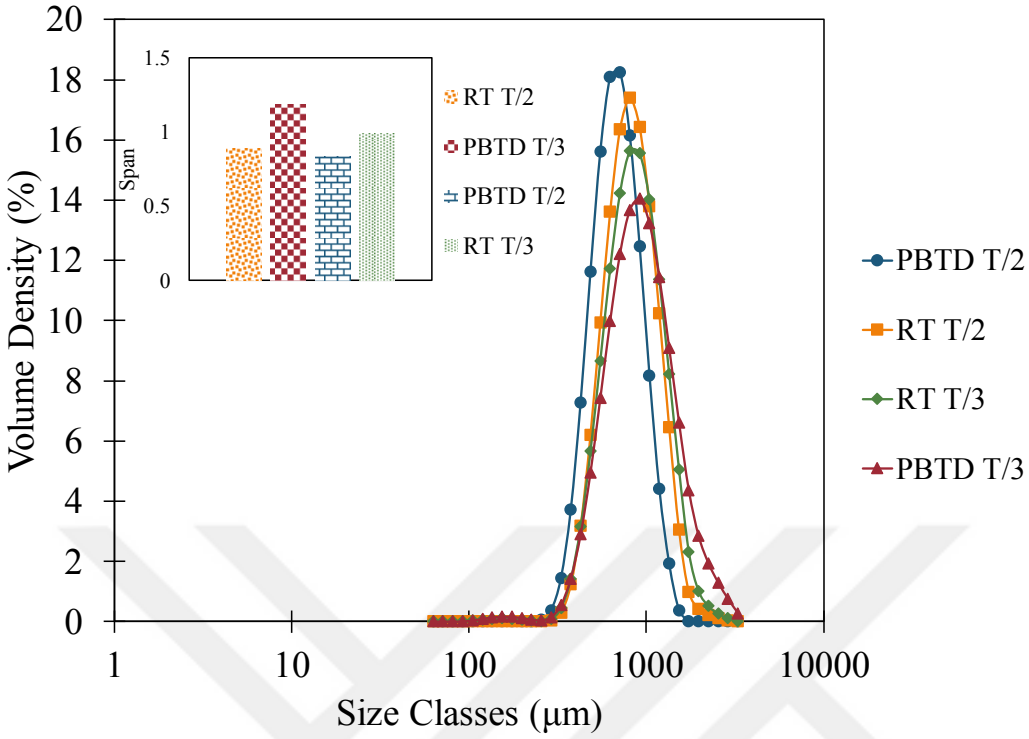

Figure 3.4. Drop size distribution of all impellers at the same impeller tip speed: 132 m/min

3.1.2. Effect of Impeller Reynolds Number

Impeller Reynolds number is another important design parameter in a stirred tank. Reynolds number is an indicator of the flow regime in the tank. When Reynolds number is greater than 20 000, agitation is carried out in turbulent regime. In this thesis, emulsification is performed in turbulent regime to provide effective agitation. Reynolds number is expressed with the following relation:

$$Re = \frac{ND^2\rho}{\mu} \tag{3.2}$$

N represents the impeller speed (rps), D represents the impeller diameter (m), ρ and μ are density (kg/m^3) and viscosity (kg/m s) respectively. At the same Reynolds number,

the impeller speeds are the same for the same size impellers if they are used to agitate the same liquid. In Table 3.2 the selected Reynolds numbers and corresponding impeller speeds are given. In selection of these speeds, fluid overflow and operation in turbulent regime were considered.

Table 3.2. *Selected Reynolds numbers and corresponding impeller speeds*

Reynolds number	**N (rpm) T/2 impellers**	**N (rpm) T/3 impellers**
22 000	605	1360
26 000	715	1610
30 000	825	1855

In Figure 3.5, the effect of Reynolds number on drop size with different impellers is shown. For the large impellers, when Reynolds number increases, average drop size decreases. This is expected, since turbulence intensity and energy dissipation within the system increases as Reynolds number increases. Thus, drop breakup becomes easier and smaller drops are produced. When Reynolds numbers are 22 000 and 26 000, the central vortex does not reach the impeller, so the impeller blades are in contact with the liquid. Since RT is high shear impeller, it would be expected of RT to produce smaller drops. However, at these Reynolds numbers, RT T/2 and PBTD T/2 give almost the same size drops. According to the studies, performed in baffled tanks with T/2 and T/3 PBT impellers, it has been found that the radial component of the impeller discharge becomes dominant when T/2 impeller is used (Jaworski et al., 2001; Özcan-Taşkin and Wei, 2011). Haque et al. (2006) modelled turbulent flows for RT T/2 impeller at T/3 off-bottom clearance with free surface in unbaffled stirred tanks. They

modeled the flow pattern of the impeller for the case where the vortex does not reach the impeller. The result of this study indicates that the flow pattern includes two loops one above and one below the impeller similar to flow pattern of RT impeller in baffled tanks. However, they also found that RT impeller in a unbaffled tank forms a radial flow with downward inclination. Based on these results, in a unbaffled tank the flow fields produced by RT and PBTD are similar when the vortex does not reach the impeller, and this causes producing similar size drops.

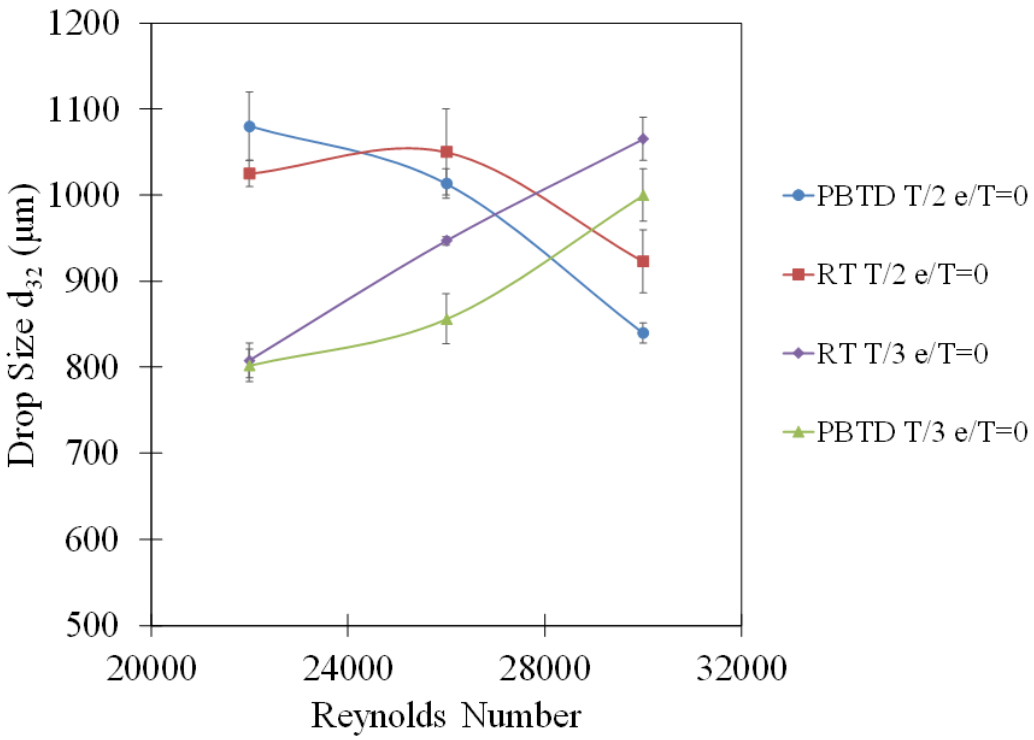

Figure 3.5. The effect of Reynolds number on drop size

When Reynolds number increases, PBTD T/2 yields slightly smaller drops than RT T/2. This is related to the size of formed central vortex. When Reynolds number increases, formed vortex at free surface gets larger and reaches the impeller blades. This prevents the contact of the impeller with the liquid in full and causes a decrease

in the transfer of shear to the system. At the same Reynolds number, the size of formed vortex and air cavity under the impeller are larger for RT T/2 compared to PBTD T/2. Therefore, shear capacity of RT impeller cannot be transferred to the system completely.

Pumping capacity of impellers can affect the drop size. Impeller flow number depends on the type of the impeller and represents pumping capacity of an impeller. Impeller flow number of PBTD is higher than Rushton turbine (Hemrajani and Tatterson, 2004; Grenville et al., 2017). This means PBTD impeller has better pumping capacity than RT impeller. Therefore, better particle dispersion occurs when PBTD is used. Better particle dispersion can make surface coverage better and result in formation of smaller drops.

Circulation time can be another reason of the production of smaller drops with PBTD. Circulation time is the time between discharge of the impeller leaving the impeller and coming back to impeller zone. It is expressed by the following relation (Leng and Calabrese, 2004):

$$t_{circ} = \frac{V_{tank}}{N_q \times D^3 \times N} \tag{3.3}$$

In this relation, t_{circ} represents the mean circulation time, N_q is the impeller flow number, N and D are impeller speed and impeller diameter respectively. At the same impeller speed, PBTD impeller has larger N_q and therefore smaller circulation time than RT impeller when their sizes are equal. Therefore, drops come back to impeller zone more quickly and are exposed to shear more frequently. This case results in formation of smaller drops.

For the small impellers, when Reynolds number increases, average drop size increases. At the same Reynolds number, impeller speeds are higher for the small impellers and more energy is dissipated into the system. Turbulence fluctuations are also larger. Increase in turbulence fluctuations leads to increase in collision frequency of drops (Coulaloglou and Tavlarides, 1977; Tsabet and Fradette, 2015a). Particle

detachment from the interface occurs due to collisions. Drop collisions also cause decrease in film drainage and increase in film rupture (Chesters, 1991). According to Tsabet and Fradette (2015b), when the surface of the drops is not covered completely, they come together and form larger drops.

At the lowest Reynolds number RT T/3 and PBTD T/3 give the same size drops. The shear capacity RT impeller at low Reynolds number can be compensated by the pumping capacity of PBTD impeller. As Reynolds number increases, PBTD T/3 gives smaller drops than RT T/3. Formation of central vortex prevents contact of the impellers with the emulsion system. Even if formed shear by RT impeller is higher, it cannot be transferred to the system completely due to presence of central vortex. Since circulation time of PBTD impeller is smaller, drops come to the impeller zone more quickly and spend more time in the impeller zone. Drop breakup occurs mostly in the impeller zone, so PBTD impeller creates smaller drops compared to RT impeller. In the overall, however, drop collisions begin to dominate over drop breakup as seen by the increasing drop size trend.

Figure 3.5 shows that at the lower Reynolds numbers the small impellers give smaller drops than the large impellers. At the same Reynolds number, impeller speeds are higher for the small impellers. Operating at higher impeller speeds causes increase in the energy dissipated into the system and therefore, increase in turbulence fluctuations. This brings about formation of smaller drops. However, as Reynolds number continues to increase, there is an increase in drop collisions and particle detachment occurs. This situation leads to drop coalescence. With the small impellers at the highest two Reynolds numbers, the impeller speeds are so high that drop coalescence dominates over drop breakup. Large impellers, however, over the full range of Reynolds numbers tested have moderate-high impeller speeds that drop breakup can still dominate and yield smaller drops.

Figure 3.6 shows the drop size distribution of all impellers at Reynolds number 22000. A little bit narrower drop size distribution is obtained with PBTD at both sizes than RT. This can be attributed to better particle dispersion property of PBTD impellers.

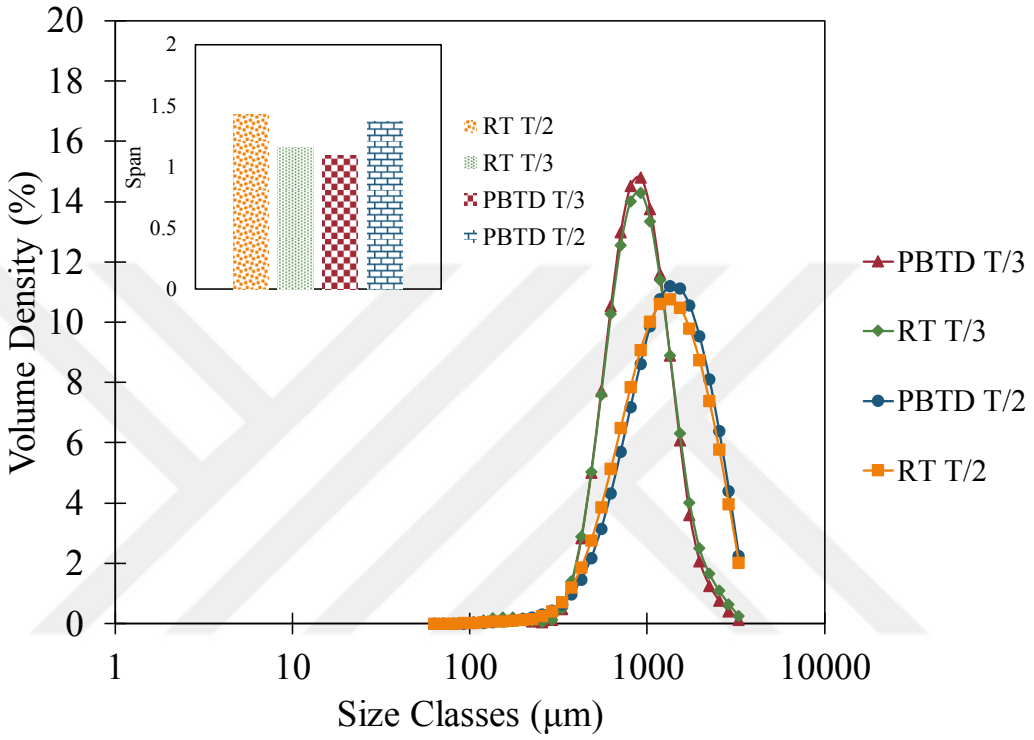

Figure 3.6. Drop size distribution of all impellers at Reynolds number 22 000

Figure 3.7 shows that the drops size distribution of all impellers at Reynolds number 30000. Narrowest drop size distribution is obtained with PBTD T/2. PBTD T/2 also gives smaller drop size. The rest of the distributions are very close to each other, even though there are variations in drop sizes. However, even if RT T/2 produces smaller drops than RT T/3, drops size distribution obtained by RT impellers are almost the same.

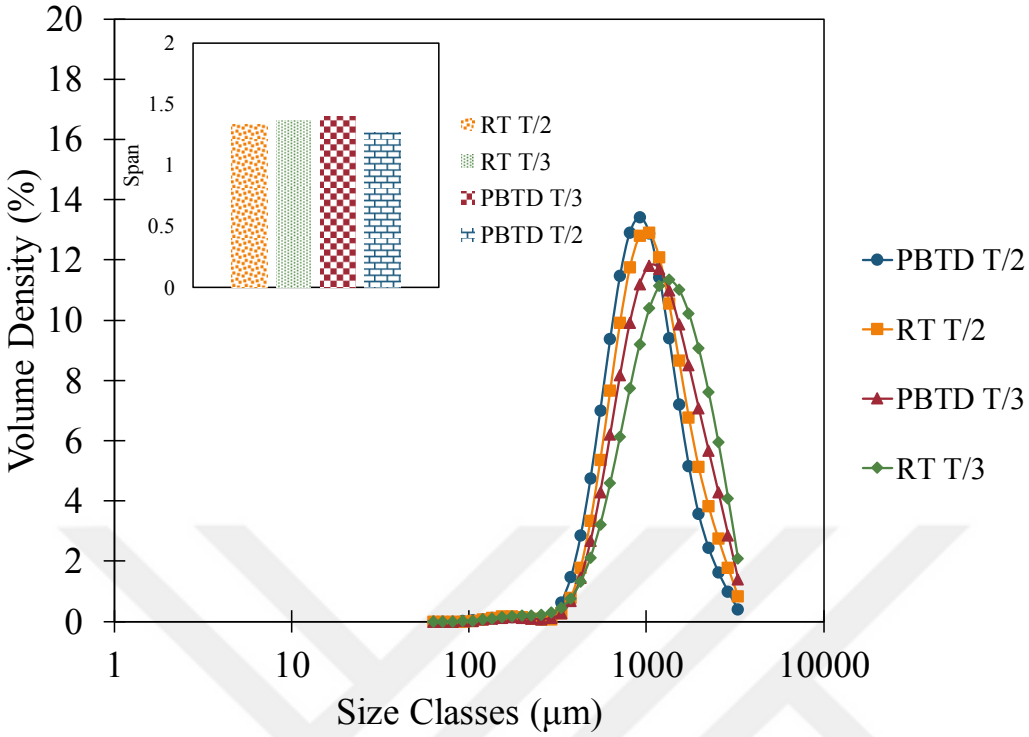

Figure 3.7. Drop size distribution of all impellers at Reynolds number 30000

3.1.3. Effect of Weber Number

The interfacial tension between the phases of an emulsion is an important factor that affects the drop size. Since Weber number is a parameter associated with the interfacial tension, the effect of change in Weber number on Pickering emulsion formation was investigated. Weber number is defined as:

$$We = \frac{\rho_c N^2 D^3}{\sigma} \tag{3.4}$$

Here, ρ_c refers to the density of the continuous phase (kg/m^3), N is the impeller speed (rps), D is the impeller diameter (m), and σ is the interfacial tension (N/m). In calculation of the density of the continuous phase, the amount and density of the continuous phase, distilled water, and the glass beads were taken into account:

$$\rho_c = \frac{m_w + m_p}{m_w/\rho_w + m_p/\rho_p} \tag{3.5}$$

Here, m_w and m_p represent the mass of water and the mass of particles respectively. ρ_w is the water density and ρ_p is the particle density. In determining the Weber number values for testing, overflow and turbulent regime were considered as was the case for the other hydrodynamic parameters. In Table 3.3 selected Weber numbers and corresponding impeller speeds are given.

Table 3.3. Selected Weber numbers and corresponding impeller speeds

Weber Number	N (rpm) T/2 impellers	N (rpm) T/3 impellers
350	774	1425
400	828	1523
450	878	1615

Figure 3.8 shows that for the large impellers, increase in Weber number causes decrease in drop size of the emulsions. Impeller speed increases as the Weber number increases and more energy is dissipated into the system. This brings about increase in drop breakup and formation of smaller drops. At low Weber numbers, RT T/2 and PBTD T/2 produce almost the same size drops. This means that at low Weber numbers, the type of impeller does not affect the drop size. Shear capacity of RT impeller can be compensated by pumping capacity of PBTD impeller at low Weber numbers. The system is exposed to more shear when RT impeller is used. Therefore, formation of smaller drops would be expected. However, particle dispersion is better when PBTD impeller is used because flow number of PBTD is higher than flow number of RT impeller. Better particle dispersion enables the coverage of newly formed drops and allows the formation of smaller drops. PBTD impeller is known as

mixed flow impeller that means its flow pattern includes axial and radial components. However, radial component of flow pattern created by PBTD T/2 is dominant. Also, flow pattern created by RT T/2 has a downward inclination. Thus, RT T/2 and PBTD T/2 create similar flow patterns in the tank. Therefore, the sizes of drops generated by RT T/2 and PBTD T/2 impellers are almost the same.

PBTD T/2 produces smaller drops than RT T/2 at the largest Weber number. Formed vortex at free surface, gets larger as the impeller speed increases. Impeller blades remain in the vortex and shear generated by the impellers cannot be transferred into the system effectively. In this case, how long the drops remain in the impeller zone plays an important role in determination of the drops size. Since the circulation time of PBTD impeller is smaller than the circulation time of RT impeller, drops come to impeller zone more frequently and spend more time in the impeller zone. Drops in the impeller zone are exposed to more shear, and this results in formation of smaller drops.

At low Weber numbers, PBTD T/3 and RT T/3 produce almost the same size drops. Again, at low Weber numbers the type of impeller does not affect the drop size even if the size of impellers is changed. The drop size obtained by RT T/3 increases as Weber number increases. The increase in Weber number means an increase in the amount of energy dissipated into the system due to an increase in the impeller speed. At high impeller speeds, drop collisions lead to particle detachment from the interface. Coalescence takes place due to partial surface coverage of newly formed drops. The decrease in effectively covered interface due to drop collisions at high Weber numbers is also observed in the study conducted by Tsabet and Fradette (2015a). However, even if the dissipated energy into the system increases, smaller drops are produced with PBTD T/3 as Weber number increases. According to Tsabet and Fradette (2016), after initial particle adsorption, slow adsorption occurs, so reaching the final drop size takes time. Since the circulation time of PBTD is smaller than the circulation time of RT impeller, drops come to the impeller zone more quickly and are exposed to more shear. Therefore, it would be expected that increase in drop size would occur as Weber number increases due to smaller adsorption time. However, the opposite result was

obtained in this study. This is attributed to the better particle dispersion property of PBTD impeller. The presence of better particle dispersion within the system provides better surface coverage before coalescence takes place.

In Figure 3.8, it is seen that the size of the impeller does not have much effect on drop size at the highest Weber number. For the small impellers, the amount of energy dissipated into the system is larger than the large impellers. For the large impellers, impeller zone is larger than the small impellers. The effect of having higher energy dissipation with the small impellers is compensated with the effect of larger impeller zone of the large impellers. Therefore, RT T/2 gives similar size drops with RT T/3 and PBTD T/2 gives similar size drops with PBTD T/3. Among the impellers, PBTD produces smaller drops than RT due to better particle dispersion property. At low Weber numbers, formed vortex does not cover completely the impeller and it is seen that the energy dissipated into the system is more effective than the size of impeller zone in producing smaller drops.

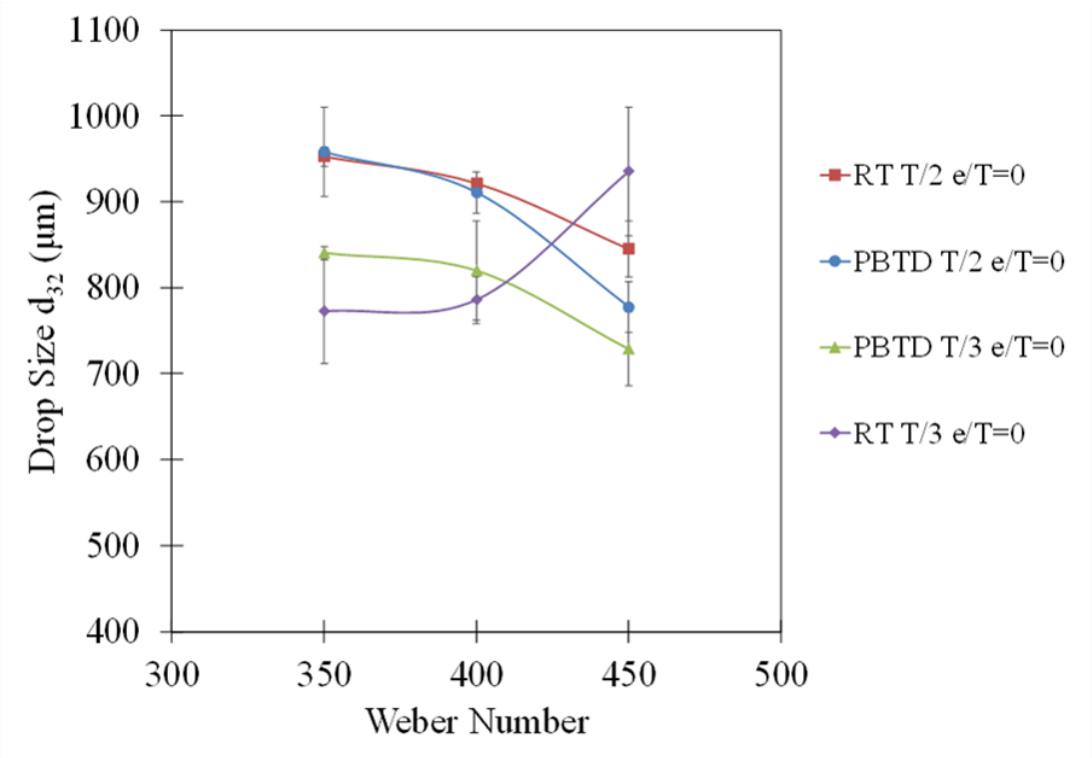

Figure 3.8. The effect of Weber number on drop size

Figure 3.9 shows the drops size distribution of all impellers at Weber number 350. At low Weber number, the drop size is affected by the size of the impellers rather than the type of the impellers. The small impellers give smaller drops at low Weber number, but their drop size distribution is wider. This is an indication of the importance of the impeller zone because narrower drops size distribution is obtained with the large impellers.

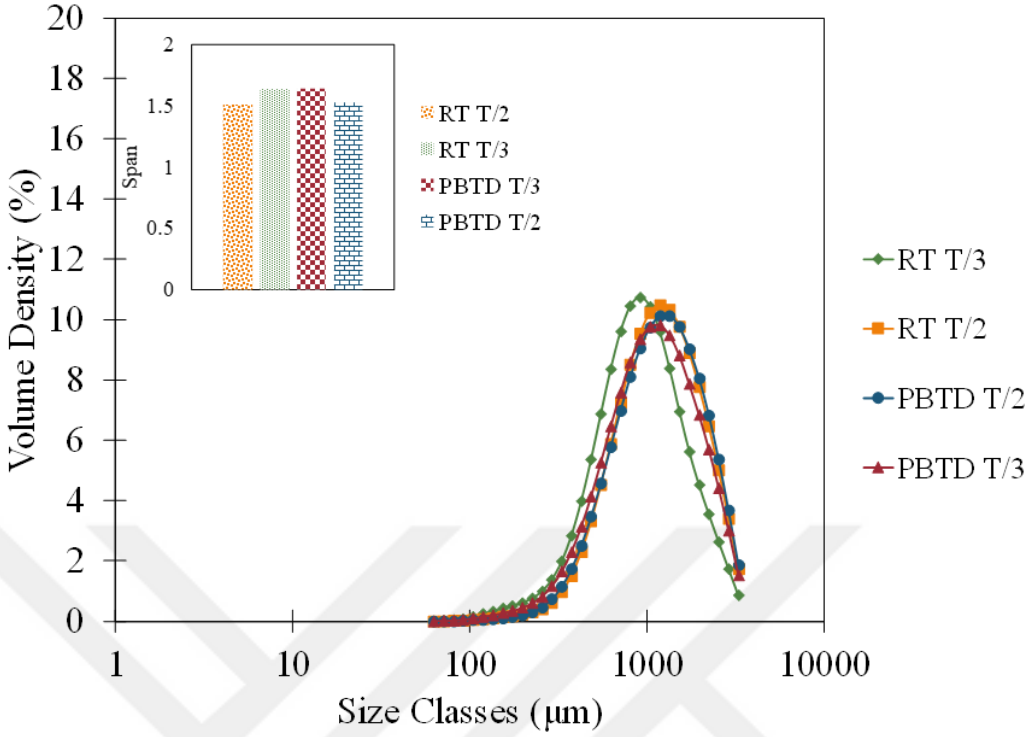

Figure 3.9. Drop size distribution of all impellers at Weber number 350

Figure 3.10 shows the drops size distribution of all impellers at Weber number 450. At high Weber number, the drop size is affected by the type of the impellers rather than the size of the impellers. Even if RT T/2 and RT T/3 produce almost the same size drops, RT T/3 gives narrower drop size distribution than RT T/2. Even if PBTD T/2 and PBTD T/3 produce almost the same size drops, PBTD T/2 gives narrower drop size distribution than PBTD T/3.

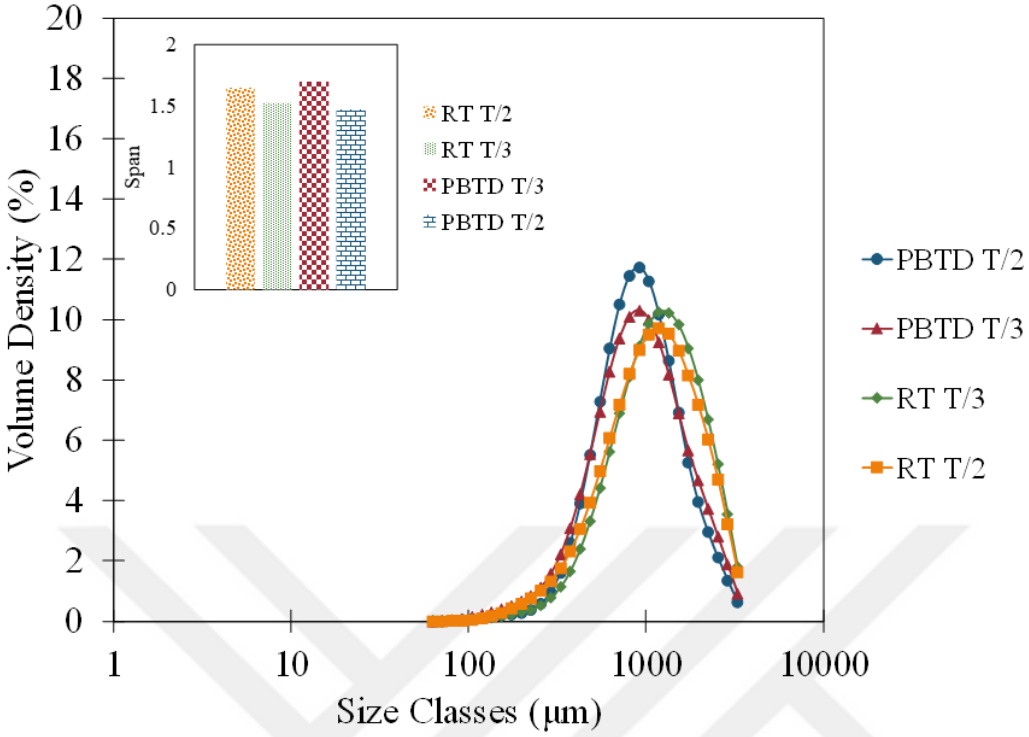

Figure 3.10. Drop size distribution of all impellers at Weber number 450

3.1.4. Effect of Power/Mass Ratio

Power/mass is an indication of breakup potential of an emulsion system in a stirred tank. Mass includes volume. When the impeller swept volume is used, the power/mass is known as the maximum energy dissipation in the tank. At the same power/mass ratio with different impellers, the same amount of energy is dissipated into the system. In this thesis, the effect of varying power/mass ratios on drop sizes was investigated. This ratio is expressed with the following relation:

$$\varepsilon = \frac{Power}{Mass} = \frac{P}{\rho V_{imp}} = \frac{\rho N^3 D^5 N_p}{\rho V_{imp}} = \frac{N^3 D^5 N_p}{V_{imp}} \tag{3.6}$$

N (rps) refers to the impeller speed, D (m) is the impeller diameter, N_p is the impeller power number and V_{imp} is the impeller swept volume. V_{imp} is calculated by the relation given below.

$$V_{imp} = \frac{\pi D^2}{4} * H_{imp} \tag{3.7}$$

$$H_{imp} = \frac{D}{5} \tag{3.8}$$

In Table 3.4, the selected power/mass ratios and corresponding impeller speeds are given. In selection of these values, liquid overflow and operating in turbulent regime were taken into account. For better understanding of the effect of power/mass on drop size, only two common values could be determined for all impellers. However, required impeller speeds for these common values caused liquid overflow when the large impellers are used. Therefore, a longer tank which has the same diameter with the original tank was used in the experiments for the large impellers.

Table 3.4. Selected power/mass ratios and corresponding impeller speed

Power/mass (W/kg)	**N (rpm) RT T/2 impellers**	**N (rpm) PBTD T/2 impellers**	**N (rpm) RT T/3 impellers**	**N (rpm) PBTD T/3 impellers**
300	923	1493	-	-
350	971	1571	1274	2060
400	1016	1643	1332	2155
450	-	-	1386	2240
500	-	-	1435	2320

Impeller power number depends on the type of the impeller. The power number of RT impeller is higher than the PBTD impeller (Chapple et al., 2002; Grenville et al.,

2017). Therefore, at the same power per mass ratio, impeller speed of RT is smaller than the impeller speed of PBTD. Power numbers of the impellers are constant in turbulent regime for baffled tanks (Hemrajani and Tatterson, 2004). However, according to studies performed with RT impeller in unbaffled stirred tanks filled with water, power number of the impeller changes with the vortex depth. When the central vortex does not reach the impeller, power number slightly decreases as Reynolds number increases. When the central vortex reaches the impeller, a steep reduction in power number occurs (Scargiali et al., 2013; Scargiali et al. 2017). These results do not reach an agreement with another study conducted by Assirelli et al. (2008). This paper used RT impeller in unbaffled stirred tanks filled with water. According to this study, power number is constant in turbulent regime in the unbaffled tank as in the baffled tank but smaller than in the baffled tank. Because of the contradiction in these results and lack of information about the change in power number in the eccentric shaft position, the power number values for baffled tanks were used in the experiments to make comparisons more accurate.

Figure 3.11 shows the effect of power per mass ratio on drop size. When power/mass ratio is 350, PBTD T/3 gives the smallest drops. This is followed by PBTD T/2. At the same power/mass ratio, PBTD impellers produce smaller drops than RT impellers. This can be explained by circulation time of the impellers. Since PBTD impellers have larger flow number than RT impellers, they have smaller circulation time. This case can be shown in detail for the same size impellers by the following relations:

$$P = \rho N^3 D^5 N_p \tag{3.9}$$

$$N \sim {N_p}^{-1/3} \tag{3.10}$$

$$t_{circ} = \frac{V_{tank}}{N_q \times D^3 \times N} \tag{3.11}$$

$$t_{circ} \sim {N_p}^{1/3} / N_q \tag{3.12}$$

The smaller the circulation time, the more often the drops come to the impeller zone. Since drop breakup occurs mostly in the impeller zone, drops are exposed to shear more frequently and smaller drops are produced. Similar results have been obtained in the study performed to investigate liquid-liquid dispersion in baffled tanks by Pacek et al. (1999). According to this study, an impeller with smaller power number gives smaller drops.

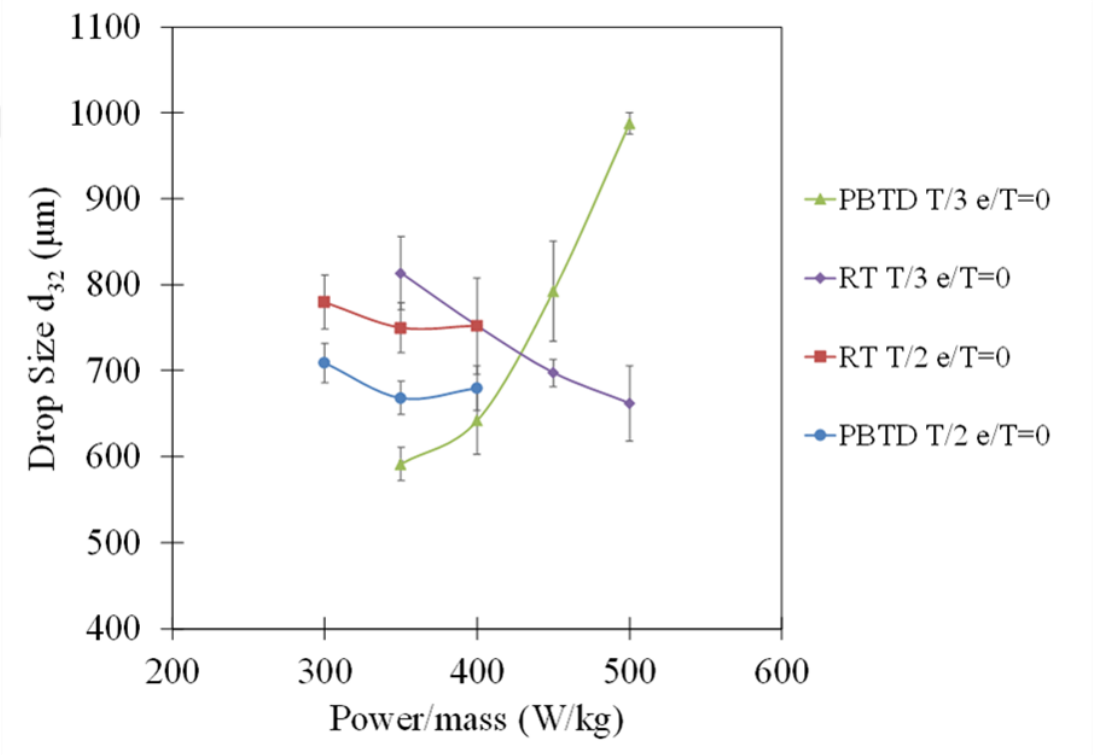

Figure 3.11. The effect of power/mass on drop size

Formation of smaller drops with PBTD T/3 than PBTD T/2 is related with their impeller speeds. At the same power/mass ratio, the impeller speed of PBTD T/3 is larger than the impeller speed of PBTD T/2. Therefore, turbulence fluctuations in the system are higher when PBTD T/3 is used and this case makes drop breakup easier. However, as power/mass ratio continues to increase, drop sizes with PBTD T/3

increase. Increase in turbulence fluctuations in the system with increase in the impeller speeds causes also increase in drop collision frequency. At low power/mass ratio, drop collisions cause drop breakup however, after a certain impeller speed, particle detachment from the interface occurs. The time required for particle attachment on the interface is not sufficient at higher impeller speeds. Thus, drops that are not covered completely coalesce and bigger drops are formed. The reason of the formation of the same size drops with PBTD T/2 and PBTD T/3 when power/mass ratio is 400 is that drop sizes increase with PBTD T/3 as power/mass ratio increases; therefore, data of the two impellers overlaps.

At the same power/mass ratio RT T/2 and RT T/3 impellers give the same size drops. This indicates that power/mass ratio is the determining factor for drop size for this impeller. Impeller size of RT impeller does not affect the drop size at the same power/mass ratio. As power/mass ratio increases, drops size decreases with RT T/3. At higher power/mass ratio, RT T/3 produces smaller drops than PBTD T/3. This is related to again their impeller speeds. At the same power/mass ratio, the impeller speed of RT T/3 is smaller than PBTD T/3. Therefore, there is less turbulence fluctuations that do not cause particle detachment in the system, so smaller drops are formed with RT T/3 compared to PBTD T/3.

In Figure 3.12 drop size distribution of all impellers at the same power/mass ratio, 350, is given. PBTD T/3 impeller that produces the smallest drop size has the largest drop size distribution. This is an indication that more frequent exposure of the drops to the shear causes drop breakup, as well as particle detachment from the surface and thus the drop coalescence. Even though RT T/2 and RT T/3 impellers produce the same size drops, RT T/2 impeller has narrower drop size distribution. Since the impeller speed of RT T/3 impeller is higher than the impeller speed of RT T/3 when power/mass ratio is 350, turbulence fluctuations in the system are more and this brings about formation of smaller drops and drop coalescence due to particle detachment from the interface.

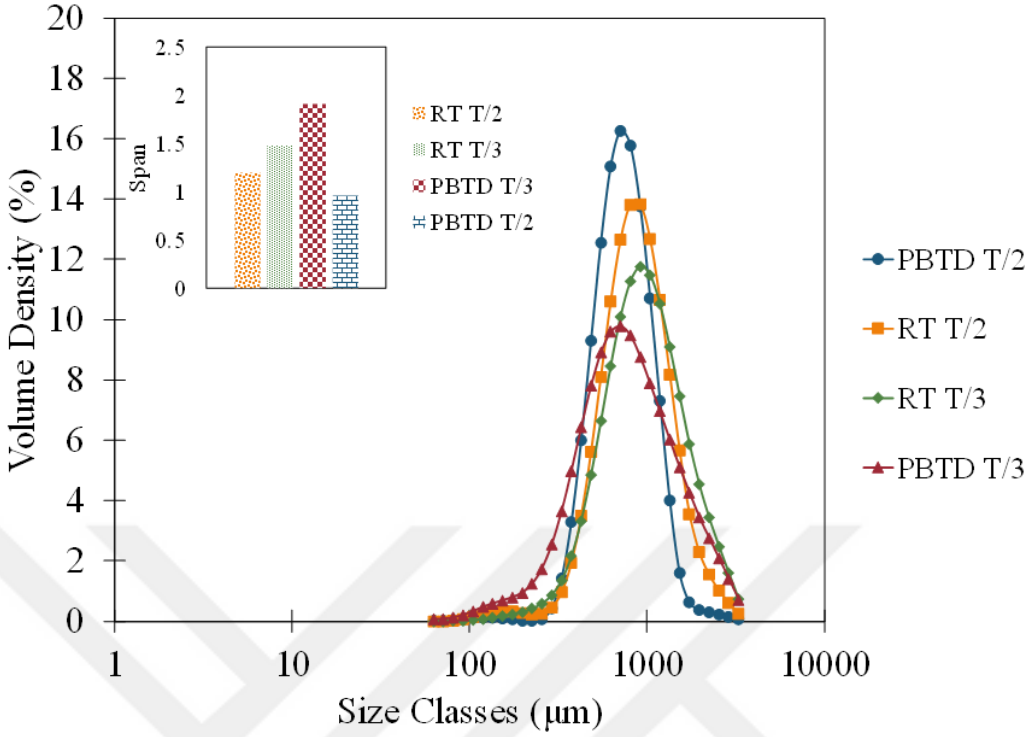

Figure 3.12. Drop size distribution of all impellers at the same power/mass ratio: 350

3.2. Effect of Hydrodynamics on the Production of Pickering Emulsions in Unbaffled Stirred Tanks with Eccentric Shaft

In this section, the effect of shaft position on drop size was investigated. Shaft was positioned at 1 cm (e/T=0.1) and 2 cm (e/T=0.2) away from the tank center in the experiments. The values specified for the centered shaft for each parameter and corresponding impeller speeds were also used in this section.

When the baffles are removed, and the shaft is located at e/T=0, a central vortex form. When the shaft is located eccentrically, an upper and a lower vortices form. These vortices periodically oscillate in the system; they are not steady (Galletti et al., 2008). According to studies conducted by Galletti et al. (2008) and Musik and Talaga (2016), when the shaft is located eccentrically, asymmetric vortex forms at the region where the shaft is away from the tank wall instead of symmetric, central vortex. As the

eccentricity ratio increases, inclination of the vortex relative to vertical axis increases and vortex oscillation decreases. These studies were performed with RT T/3 impeller in a stirred tank filled with single phase fluid. These results were also observed in this study where Pickering emulsion, a multiphase system, was produced. Formation of asymmetric vortex and increase in vortex inclination were observed not only with RT T/3 but also with other impellers. Figure 3.13 shows change in vortex formation with PBTD T/3 owing to the change in eccentricity ratio. These photographs were taken when the impeller speeds were suitable for the best visibility of the vortices.

a) e/T=0 b) e/T=0.1 c) e/T=0.2

Figure 3.13. Vortex formations at different eccentricity ratios with PBTD T/3

Montante et al. (2006) conducted a study to investigate the effect of the shaft eccentricity on the hydrodynamics of unbaffled stirred tanks filled with water using RT T/3 impeller and they positioned the shaft at e/T=0.25. According to their study, two vortices that have an inclination with the vertical axis formed in the system: one is above the impeller and one is below the impeller. Their findings are coinciding with the observations of this study when RT T/3 and RT T/2 impellers are located at e/T=0.2. Two vortices form in the system. However, the lower vortex appears after a certain impeller speed and is weaker compared to the upper vortex. In the study conducted by Galletti et al. (2008) which was performed with RT T/3 at e/T=0.21, it

was also observed that the upper vortex affects the system mostly. In Figure 3.14 vortex formations for RT impellers at e/T=0.2 at suitable impeller speeds where vortices are visible for both impellers are shown. The tanks are filled with water. The lower and the upper vortices formed in the tanks can be seen in this figure. The upper vortex is more dominant in the system and the size of the upper vortex formed with RT T/2 is larger compared to RT T/3. Therefore, the height of liquid in the tank is higher when RT T/2 is used.

a) RT T/3 b) RT T/2

Figure 3.14. Vortex formations with RT impellers at e/T=0.2

When PBTD T/3 and PBTD T/2 impellers are at e/T=0.2, the lower vortex does not appear in the system. There is just an upper vortex affecting the flow pattern in the tank. In Figure 3.15, vortex formations with PBTD impellers at e/T=0.2 at suitable impeller speeds where vortices are visible for both impellers are shown. The size of the upper vortex formed with PBTD T/2 is slightly larger; therefore, the height of the liquid in the tank is slightly higher when PBTD T/2 is used.

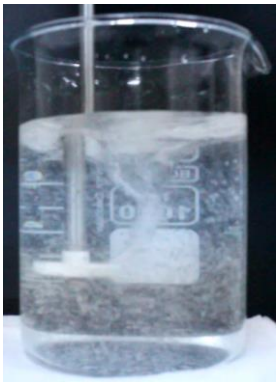

a) PBTD T/3

b) PBTD T/2

Figure 3.15. Vortex formations with PBTD impellers at e/T=0.2

When RT T/3 and RT T/2 are at e/T=0.1, an air cavity forms instead of the lower vortex below the impellers. In Figure 3.16, vortex formations with RT impellers at e/T=0.1 at suitable impeller speeds where air cavities under the impeller are visible for both impellers are shown.

a) RT T/3

b) RT T/2

Figure 3.16. Vortex formations with RT impellers at e/T=0.1

When PBTD T/3 and PBTD T/2 are at e/T=0.1, while the lower vortex is formed with PBTD T/3, an air cavity is formed instead of the lower vortex with PBTD T/2. In vortex formations with PBTD impellers at e/T=0.1 at suitable impeller speeds where vortices are visible for both impellers are shown in Figure 3.17.

a) PBTD T/3 b) PBTD T/2

Figure 3.17. Vortex formations with PBTD impellers at e/T=0.1

This overview provides information about the hydrodynamics related observations when the shaft is off-centered. The following results at varying values of V_{tip}, Reynolds number, Weber number and power per mass are explained in the light of these observations.

3.2.1. Effect of Impeller Tip Speed

In Figure 3.18 the effect of impeller tip speed on drop size when the shaft is located at e/T=0.1 is shown. For better understanding of differences in performances of different impellers, comparison should be done at the same impeller tip speed. Experiments could be performed at only one common impeller tip speed for all impellers: 132 m/min. At the same impeller tip speed, PBTD T/2 and RT T/3 give the same size

drops, PBTD T/3 produces slightly larger drops considering the error bars and RT T/2 produces the largest drops.

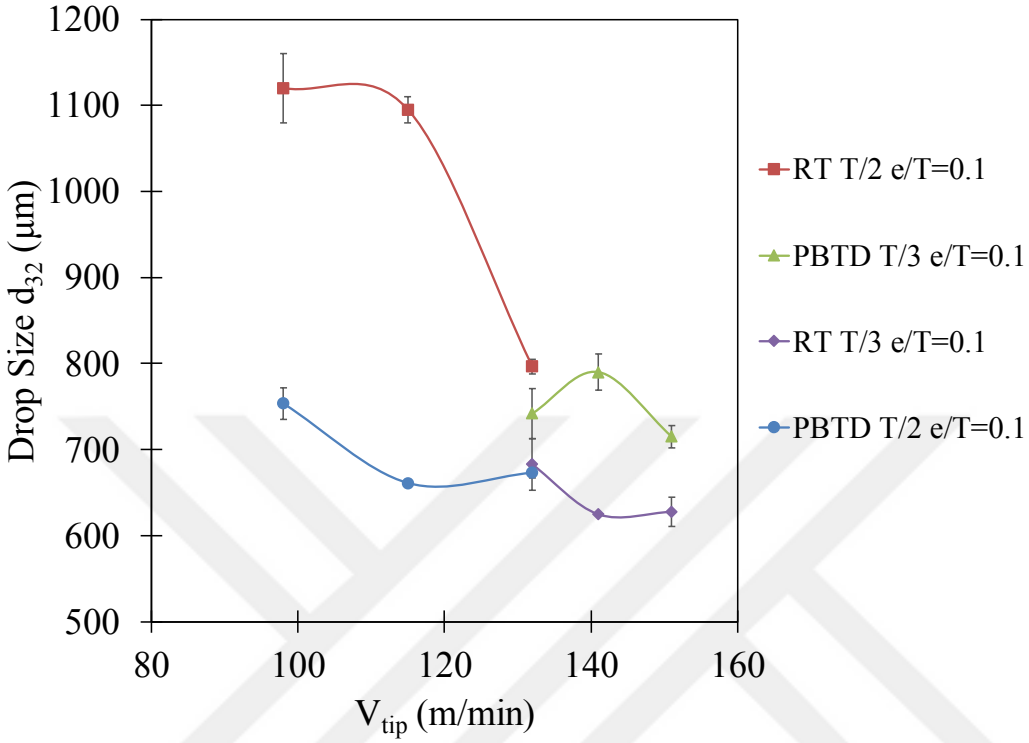

Figure 3.18. The effect of impeller tip speed on drop size at e/T=0.1

In the studies conducted by Soto et al. (2011) with eccentrically located RT T/3 and PBTD T/3 and conducted by Musik and Talaga (2016) with eccentrically located RT T/3, it is observed that when the shaft is located approximately at e/T=0.1, regardless of the type of the impeller, the impeller discharge circulates in the tank as two loops at the region where the shaft is close to the tank wall: one is below and the other is above the impeller. This is caused by interaction of the impeller discharge with the tank wall. Two loops are also generated with RT T/3 at the region where the shaft is away from the tank wall. However, one single loop is observed with PBTD T/3 at the region where the shaft is away from the tank wall. Even if larger vortex is formed with RT T/3, it produces smaller drops than PBTD T/3 because more energy is dissipated

into the system with RT T/3 at the same impeller tip speed when they are located at e/T=0.1. Figure 3.19 shows larger vortex formation with RT T/3.

a) RT T/3 b) PBTD T/3

Figure 3.19. Formed vortices at the same impeller tip speed (132 m/min) for the small impellers at e/T=0.1

As mentioned previously, RT T/2 and PBTD T/2 have similar flow pattern due to having larger impeller size. When they are located eccentrically, two loops are generated at the region where the shaft is close to the tank. They also have similar flow pattern at the region where the shaft is away from the tank wall. The flow discharge at the region where the shaft is away from the tank wall has a downward inclination. Even if they have similar flow patterns, RT T/2 produces larger drops. This can be attributed to the size of the vortex. As seen in Figure 3.20, when RT T/2 is used, the size of the vortex is larger than PBTD T/2 and larger air cavity is formed below the impeller. These formations decrease contact of the impeller blades with the liquid in the tank and reduce the effect of shear. Therefore, larger drops are formed with RT T/2.

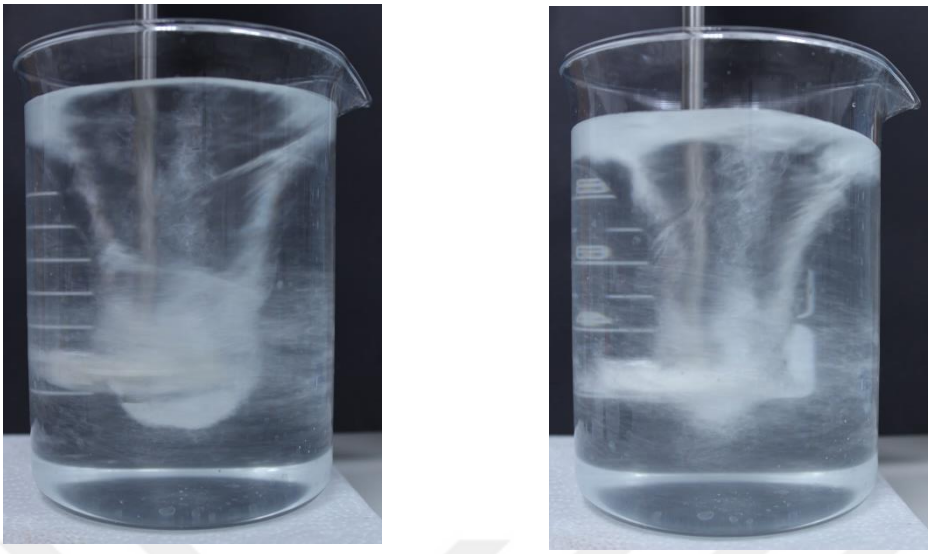

a) RT T/2 b) PBTD T/2

Figure 3.20. Formed vortices at the same impeller tip speed (132 m/min) for the large impellers at e/T=0.1

In Figure 3.21 drop size distribution of all impellers at the same impeller tip speed at e/T=0.1 is given. PBTD T/2 and RT /3 produce not only the same size drops but also have the same drop size distribution. PBTD T/3 has the largest drop size distribution. This situation indicates the importance of energy dissipation to the system and the size of impeller region. PBTD T/3 has less energy dissipation than RT T/3 and smaller impeller zone than PBTD T/2. Therefore, the performance of PBTD T/3 is worse than the other two impellers.

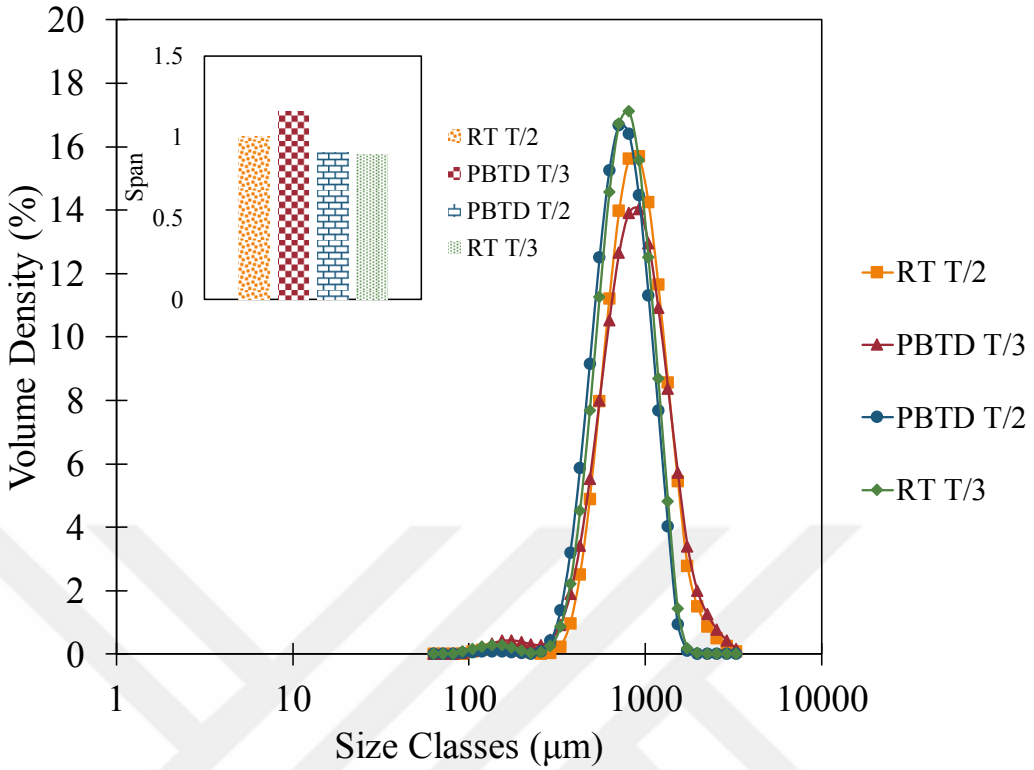

Figure 3.21. Drop size distribution of all impellers at the same impeller tip speed: 132 m/min at e/T=0.1

In Figure 3.22 the effect of impeller tip speed on drop size when the shaft is located at e/T=0.2 is shown. At the same impeller tip speed, among different impellers, PBTD T/2 produces the smallest drops. RT T/3, RT T/2 and PBTD T/3 give the same size drops at the same impeller tip speed: 132 m/min.

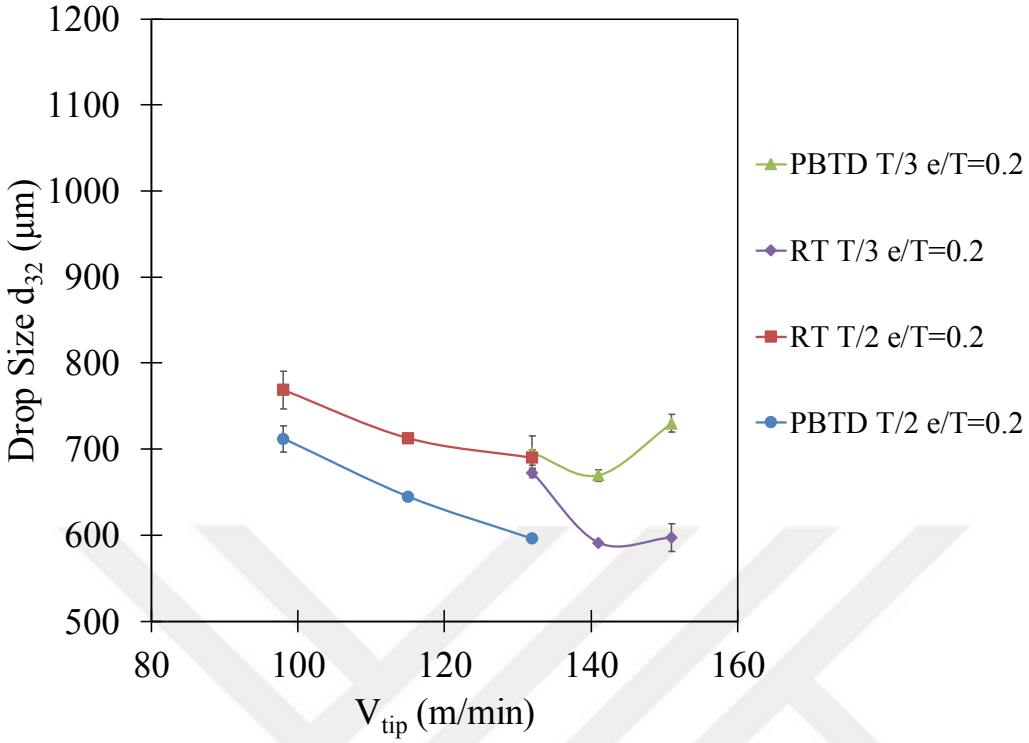

Figure 3.22. The effect of impeller tip speed on drop size at e/T=0.2

Musik and Talaga (2016) showed that RT T/3 impeller at e/T=0.25 has different flow pattern than it has in smaller eccentricity ratio. While the impeller discharge circulates in the tank as two loops at the region where the shaft is close to the tank wall, one single loop forms at the region where the shaft is away from the tank wall. Montante et al. (2006) observed a similar flow pattern with RT T/3 at e/T=0.25. According to their study, overall elliptic vertical flow pattern is generated instead of double loop at the region where the shaft is away from the tank wall. Based on these studies, it can be said that RT T/3 and PBTD T/3 have similar flow pattern when they are located at e/T=0.2. RT T/2 and PBTD T/2 also have similar flow patterns due to their impeller size: double loop at the region where the shaft is close to the tank wall and single elliptic loop at the region where the shaft is away from the tank wall. In the end, it can

be said that all impellers regardless of their types and sizes have almost the same flow pattern in the tank when they are located at e/T=0.2.

When the large impellers are located at e/T=0.2, upper vortex begins to disappear and the liquid in the tank moves in an elliptic path. Although RT T/2 and PBTD T/2 have the same flow pattern, as seen in Figure 3.23, with RT T/2, the liquid height in the tank is higher. It takes more time for the drops with RT T/2 to come to the impeller region as there is more area to circulate in the tank to reach the impeller region. Larger drops are produced because they are less exposed to shear.

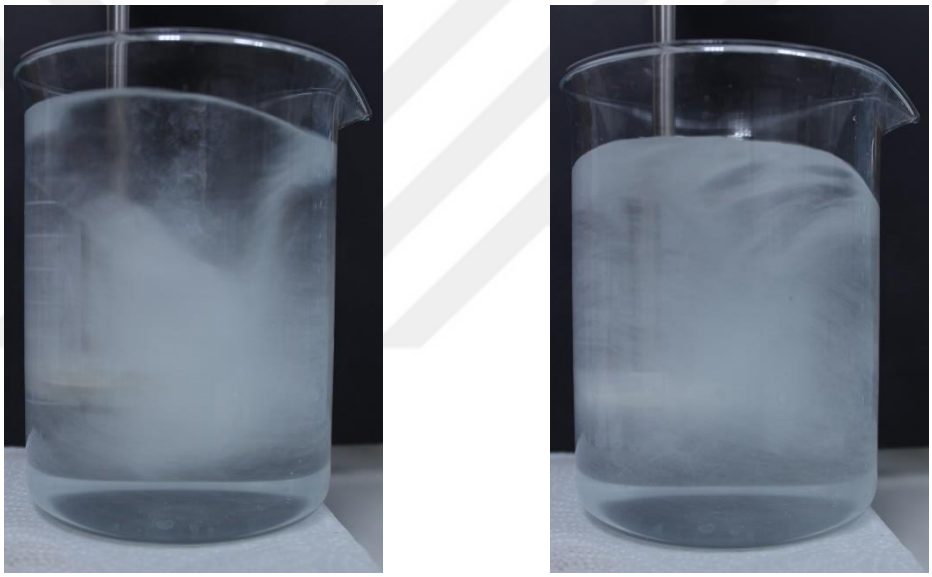

b) RT T/2 c) PBTD T/2

Figure 3.23. Formed vortices at the same impeller tip speed (132 m/min) for the large impellers at e/T=0.2

At the same impeller tip speed, RT T/3 and PBTD T/3 produce the same size drops. They have similar flow pattern but different energy dissipation and different size of the vortex. Even though the energy dissipated to the system is larger with RT T/3, size of the vortex in the system is larger and this affects the applied shear by the impeller.

As seen in Figure 3.24, a lower vortex forms below RT T/3 at that impeller speed. This also leads to a decrease in applied shear to the system. Therefore, they show similar drop breakup performance.

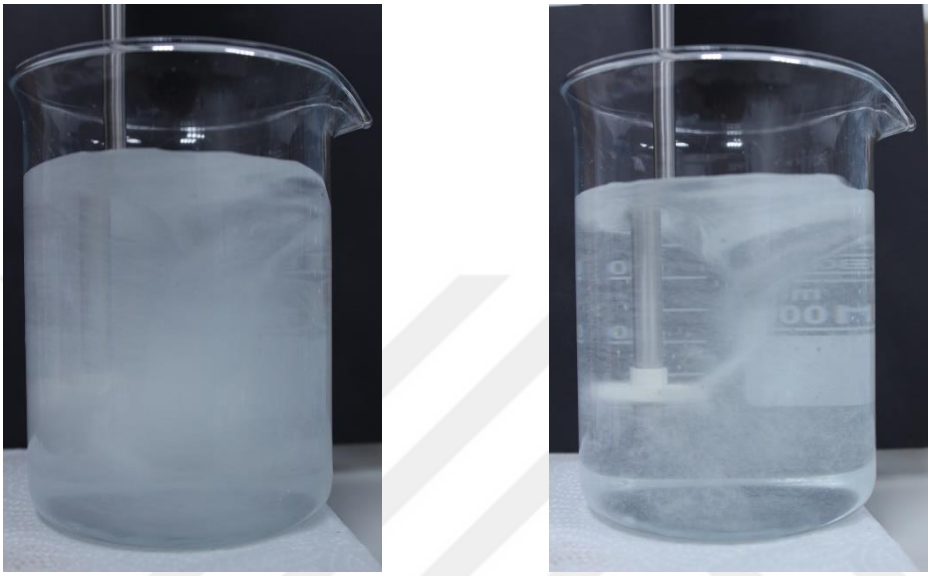

m) RT T/3 n) PBTD T/3

Figure 3.24. Formed vortices at the same impeller tip speed (132 m/min) for the small impellers at e/T=0.2

Figure 3.25 shows drop size distribution of all impellers at the same impeller tip speed at e/T=0.2. Even though RT T/2, RT T/3 and PBTD T/3 produce the same size drops, RT T/2 has the narrowest drop size distribution. This is an indication of the importance of the impeller zone. In the formation of narrower drop size distribution, having larger impeller zone is more effective. While the drops sizes obtained with PBTD T/2 are smaller than RT T/2, narrower drop size distribution is obtained with RT T/2. Based on this result, it can be said that energy dissipation also plays an important role in determination of the performances of different impellers.

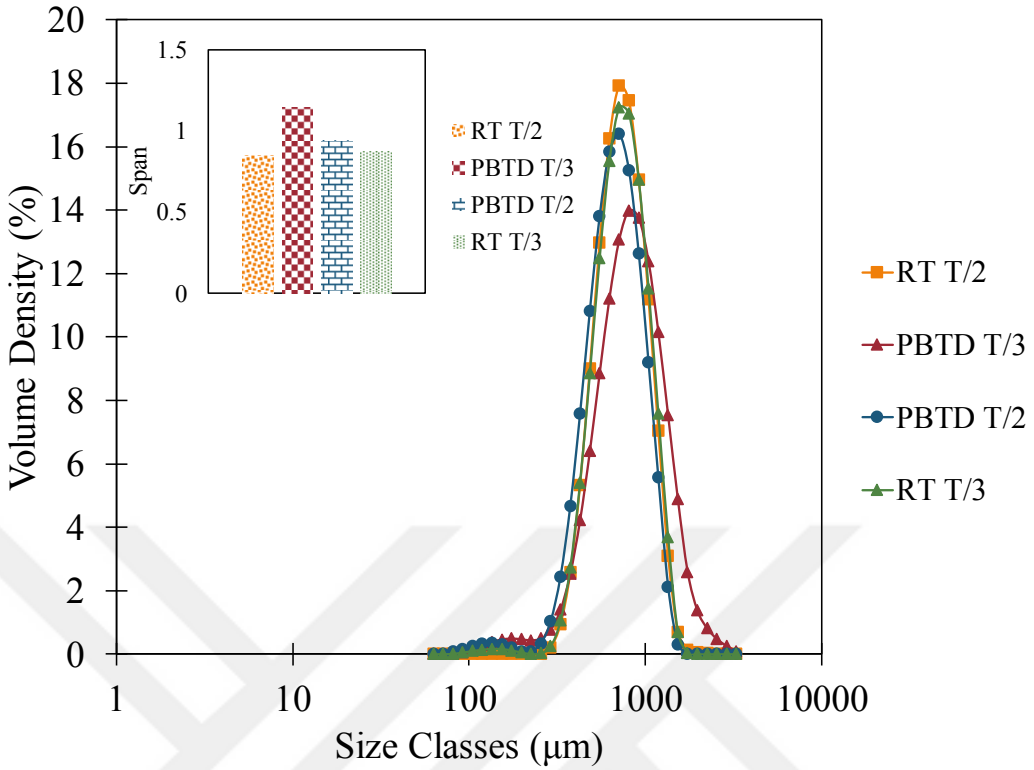

Figure 3.25. Drop size distribution of all impellers at the same impeller tip speed: 132 m/min at e/T=0.2

Figure 3.26 show the effect of eccentricity on drop size for all impellers at the same impeller tip speed. Generally, when the eccentricity is e/T=0.2, smaller drops are produced. This is because when the eccentric ratio increases, the size of vortex decreases, and the vortex moves toward to the tank wall. Therefore, impellers are in contact with the liquid more and drops can be exposure more shear so, drop breakup occurs more efficiently. Lipin (2017) conducted a study with eccentrically located RT T/3 and observed that when the eccentricity increases, turbulence kinetic energy also increases. Thus, more energy is dissipated to the system and this contributes to formation of smaller drops.

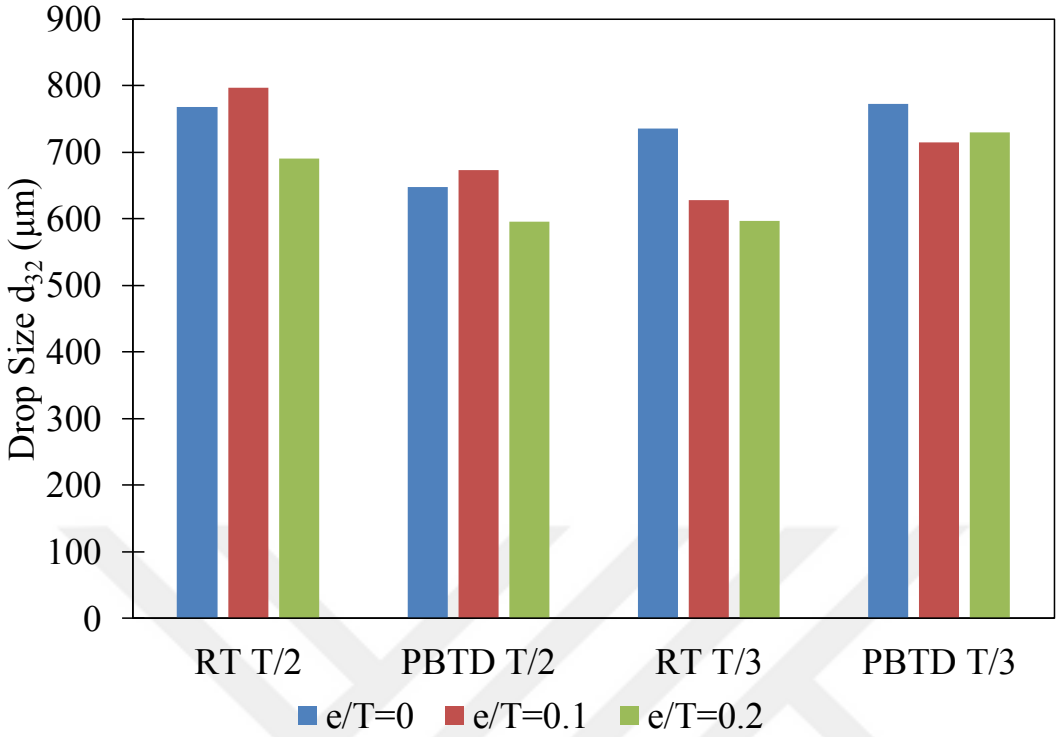

Figure 3.26. Effect of eccentricity on drop size at the same impeller tip speed (V_{tip}= 132 m/min)

3.2.2. Effect of Impeller Reynolds Number

In Figure 3.27, the effect of Reynolds number on drop size when the impellers are located at e/T=0.1 is shown. Drop sizes produced with PBTD T/2 decreases until a certain Reynolds number of 26 000 and then remain almost constant. For the other impellers, drop sizes do not change substantially as Reynolds number increases. The contact of the impellers with the liquid decreases when the impeller speed increases because air cavity or lower vortex begin to form. Therefore, the effect of the shear applied by the impellers decreases. Even if energy dissipated into the system increases with increase in Reynolds number, drops size remains almost constant due to formations of air cavity and lower vortex. While RT T/3 gives the smallest drop size, RT T/2 produces the largest drop size.

Among the small impellers, RT T/3 gives smaller drops. Flow patterns of RT T/3 and PBTD T/3 are similar at the region where the shaft is close to the tank wall. Fluid impinges to the tank wall and separates as two loops due to interaction of fluid with the tank wall: one is above and the other is below the impeller. At the region where the shaft is away from the tank wall, while flow pattern of RT T/3 contains two loops, flow pattern of PBTD T/3 contains one loop. Power number of RT T/3 is greater than PBTD T/3. Therefore, more energy is dissipated to the system when RT T/3 is used. Dissipating more energy to the system makes drop breakup easier, so smaller drops are obtained with RT T/3. When RT T/3 is used, a smaller air cavity forms below the impeller when the shaft is at e/T=0.1 compared to centered position. Despite this air cavity, RT T/3 produces smaller drops than PBTD T/3. This an indication that at the same Reynolds number, among the small impellers, the energy dissipated to the system is more dominant in determining drop size and the effect of air cavity which does not cover under the impeller completely is negligible when the impellers are positioned at e/T=0.1.

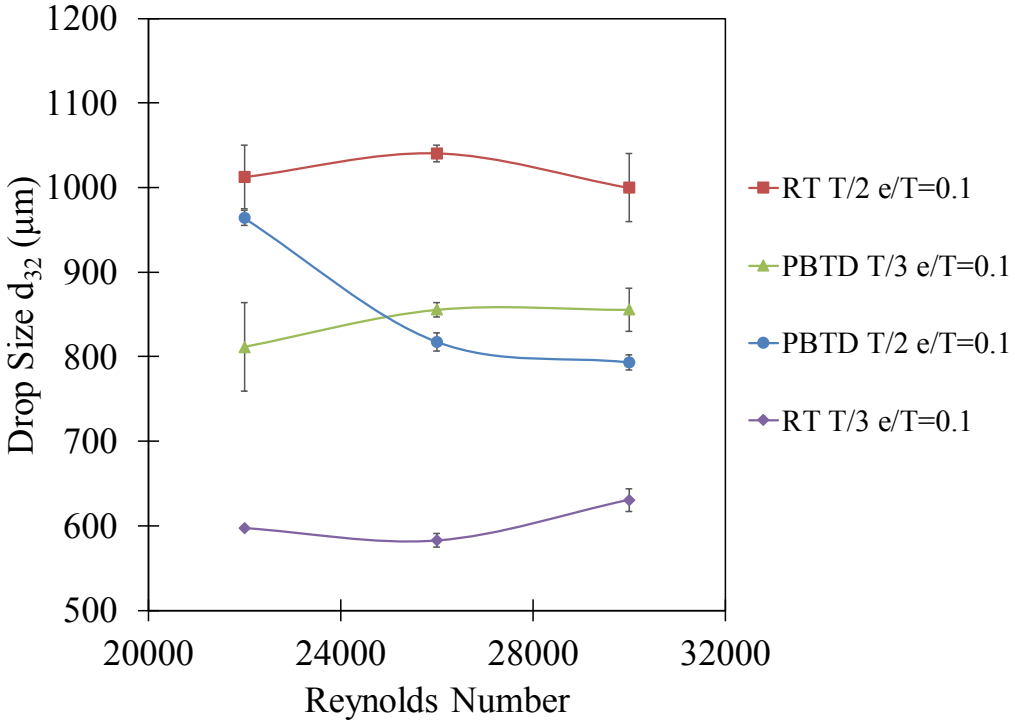

Figure 3.27. The effect of Reynolds number on drop size for all impellers located at e/T=0.1

Among the large impellers, PBTD T/2 gives smaller drops. Smaller upper vortex is formed with PBTD T/2. Also, there is no air cavity or lower vortex below the impeller. Therefore, contact of PBTD T/2 with the liquid in the tank is larger and the effect of shear applied by the impeller is larger compared to RT T/2. This situation contributes to formation of smaller drops.

Figure 3.28 shows drop size distribution of all impellers at the same Reynolds number of 30 000 at e/T=0.1. The impeller that produces the smallest drops sizes, RT T/3, also gives the narrowest drop size distribution. This is an indication that the performance of RT T/3 is better than the others in both respects: drop size and drop size distribution. Although PBTD T/3 gives smaller drop size than RT T/2, it has larger drop size distribution. This is an indication that the size of impeller zone also influences drop

size distribution in addition to energy dissipated to the system when the impellers are positioned at e/T=0.1.

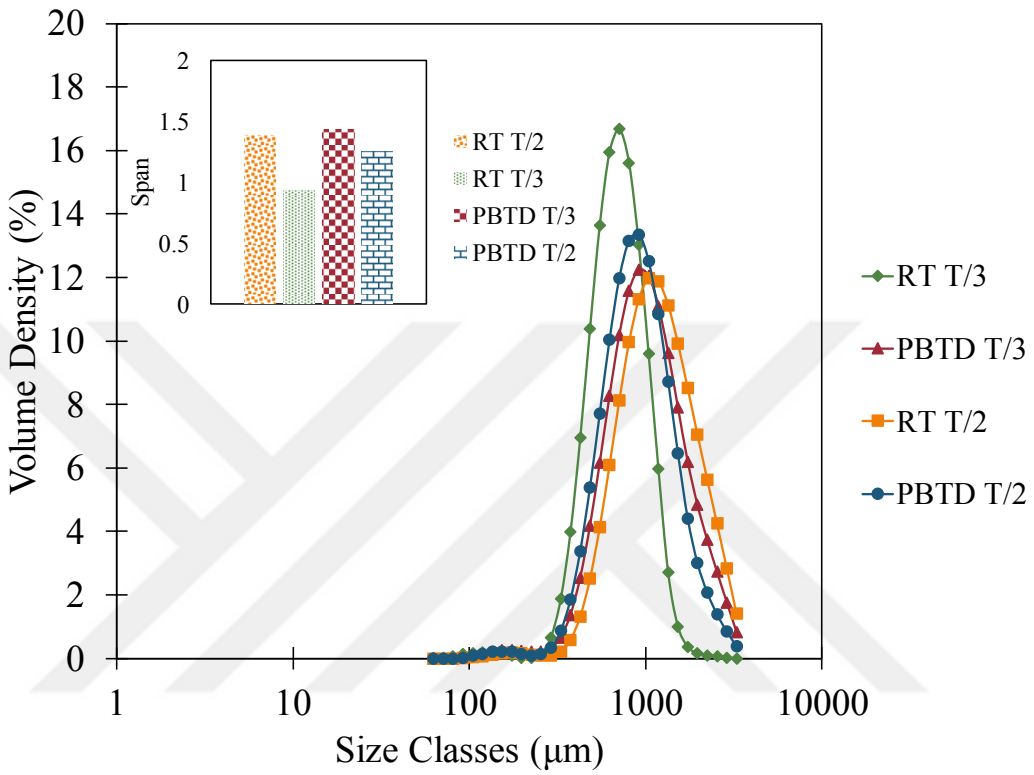

Figure 3.28. Drop size distribution of all impellers at the same Reynolds number: 30 000 at e/T=0.1

Figure 3.29 the effect of Reynolds number on drop size when the impellers are located at e/T=0.2 is shown. While RT T/3 gives the smallest drops at low Reynolds numbers, RT T/2 gives the smallest drops as Reynolds number increases.

As Reynolds number increases, drop sizes decrease until intermediate Reynolds number and then remain almost constant when the large impellers are used. RT T/2 produces smaller drops than PBTD T/2. The flow patterns of these impellers are the same when they are located at e/T=0.2. At the region where the shaft is close to the tank wall, the impeller discharge circulates in the tank as radial two loops and at the

region where the shaft is away from the tank wall, the impeller discharge circulates in the tank elliptically. Even if their flow patterns are similar, their flow numbers, circulation times and power numbers are different. Formation of different drop sizes can be attributed to these differences. While power number and circulation time of RT T/2 impeller are higher than PBTD T/2 impeller, flow number of PBTD T/2 is higher than RT T/2. When the large impellers are positioned at e/T=0.2, the formed vortex in the tank begins to disappear and the parts of the impellers which are in contact with the liquid increases as Reynolds number increases. Therefore, shear capacity of the impellers is transferred to the system better. Formation of smaller drops with RT T/2 is an indication that for the large impellers, the effect of the amount of energy dissipated into the system in determining drop size is more dominant than pumping capacity when the vortex begins to disappear.

Among the small impellers, RT T/3 gives smaller drops at low Reynolds number owing to having higher power number. However, as Reynolds number increases, drops sizes obtained with RT T/3 and PBTD T/3 get close to each other and at high Reynolds number, these two impellers produce the same drop sizes. This result is caused by particle detachment from the interface at high Reynolds number. Since RT T/3 has greater power number, energy dissipated to the system is higher and particle detachment occurs due to increase in drop collisions. Therefore, drop coalescence occurs and larger drops are produced.

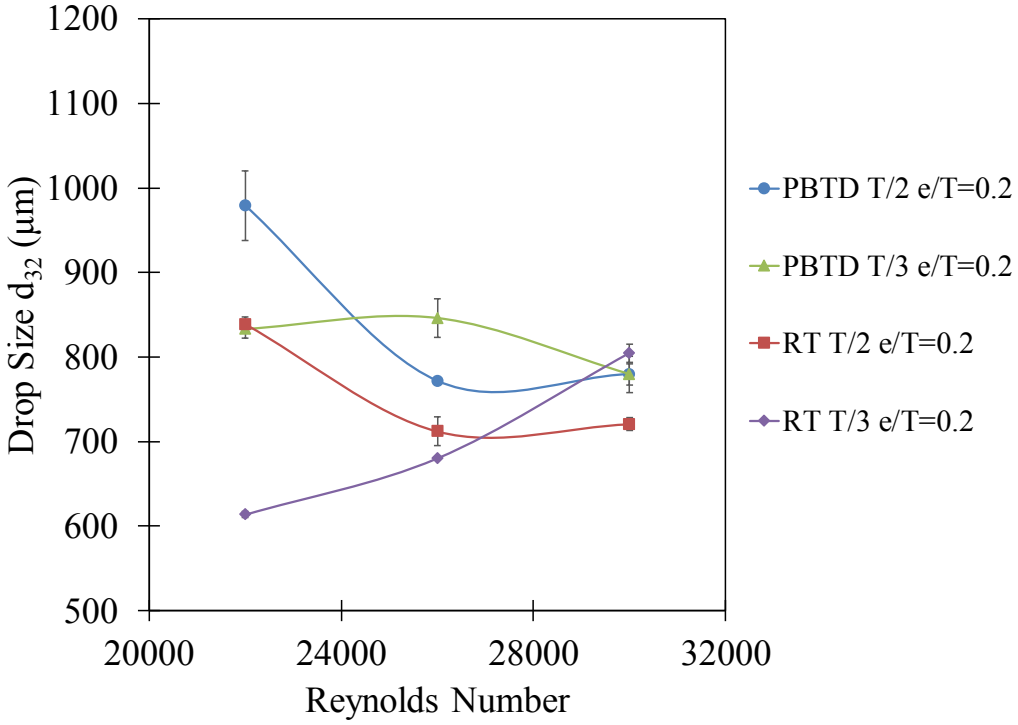

Figure 3.29. The effect of Reynolds number on drop size for all impellers located at e/T=0.2

At higher Reynolds number PBTD T/2, PBTD T/3 and RT T/3 produce the same size drops. At same Reynolds number, the impeller speeds are higher than the large impellers, so more energy is dissipated to the system. Based on this, it is expected that the small impellers would produce smaller drops. However, increase in dissipated energy causes increase in drop collisions and particle detachment from the interface. Also, the small impellers have larger coalescence zone. Therefore, smaller drops are not produced as expected. PBTD T/2, on the other hand, has larger impeller zone and this contributes to formation of smaller drops. In this case, higher energy dissipation to the system due to higher impeller speed is compensated by having a larger impeller zone. Among all impellers, RT T/2 gives the smallest drops at high Reynolds number. This is an indication that the size of impeller zone is more dominant in determining drop size at high Reynolds number when the upper vortex begins to disappear. A lower vortex is formed below RT T/2 at high Reynolds number. The formation of the

smallest drops with RT T/2 despite this lower vortex is an indication that the effect of the lower vortex on the system is weak. This result is also observed in the study conducted by Galletti et al. (2008).

Figure 3.30 shows drop size distribution of all impellers at the same Reynolds number of 30 000 at e/T=0.2. Even though PBTD T/2, PBTD T/3 and RT T/3 produce the same size drops when Reynolds number is 30 000, drops size distribution of PBTD T/2 is larger than the others. This is an indication that for obtaining narrower drop size distribution, the energy dissipated into the system is more important than having larger impeller zone.

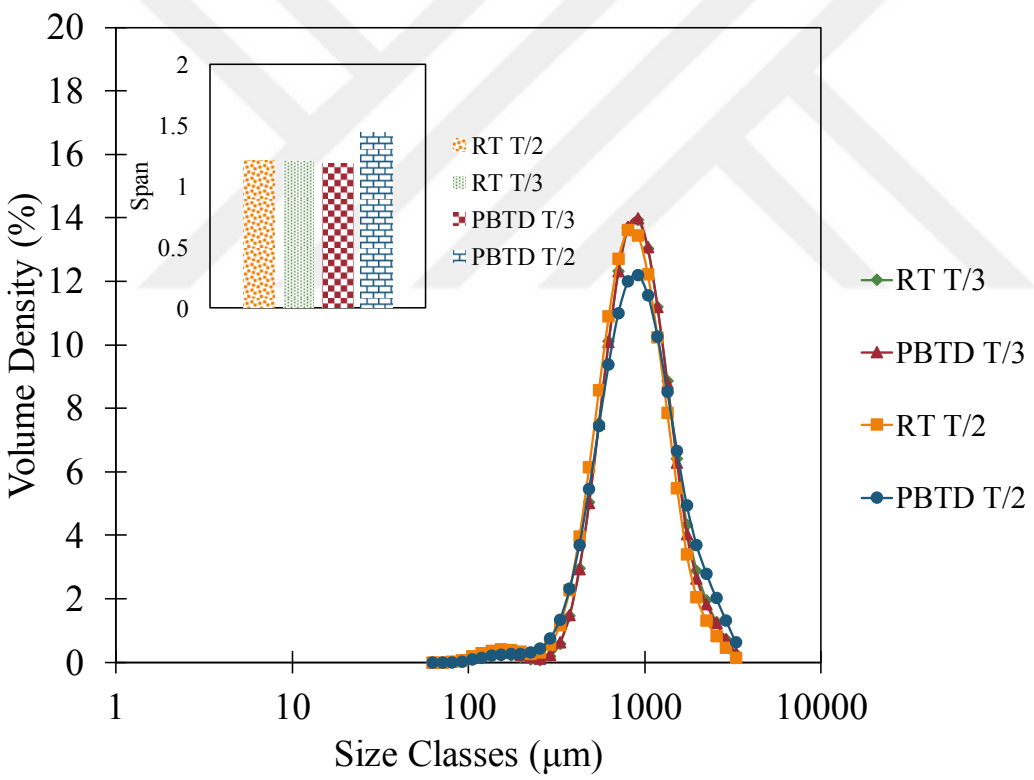

Figure 3.30. Drop size distribution of all impellers at the same Reynolds number: 30 000 at e/T=0.2

Figure 3.31 shows the effect of eccentricity on drop size for all impellers at the same Reynolds number of 30 000. Generally, when the eccentricity is e/T=0.2, smaller drops are produced. As mentioned previously, this is caused by decrease in the size of the upper vortex and increase in contact of the impellers with the liquid in the tank. Therefore, drops are exposed to shear in a more effective way and drop breakup occurs more efficiently.

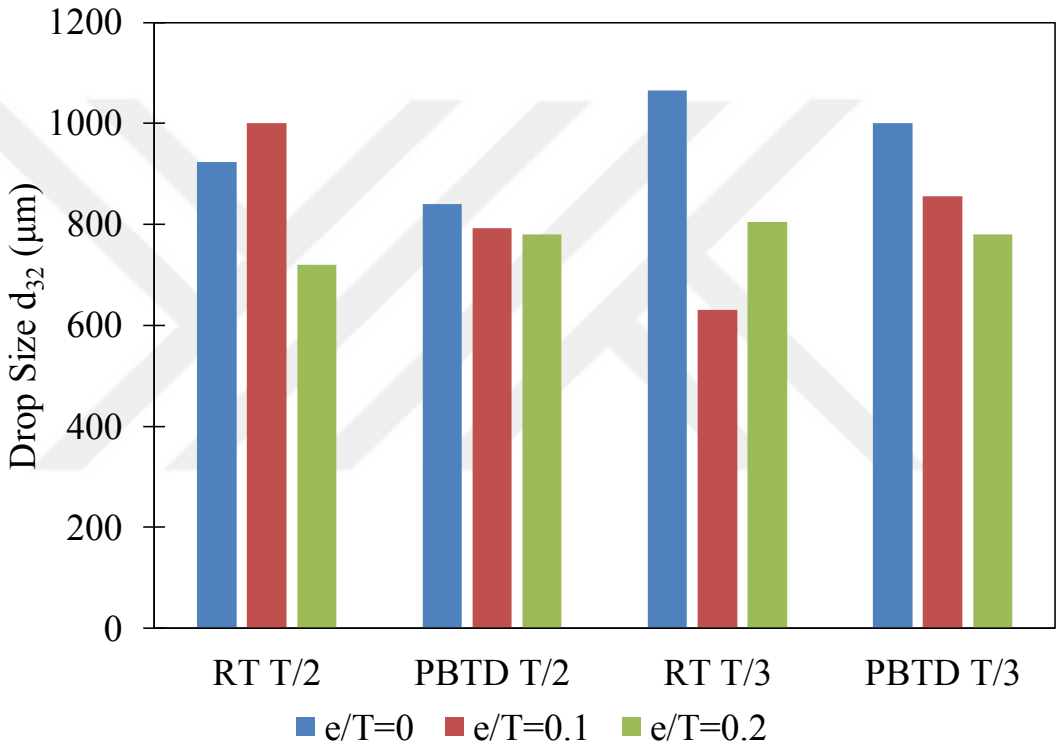

Figure 3.31. Effect of eccentricity on drop size (Re=30 000)

3.2.3. Effect of Weber Number

In Figure 3.32, the effect of Weber number on drop size when the impellers are located at e/T=0.1 is shown. The small impellers produce smaller drops. Flow patterns of the small impellers are partially similar at e/T=0.1. Flow patterns formed at the region

where the shaft is close to the tank wall are the same for both impellers. However, flow patterns at the region where the shaft is away from the tank wall differ from each other. While RT T/3 discharge has two loops, PBTD T/3 discharge has one loop. Among the small impellers RT T/3 gives smaller drops. RT T/3 has higher power number than PBTD T/3, so more energy dissipation is provided with RT T/3. Dissipating more energy to the system makes drop breakup easier, so smaller drops are obtained with RT T/3. An air cavity forms below RT T/3 as Weber number increases. This impeller produces smaller drops in spite of this air cavity. Formed air cavity at e/T=0.1 is smaller compared to that at e/T=0.2. Therefore, its effect on drop size is relatively weaker and does not affect drop size too much, so smaller drops are obtained even at the highest Weber number with RT T/3.

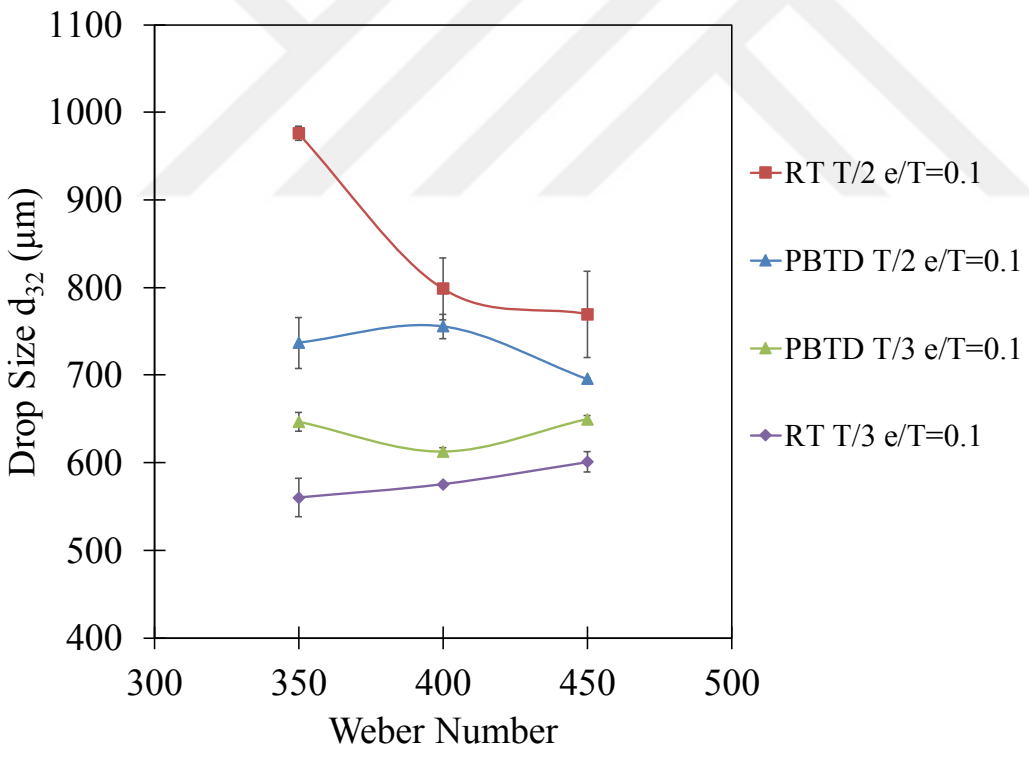

Figure 3.32. The effect of Weber number on drop size for all impellers located at e/T=0.1

Among the large impellers, although RT T/2 and PBTD T/2 form the same flow pattern in the tank at e/T=0.1, PBTD T/2 produces smaller drops. An air cavity below RT T/2 forms as Weber number increases and causes decrease in contact of the impeller with the liquid in the tanks. This decreased contact reduces shear applied by the impellers and prevents formation of smaller drops compared to full contact case. Since the effect of upper vortex on the system is more dominant, the size of the upper vortex is one of the determining factors of drop size. The higher the upper vortex, the lower the contact of the impeller with the liquid. RT T/2 has larger upper vortex. Even though RT has higher power number and can provide more energy dissipation to the system, it produces larger drops due to this larger upper vortex and air cavity.

Figure 3.33 shows drop size distribution of all impellers at the same Weber number of 450 at e/T=0.1. The impeller that produces the largest drop sizes, RT T/2, also gives the largest drop size distribution. This is an indication that decrease in contact of the impeller with the liquid causes not only formation of larger drops but also larger drop size distribution even if it has higher impeller zone and power number.

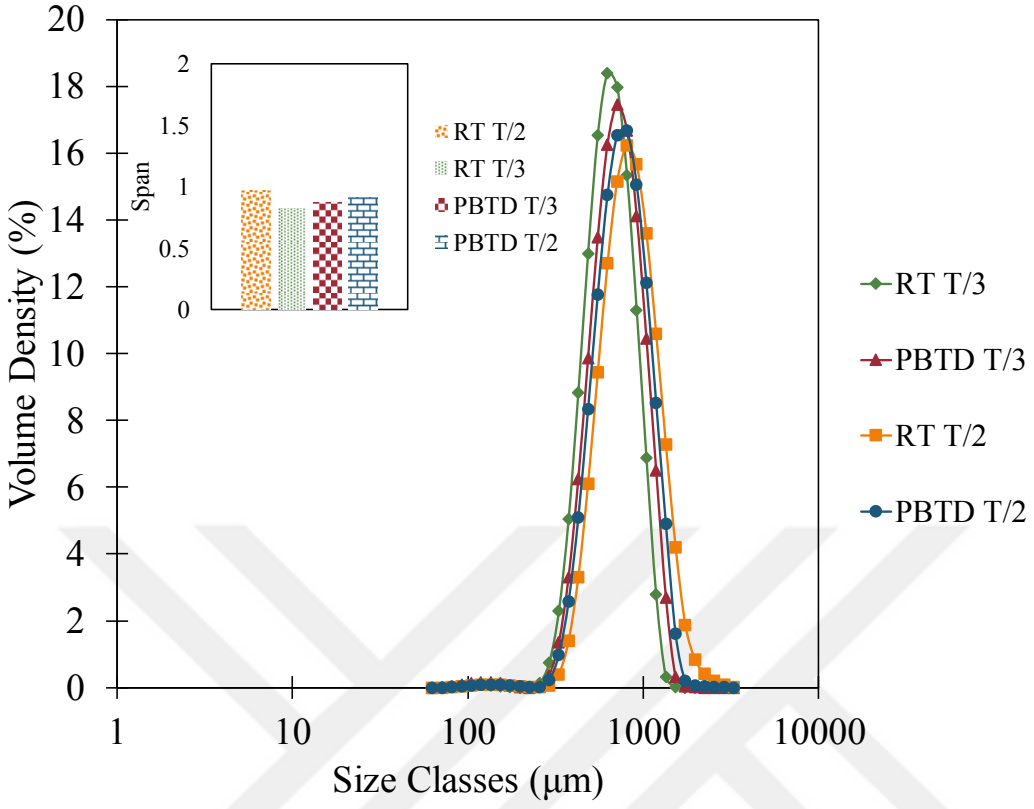

Figure 3.33. Drop size distribution at Weber number 450 at e/T=0.1

In Figure 3.34, the effect of Weber number on drop size when the impellers are located at e/T=0.2 is shown. At the lowest Weber number, RT T/3 gives the smallest drop sizes and the other impellers produce similar size drops with overlapping error bars. PBTD T/3 and RT T/3 create the same flow pattern in the tank. However, RT T/3 gives smaller drop sizes since its power number is higher and it gives more energy to the system. Increase in energy dissipation to the system makes drop breakup easier. Therefore, smaller drops are obtained with RT T/3. At the same Weber number, the impeller speeds of the small impellers are higher, and they provide more energy dissipation to the system. Even if the large impellers have larger impeller zone and it is expected to produce smaller drops, RT T/3 gives the smallest drops due to having higher impeller speed. However, after intermediate Weber number, larger drops begin

to form with RT T/3. As Weber number increases, higher turbulence intensity is created in the system. This leads to increase in drop collisions and particle detachment occurs from the interface with the time. Therefore, larger drops are produced.

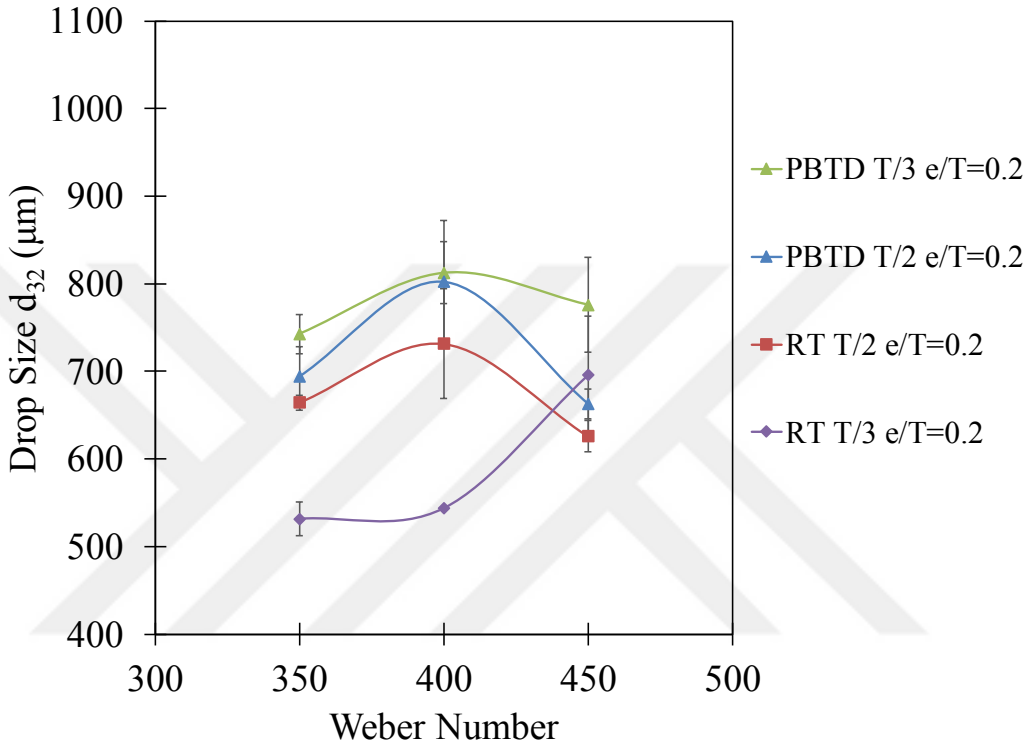

Figure 3.34. The effect of Weber number on drop size for all impellers located at e/T=0.2

When the impellers are positioned at e/T=0.2, the upper vortex begins to disappear, so impellers transfer their shear capacity almost completely. Also, they create similar flow pattern in the tank. At the largest Weber number PBTD T/3 produces the largest drops. It is followed by the RT T/3. The larger impellers produce almost the same size drops, and these are smaller than the drops produced with the small impellers. While the small impellers have higher impeller speeds and give more energy to the system,

they do not produce smaller drops than the large impellers, since particle detachment and drop coalescence occur.

Figure 3.35 shows drop size distribution of all impellers at the same Weber number of 450 at e/T=0.2. The small impellers have narrower drop size distribution. This is an indication that the effect of the amount of energy dissipated to the system on drop size distribution is more dominant on drop size distribution.

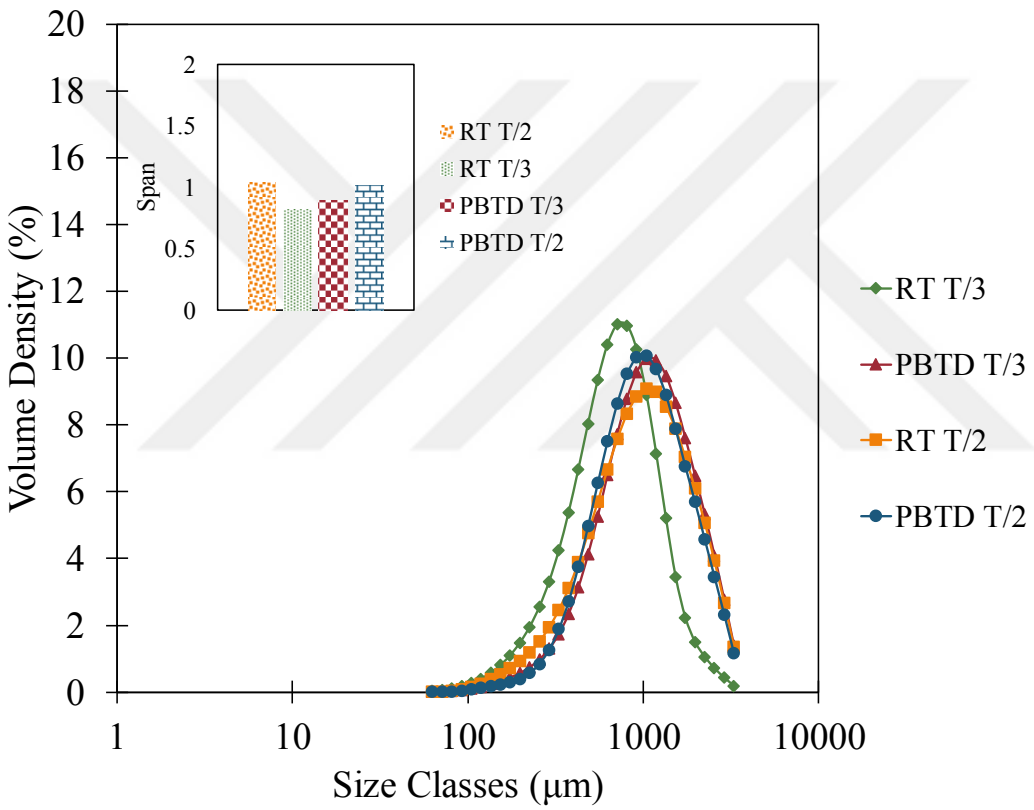

Figure 3.35. Drop size distribution at Weber number 450 at e/T=0.2

Figure 3.36 shows the effect of eccentricity on drop size for all impellers at the same Weber number of 450. The large impellers give the smallest drops at e/T=0.2, since the upper vortex begins to disappear and the contact of the impellers with the liquid

increases, so drops are exposed to shear effectively. On the other hand, the small impellers can not produces the smallest drops at e/T=0.2 because of particle detachment and drop coalescence, they produce the smallest drops at e/T=0.1 instead.

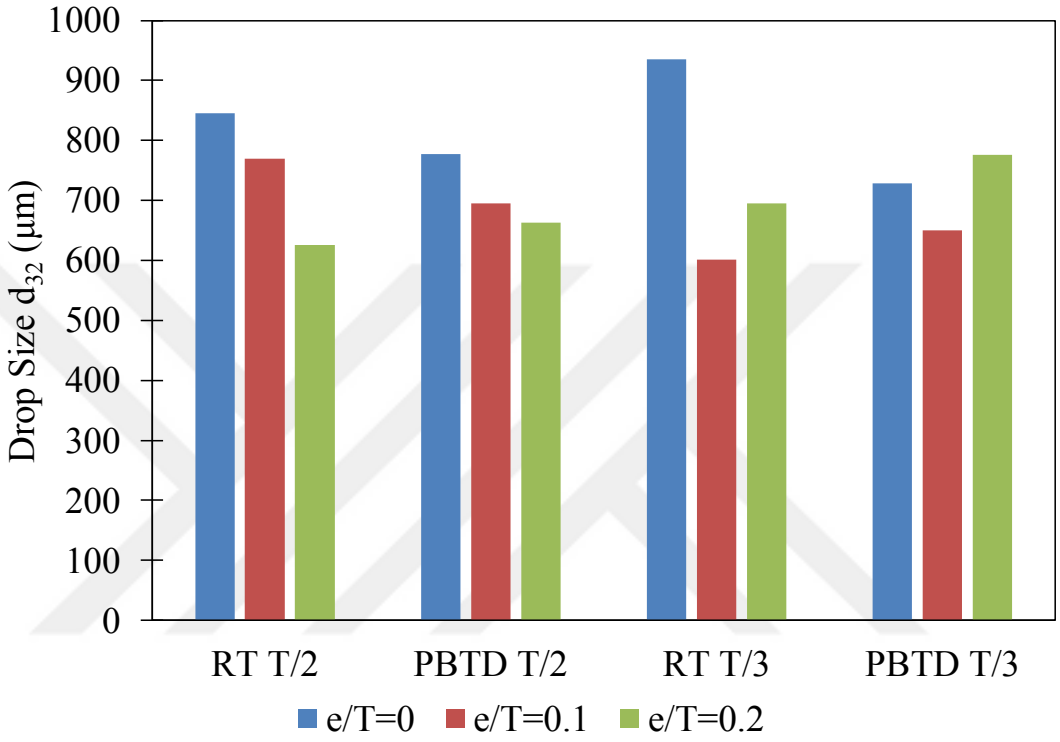

Figure 3.36. Effect of eccentricity on drop size (Weber=450)

3.2.4. Effect of Power/Mass

The energy dissipated into the system can be estimated by power per mass. This is the total power provided to the tank by rotation of the impeller, divided by the total mass of the contents of the tank. The power contains an impeller power number. A recent study conducted by Musik and Talaga (2016) with RT T/3 located at different positions in an unbaffled stirred tank shows that impeller power numbers depend on not only the type of the impeller but also the presence of baffles and position of the

shaft. They observed that impeller power number of RT impeller in unbaffled stirred tank is smaller in comparison to baffled tank and is larger in comparison with unbaffled tank when the impeller is located at the center. However, the effect of eccentricity on power number of PBTD impeller is not known. Therefore, power number values of the impellers when they are in baffled tanks were used in the experiments to make comparisons more accurate.

The effect of power/mass ratio on drop size when the impellers are positioned at e/T=0.1 is shown in Figure 3.37. At the same power/mass ratio, the impeller speed of PBTD T/3 impeller is higher than RT T/3 impeller due to having smaller power number. Therefore, turbulence intensity in the system is larger when PBTD T/3 is used and it would be expected that smaller drops are obtained with PBTD T/3. However, RT T/3 produces smaller drop sizes than PBTD T/3 because increase in turbulence intensity causes increase in drop collisions and particle detachment at that high impeller speeds. When the impellers are located at e/T=0.1, the size of the vortex is smaller compared to centered position. Therefore, contact of the impellers with the liquid is larger at this eccentricity. Also, PBTD T/3 has smaller circulation time and drops are exposed to shear more frequently. Therefore, drops are more interacting with the impellers which contributes to particle detachment and formation of larger drops with PBTD T/3. At the largest power/mass, however, the drop sizes are the same with both impellers.

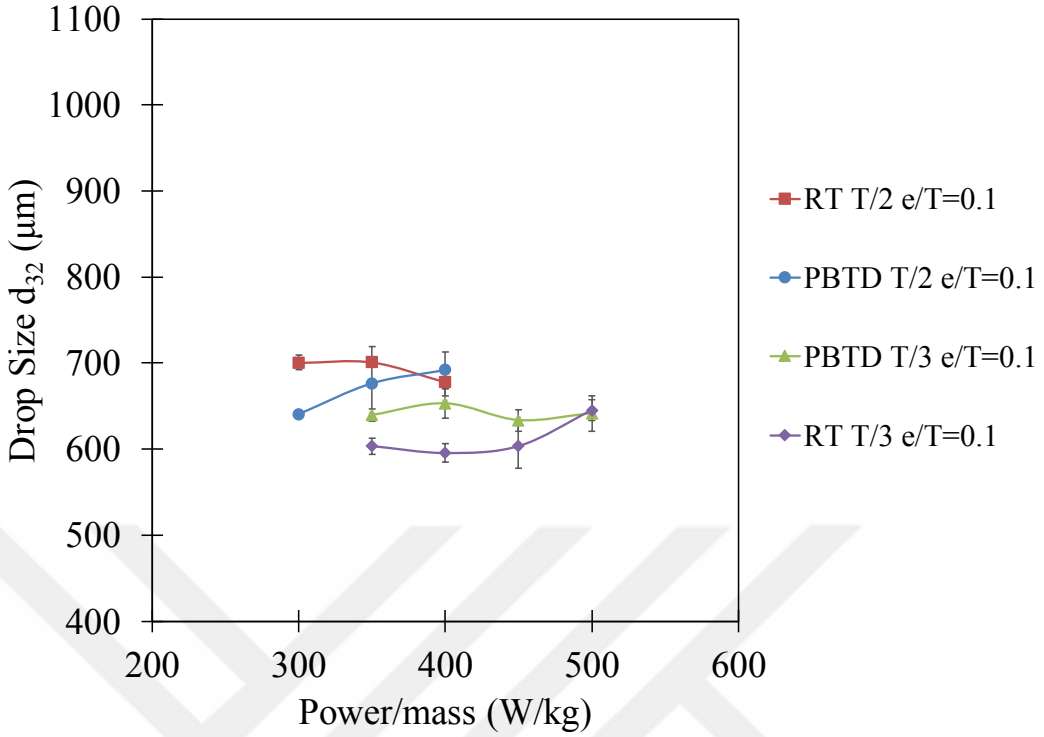

Figure 3.37. The effect of power/mass on drop size at e/T=0.1

At the same power/mass ratio RT T/2 and PBTD T/2 create the same size drops. The large impellers have the same flow patterns. Although, circulation time of PBTD impeller and the size of the formed vortex in the system are smaller with PBTD T/2, both impellers form the same size drops. This can be attributed to higher impeller speed of PBTD T/2 impeller. Since PBTD T/2 impeller has larger impeller speed, it creates more turbulence intensity in the system, and this contributes to drop collisions and particle detachment. Particle detachment results in drop coalescence and formation of larger drops. This is an indication that increase in contact of the impellers with the liquid in the tank has an adverse effect on drop breakup process if the impeller speeds of the impellers are too high.

Figure 3.38 shows drop size distribution of all impellers at the same power/mass ratio of 400, when the impellers are located at e/T=0.1. Except RT T/3 the other impellers

give the same size drops. However, PBTD impellers has larger drop size distribution. Since impeller speeds of PBTD impellers are higher than RT impellers, turbulence fluctuations in the system are more and this brings about formation of smaller drops along with drop coalescence.

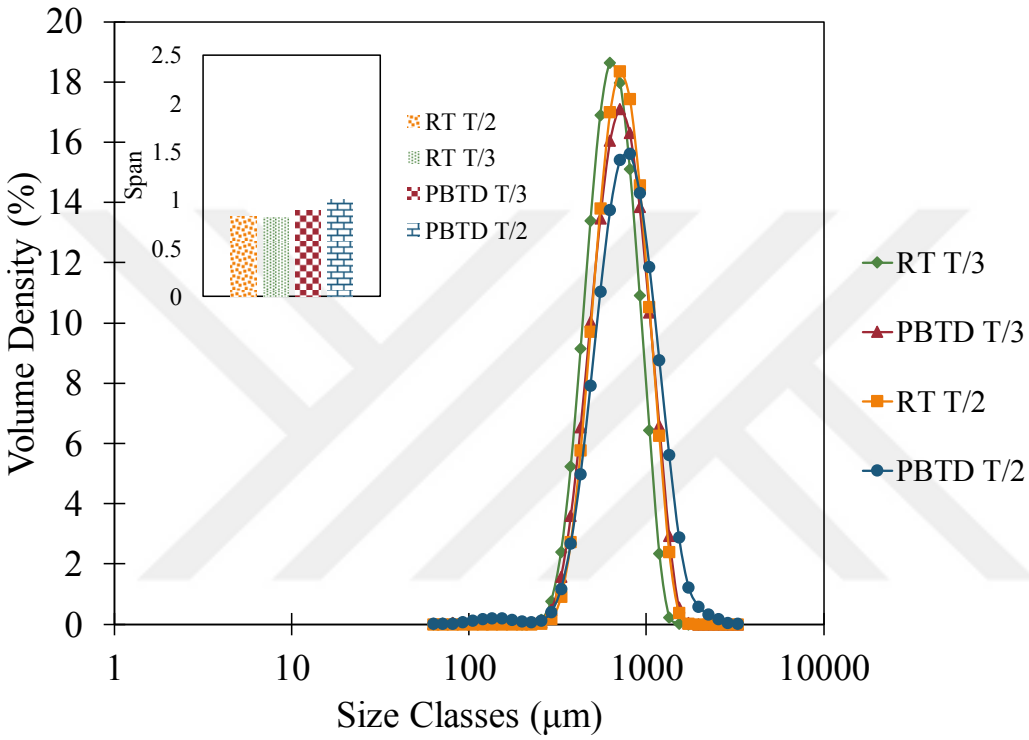

Figure 3.38. Drop size distribution of all impellers at the same power/mass ratio: 400 at e/T=0.1

The effect of power/mass ratio on drop size when the impellers are positioned at e/T=0.2 is shown in Figure 3.39. When power/mass ratio is 400, the smallest drops are obtained with RT T/3 and other impellers give similar size drops. At this eccentricity ratio, flow patterns created by the impellers are the same. Vortex in the tank begins to disappear and contact of the impellers with the liquid increases. Among the impellers, PBTD T/3 has the highest impeller speed at the same power/mass ratio.

However, when the impeller speeds are too high, drop coalescence overcome drop breakup process. Therefore, the smallest drops are not obtained with PBTD T/3.

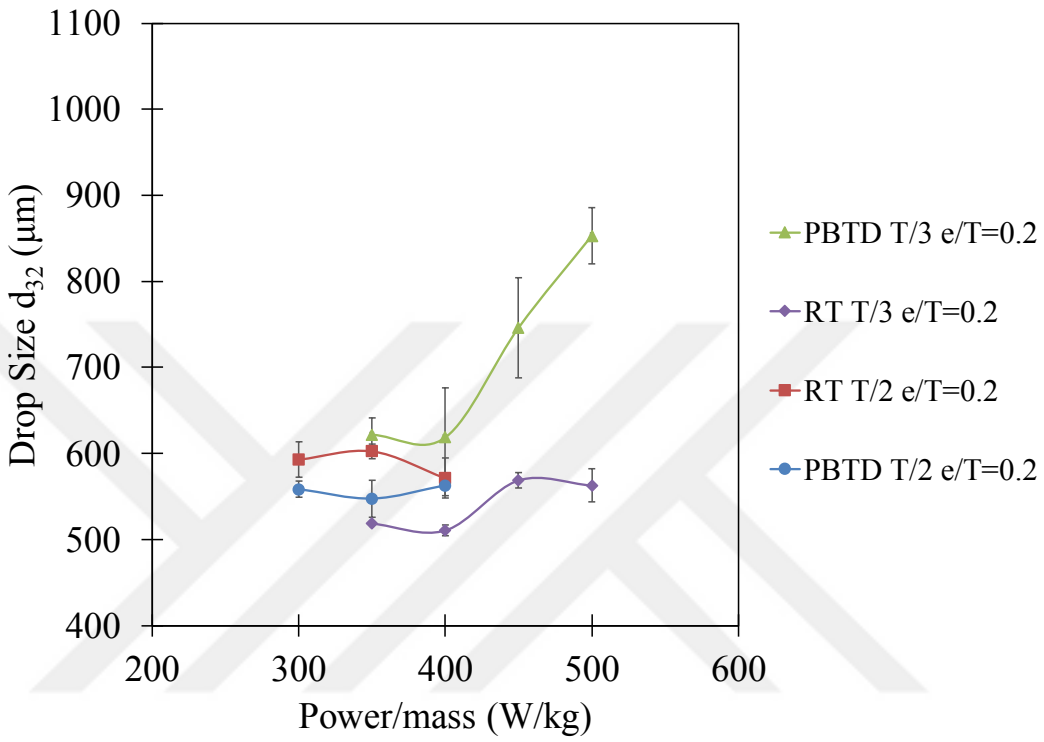

Figure 3.39. The effect of power/mass on drop size at e/T=0.2

Figure 3.40 shows drop size distribution of all impellers at the same power/mass ratio, 400, when the impellers are located at e/T=0.2. Even if RT T/2, PBTD T/2 and PBTD T/3 produce the same size drops, PBTD T/3 has the largest drop size. PBTD T/3 also has the largest drop size distribution. Even though RT T/3 gives the smallest drops, its drop size distribution is not good. The T/2 impellers perform better performances in terms of drop size distribution.

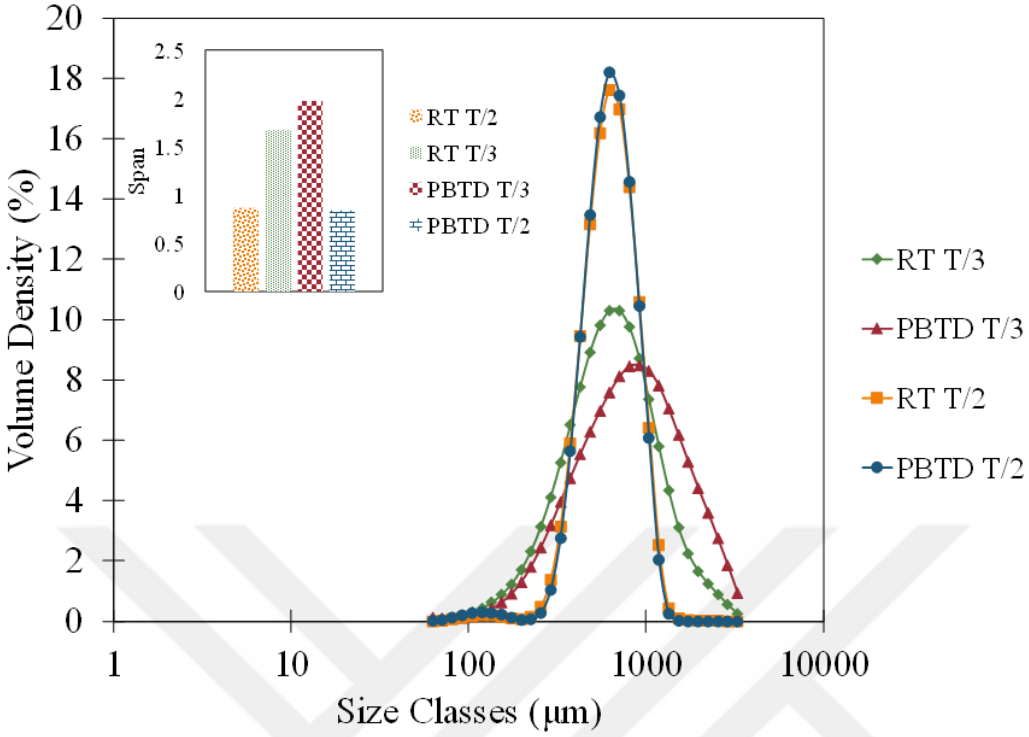

Figure 3.40. Drop size distribution of all impellers at the same power/mass ratio: 400 at e/T=0.2

Figure 3.41 shows the effect of eccentricity on drop size for all impellers at the same power/mass ratio of 400. Almost all impellers give the smallest drops when they are located at e/T=0.2. When the eccentricity ratio increases, vortex becomes smaller and begins to disappers. Therefore, contact of the impellers with the liquid in the tank increases and this leads to increase in performances of the impellers. With PBTD T/2, the smallest drops are obtained at e/T=0.2, but it should be noted that the differences between different positions of the shaft are very small.

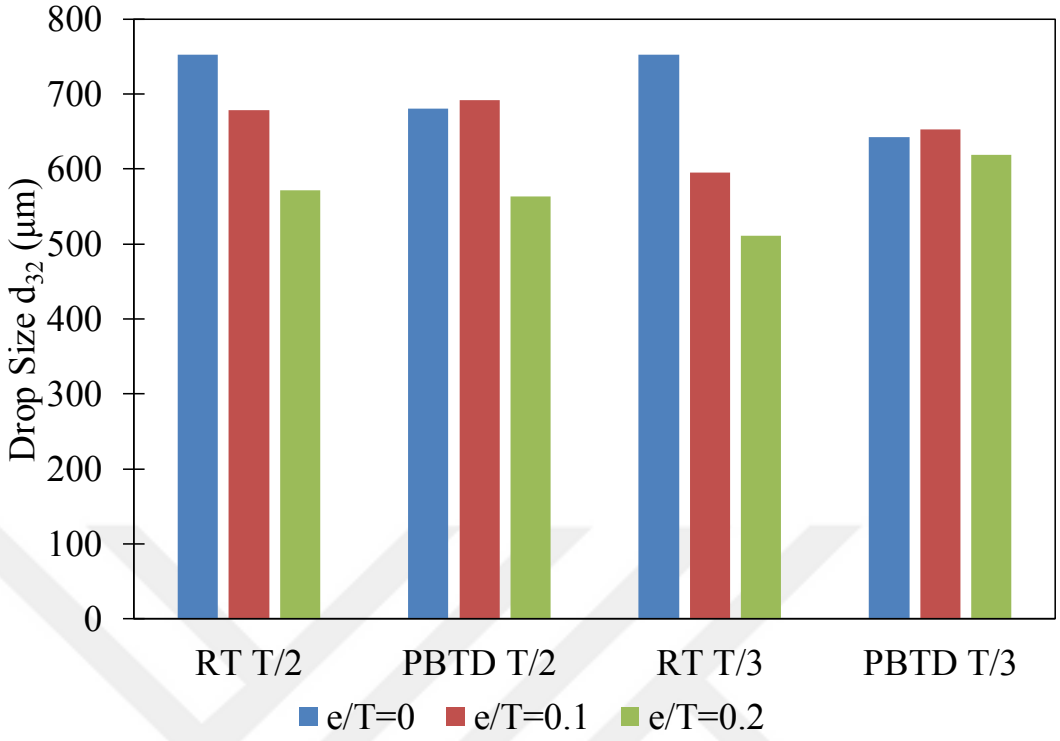

Figure 3.41. Effect of eccentricity on drop size (power/mass=400)

3.3. Comparison of Performances of PBTU and PBTD Impellers at the Same V_{tip}

PBTD impeller provides liquid to move first to bottom of the tank and then to surface of the tank. On the other hand, PBTU impeller allows liquid to move first to surface of the tank and then to bottom of the tank. Since oil dispersion and particle suspension should be done at the same time for the production of Pickering emulsions, determination of which type of PBT impeller gives the best performance in terms of drops size and drop size distribution of Pickering emulsion was aimed in this part of the study. The selected impeller tip speeds and corresponding impeller speeds are the same in chapter 3.1.1. To clarify differences in performances of PBTD and PBTU impellers, comparison should be done at the same impeller tip speed: 132 m/min. When the impellers are located at e/T=0, formed vortices in water filled tanks at the

same impeller tip speed are shown in Figure 3.42. The size of formed vortex and air cavity below the impellers are very similar for the same size impellers.

a) PBTD T/3

b) PBTD T/2

c) PBTU T/3

d) PBTU T/2

Figure 3.42. Formed vortices at the same impeller tip speed (132 m/min at e/T=0)

The large impellers have similar flow patterns. As mentioned previously, radial component of flow pattern of PBT impeller is dominant in the tank when the size of the impeller is T/2. While radial component of flow pattern created by PBTD impeller has downward inclination, radial component of flow pattern created by PBTU impeller has upward inclination. However, both impellers create double loop in the tank. As opposed to the large impellers, the small impellers create just one single loop in the tank when they are at the center of the tank. While PBTD T/3 push the fluid to the bottom of the tank, PBTU T/3 push the fluid to the surface of the tank.

The effect of impeller tip speed on drop size is seen in Figure 3.43 when the impellers are located at e/T=0. At the same impeller tip speed, the large impellers give almost the same size drops. The central vortex creates a vacuum effect, allowing the oil phase to be dispersed in the system more effectively. Since the depth of the vortex and flow patterns created by the large impellers are almost the same, they show similar performance and produce the same size drops. Among the small impellers, PBTD gives smaller drops than PBTU. This is an indication that flow pattern with downward inclination in the system is more effective to obtain smaller drops. The large impellers produce smaller drops then the small impellers. Since the large impellers have larger impeller zone and smaller circulation time, drops are exposed to shear more frequently. Therefore, smaller drops are formed.

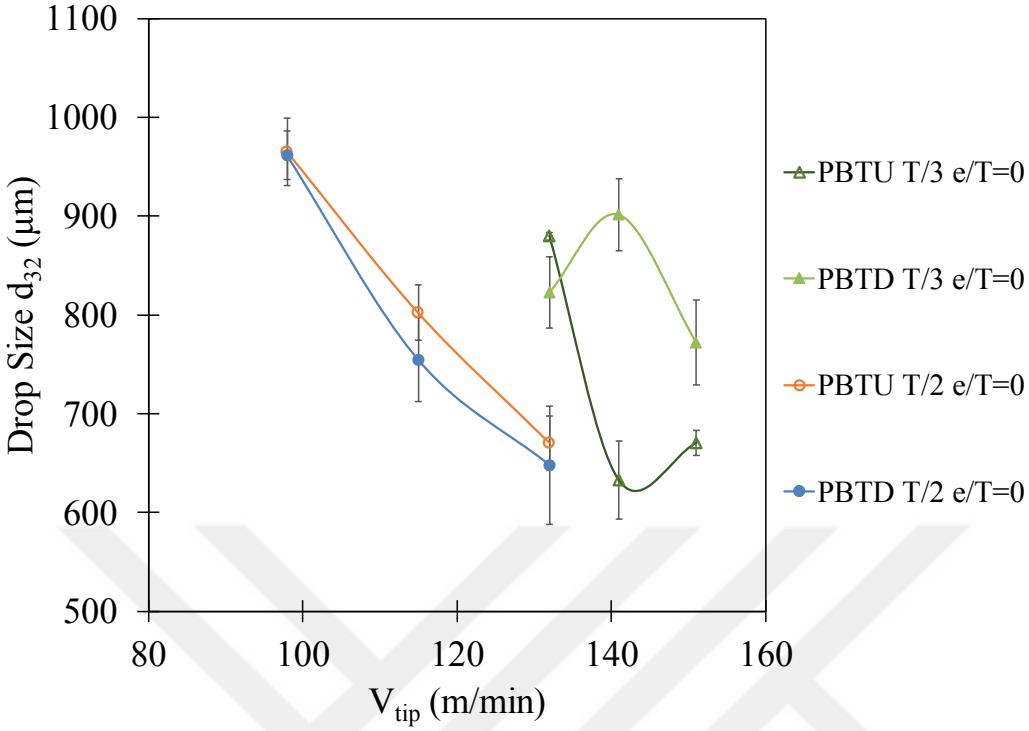

Figure 3.43. The effect of impeller tip speed on drop size at e/T=0

Figure 3.44 shows drop size distribution of all impellers at the same impeller tip speed when they are located at e/T=0. Impellers produce smaller drop size also have narrower drops size distribution. PBTU impellers show the worst performance not only in terms of drop size but also in terms of drop size distribution.

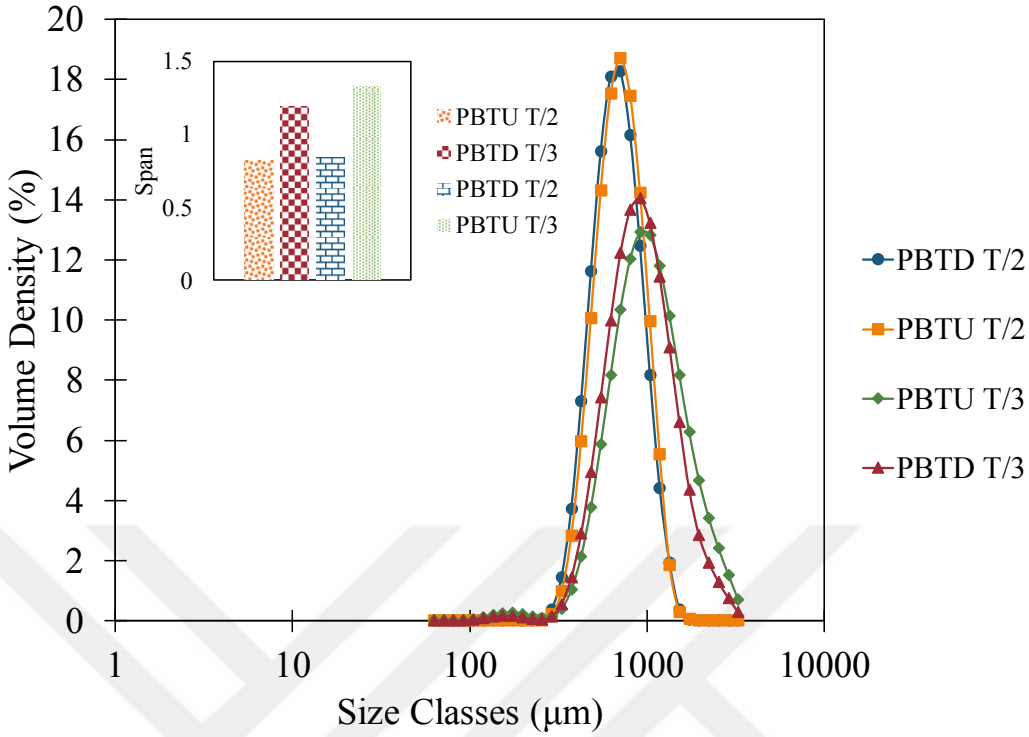

Figure 3.44. Drop size distribution of all impellers at the same V_{tip} (at e/T=0)

When the impellers are located at e/T=0.1, the sizes of the vortices are almost the same for the large impellers as seen in Figure 3.45. However, these vortices are smaller compared to centered case. Flow patterns created by the large impellers are similar also. While the sizes of the vortices created by the small impellers are similar when they are at e/T=0, they are different when the shaft is positioned at e/T=0.1. The vortex created by PBTU T/3 does not reach the impeller and smaller than the vortex created by PBTD T/3. Flow patterns created by the small impellers are also different.

a) PBTD T/3

b) PBTD T/2

c) PBTU T/3

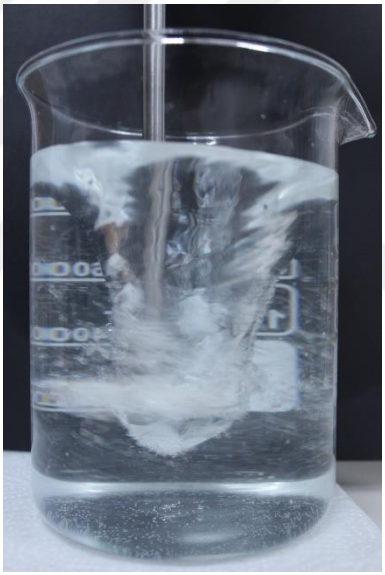

d) PBTU T/2

Figure 3.45. Formed vortices at the same impeller tip speed (132 m/min at e/T=0.1)

The effect of impeller tip speed on drop size when the impellers are located at e/T=0.1 is shown in Figure 3.46. Even though the flow patterns and the sizes of the vortices are similar for the large impellers, PBTD T/2 gives smaller drops. Since the size of the vortex becomes smaller compared to centered case, dispersion of the oil phase into

the system is affected. Based on the results, it can be said that flow pattern with downward inclination provides better dispersion of the oil phase and glass beads in the system. Thus, smaller drops are formed. This inference is also valid for the small impellers. Since the vortex created by PBTU T/3 does not reach the impeller and the fluid coming from the impeller zone goes toward the surface of the tank, entering of the oil phase that located at the upper part of the tank into the system becomes more difficult and required higher impeller speed compared to PBTD T/3. Weak dispersion of the oil phase results in formation of larger drops. PBTD impellers produce smaller drops regardless of the size of the impellers.

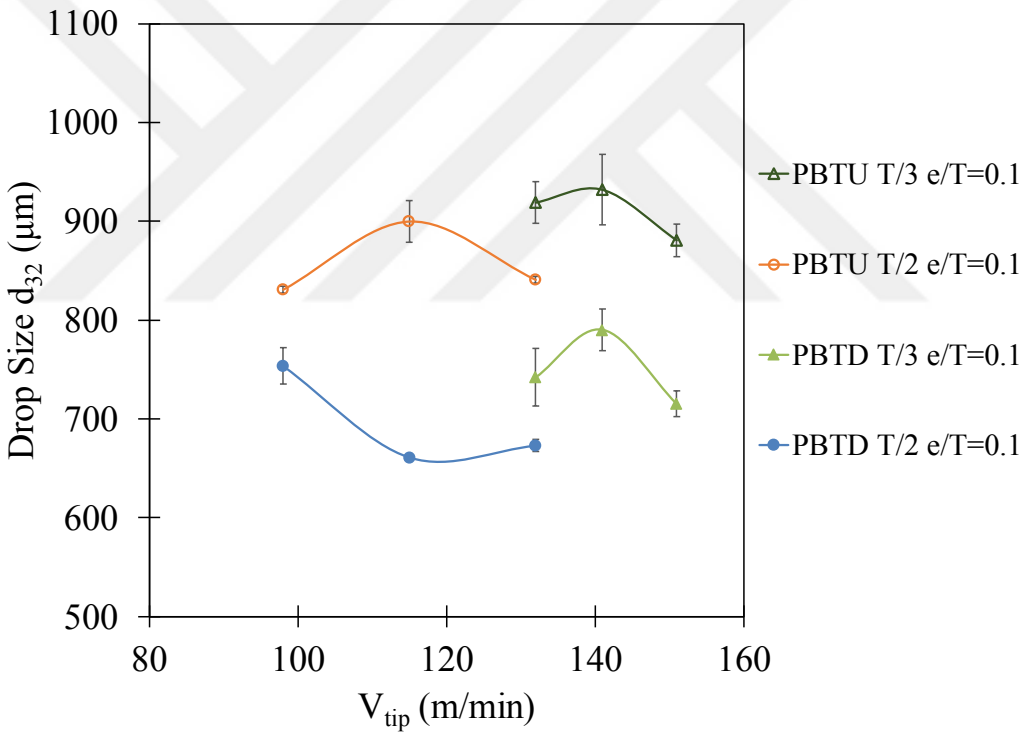

Figure 3.46. The effect of impeller tip speed on drop size at e/T=0.1

Figure 3.47 shows drop size distribution of all impellers at the same impeller tip speed when they are located at e/T=0.1. PBTD T/2 produce the smallest drop size also has

the narrowest drops size distribution. PBTU T/3 impellers show the worst performance not only in terms of drop size but also in terms of drop size distribution.

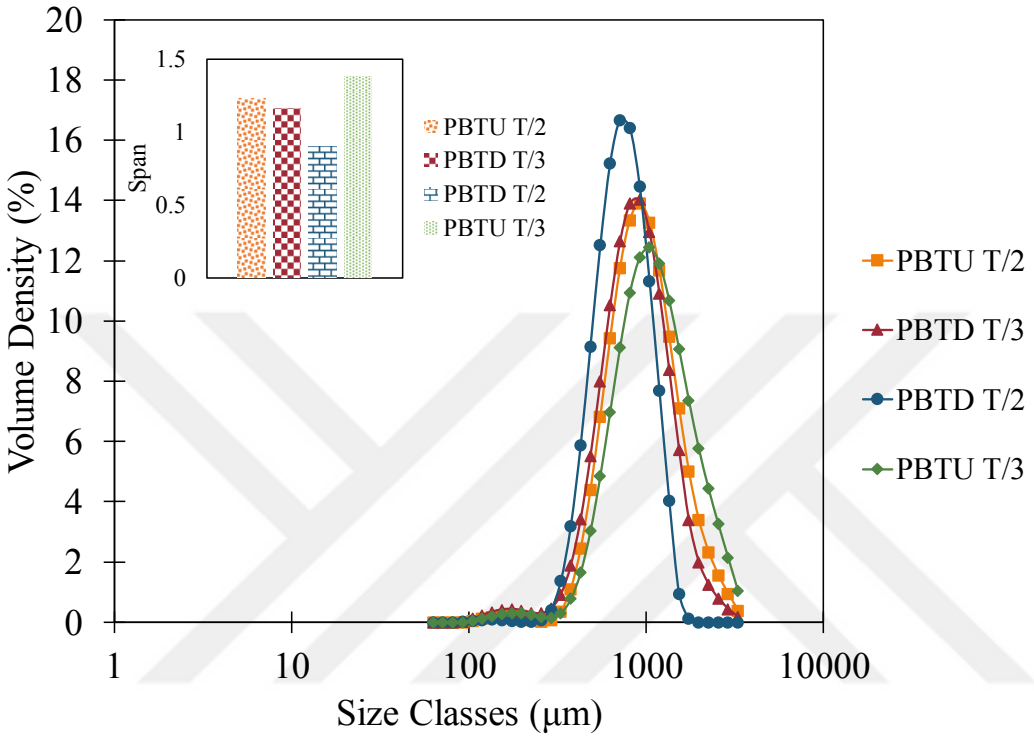

Figure 3.47. Drop size distribution of all impellers at the same V_{tip} (at e/T=0.1)

When the impellers are located at e/T=0.2, flows created by the impellers are shown in Figure 3.48. The size of the vortex created by PBTD T/3 becomes smaller compared to the other shaft positions as mentioned previously. This vortex also has a vertical inclination. When PBTU T/3 impeller is used at e/T=0.2, there is no vortex formation in the tank and higher impeller speed is required for effective dispersion especially for the oil phase. The vortex created by PBTD T/2 begins to disappear and flow gains an elliptic path in the tank. When PBTU T/2 impeller is used, a lower vortex is formed instead of an upper vortex and elliptic flow pattern is created.

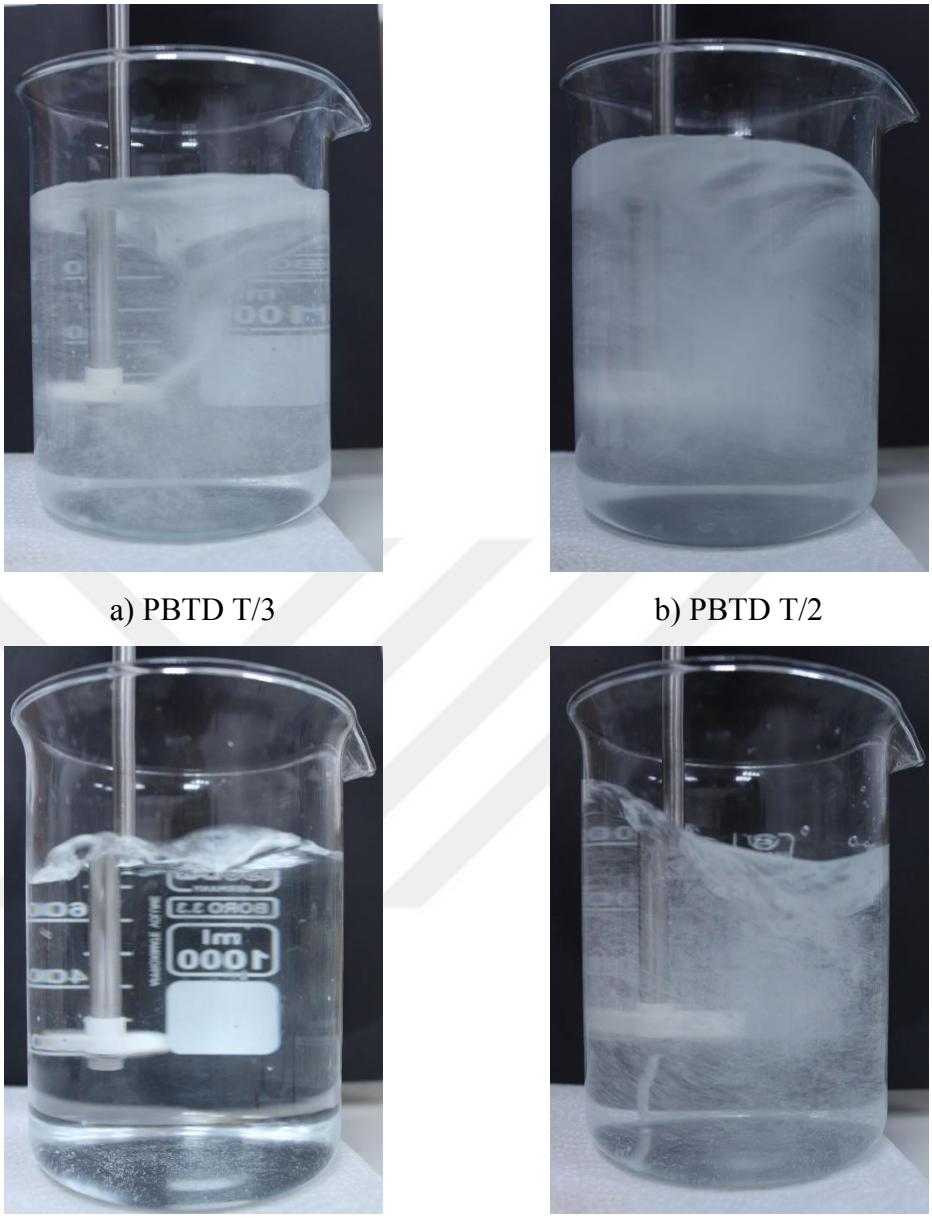

a) PBTD T/3 b) PBTD T/2

c) PBTU T/3 d) PBTU T/2

Figure 3.48. Formed vortices at the same impeller tip speed (132 m/min at e/T=0.2)

When the impellers are positioned at e/T=0.2, as seen in Figure 3.49, the large impellers give smaller drops than the small impellers. The large impellers have larger impeller zone; therefore, they form smaller drops because drop breakup occurs mostly in the impeller zone. Also, their circulation time is smaller, and drops are exposed to

shear more frequently with the large impellers. PBTD T/3 impeller produces smaller drops than PBTU T/3 impeller. There is still a vortex in the tank when PBTD T/3 is used and even if it is smaller compared to other vortices created at other shaft positions, it helps entering of oil phase to the system. For the same size impellers, PBTD creates smaller drops than PBTU. This is an indication that better dispersion and drop breakup are provided with PBTD impellers. Amira et al. (2013) performed a study with 6 bladed PBTD T/3 and PBTU T/3 and they found that PBTD has higher turbulent kinetic energy than PBTU. The higher the turbulent kinetic energy the easier the drop breakup. This is another reason to obtain smaller drops with PBTD impellers.

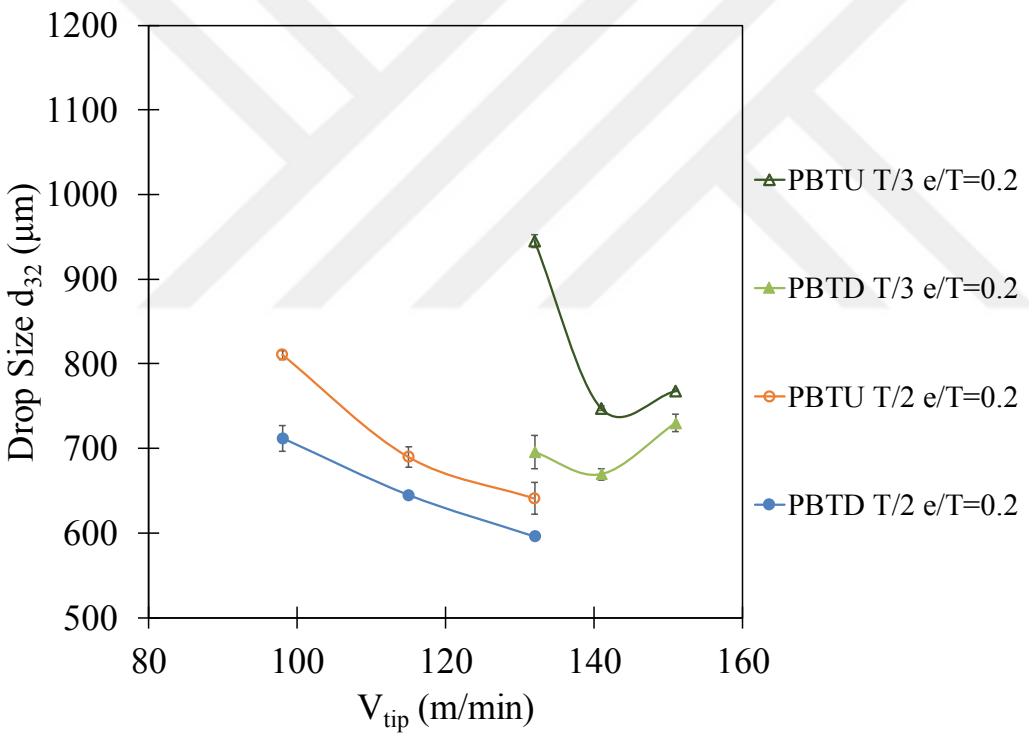

Figure 3.49. The effect of impeller tip speed on drop size at e/T=0.2

Drop size distribution of all impellers at e/T=0.2 is given in Figure 3.50. The large impellers have narrower drop size distribution than the small impellers. For the same

size impellers, PBTD impellers give narrower drop size distribution. The best performance in terms of drop size and drop size distribution is obtained with PBTD T/2.

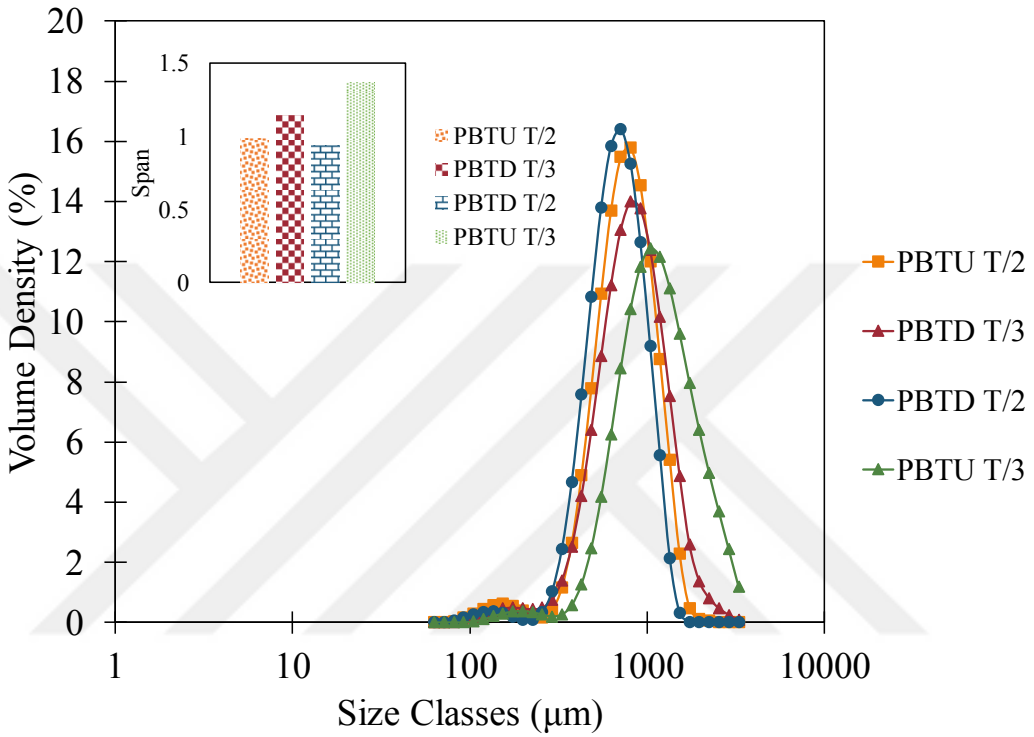

Figure 3.50. Drop size distribution of all impellers at the same V_{tip} (at e/T=0.2)

PBTD T/2 shows the best performance and produces the smallest drops when it is located at e/T=0.2 as shown in Figure 3.51. As the eccentricity ratio increases, drop size obtained with PBTU T/3 increases because increase in eccentricity ratio causes decrease in the size of vortex and this situation makes entering of oil phase into the system difficult. Also, it has smaller impeller zone, and this contributes to its poor performance.

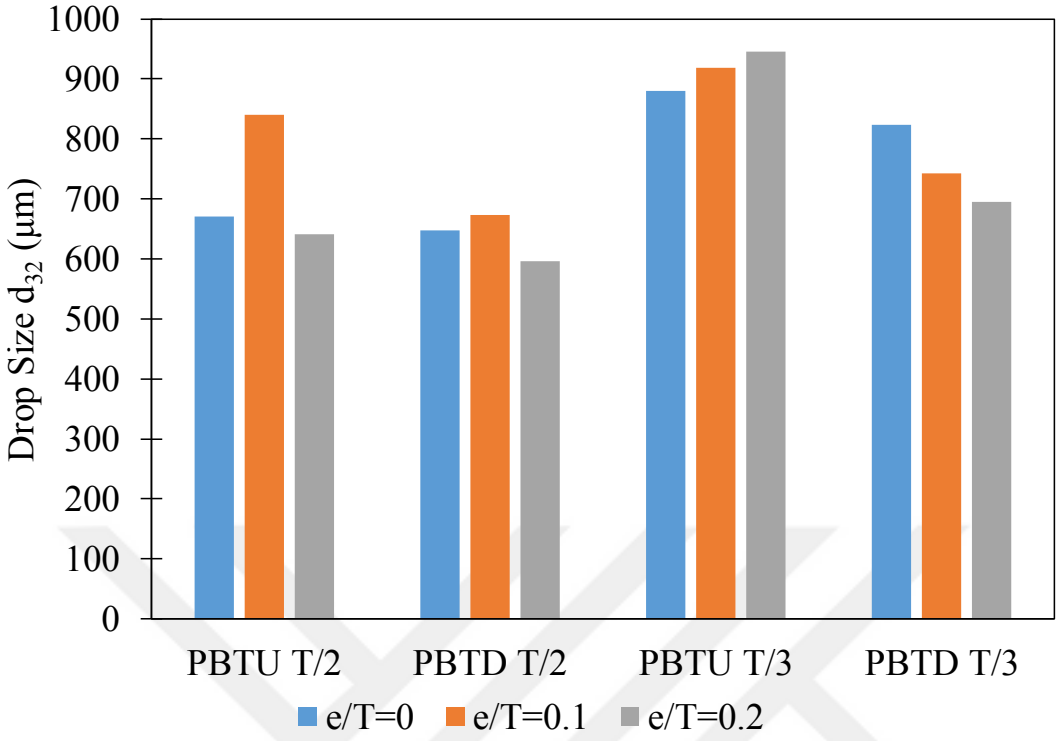

Figure 3.51. Effect of eccentricity on the impellers at the same V_{tip}

3.4. Mixing Time Analysis

Mixing time is the time taken to reach a certain degree of homogeneity (Cabaret et al., 2007). Mixing time analysis can be utilized to investigate performance differences of the impellers in a stirred tank. In this thesis, mixing time analysis was performed with three types of impeller which are PBTU, PBTD and RT when they are located at three different positions in an unbaffled stirred tank. The comparison of the performances of the impellers were done at the same impeller speed which is 865 rpm. Figure 3.52 shows the results. According to results, mixing time of the large impellers are shorter than the small impellers. This is caused by having larger impeller zone of the large impellers. Also, for the same type of an impeller, circulation time of the large impeller is smaller than the small impeller. Therefore, the large impellers provide better circulation, and this causes decrease in the time taken to achieve a certain degree of

homogeneity. The small impellers have smaller impeller zone and larger circulation time, so they provide poor circulation in the tank. Therefore, the time required to reach a certain degree of homogeneity is longer when the small impellers are used.

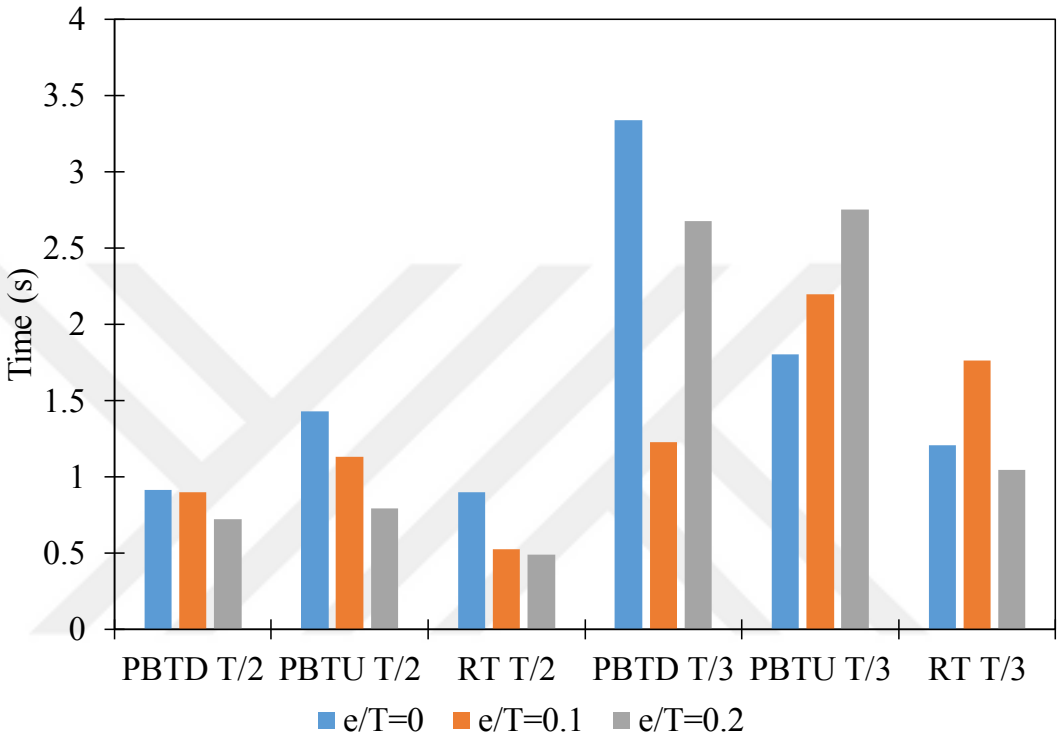

Figure 3.52. Mixing time analysis for all impellers at the same impeller speed (865 rpm)

With the large impellers, mixing time decreases as the eccentricity ratio increases. A similar result was obtained in the study conducted by Karcz and Szoplik (2004). They performed their experiments with propeller agitator in different pumping mode at centric and eccentric positions. They observed that increase in eccentricity causes decrease in mixing time and working at down pumping mode also decreases the mixing time. As seen in Figure 3.52, PBTD T/2 has smaller mixing time than PBTU T/2 impeller. However, the same observations could not be obtained with the small impellers. Even if pumping capacity of PBT impellers is higher than RT impeller, the

time require to reach a certain degree of homogeneity is shorter when RT impeller is used regardless of its size. RT T/2 at e/T=0.2 provides homogeneity in the system in a shorter time.

When the mixing time and drop size, results were considered no relationship was found. Impellers show different performances in mixing time experiments and emulsification experiments. While the smallest drops and the narrowest drop size distribution were obtained with RT T/3 impeller at e/T=0.2, the shortest time required to reach 95% homogeneity was achieved with RT T/2 at e/T=0.2. Also, mixing time experiments take seconds. On the other hand, emulsification experiments take 3 hours and homogeneity in the tank has already been achieved in 3 hours. The most important common result of mixing time and drop size analysis is that the best performances were obtained when the shaft is located at e/T=0.2.

CHAPTER 4

SUMMARY, OUTCOMES AND FUTURE WORK

4.1. Summary and Outcomes

In this thesis, the effect of different hydrodynamic conditions on the production of Pickering emulsions in unbaffled stirred tanks was investigated. Oil in water Pickering emulsions were produced. Physicochemical properties of the emulsions such as the type of oil, oil to water volumetric ratio, the amount of glass beads and the viscosity of the oil were kept constant to observe only the effect of hydrodynamics on drop size and drop size distribution. Hydrodynamic parameters such as impeller tip speed, Reynolds number, Weber number and power per mass were varied to create different hydrodynamic conditions. Performances of two different types of impellers at two different sizes to find optimum mixing geometry were compared: PBTD and RT. Apart from RT and PBTD impellers, performance of PBTU at two different sizes was also compared at different impeller tip speeds. Shaft was located at three different positions: e/T=0, e/T=0.1 and e/T=0.2. The conclusions of this thesis are given as the following:

- Drop size and drop size distributions are affected by the following factors: change in flow patterns created by the impellers due to change in the location of the shaft, the size of the vortex, the amount of energy dissipated into the system, the size of the impeller zone and circulation time of the impellers.
- When the shaft is located at the center, a central vortex forms at the free surface. The depth of the vortex increases with increase in the impeller speed. When the vortex reaches the impeller, air entrainment occurs into the system. After a certain impeller speed, an air cavity also forms below the impellers. At

the same impeller speed, the size of the vortex is larger with RT impellers compared to PBTD impellers.

- When the impellers are located eccentrically, asymmetric upper vortex forms at the region where the shaft is away from the tank wall instead of symmetric, central vortex. As the eccentricity ratio increases, inclination of the upper vortex relative to vertical axis increases. A lower vortex forms below the impellers after certain impeller speeds. The flow is mostly dominated by the upper vortex. The effect of the lower vortex on the system is very weak. When the impellers are located at e/T=0.2. All impellers create the same flow pattern. At the region where the shaft is close to the tank wall, double loops are created. At the region where the shaft is away from the tank, the vortex begins to disappear, and the liquid circulates as elliptic vertical.
- The large impellers create similar flow patterns in the tank regardless of the shaft position. When most parts of the large impellers remain in the vortex, they produce almost the same size drops. Since the contact of the impellers with the liquid in the tank is small due to vortex, shear created by the impellers cannot be transferred to the system effectively. High shear property of RT impellers compensated with having smaller circulation time with PBTD impellers. When the vortex begins to disappear on the other hand, the amount of energy dissipated into the system is dominant in determining of drop size rather than having smaller circulation time. To conclude, for the large impellers, the depth of the vortex in the tank has more impact on drop size than the amount of energy dissipated into the system or circulation time.
- When the shaft is at the center, at low impeller speeds, the small impellers produce smaller drops since more energy is dissipated into the system with the small impellers and more turbulence intensity created in the system due to having higher impeller speeds. The higher the energy dissipated into the system the smaller the drops are formed. However, at high impeller speeds, the large impellers produce the smaller drops because at high impeller speeds,

particle detachment occurs when the small impellers are used. Therefore, coalescence occurs, and large drops are formed. On the other hand, the large impellers produce smaller drops at high impeller speeds because drop breakup still dominates at that impeller speeds. Also, they have larger impeller zone and drops are exposed to shear more effectively. According to these results, while at low impeller speeds, the amount of energy dissipated into the system has more effect on drop size, at high impeller speeds, having larger impeller zone mostly affects the formation of smaller drops.

- When the shaft is located eccentrically, the amount of energy dissipated into the system has an important effect on drop size. Since power number of RT impeller is larger, it gives more energy into the system and produces the smallest drops. Since increase in eccentricity leads to increase in contact of the impellers with the liquid, the smallest drops are obtained with RT T/3 when it is positioned at e/T=0.2
- The usage of PBTD T/3 impeller for the production of Pickering emulsions is not suitable. Since oil dispersion and particle suspension could not be done effectively at the same time. Also, particle adsorption could not be sufficient with this impeller. Therefore, when PBTD T/3 impeller is used, coalescence occurs, larger drops are formed, and larger drop size distribution is obtained. The same observation is also obtained in the study that the production of Pickering emulsion was performed in baffled stirred tanks (Abdulrasaq and Ayranci, 2019).
- When the performance of PBTD and PBTU impellers are compared at the same impeller tip speed, it is found that performance of PBTD impellers is better than PBTU impellers. The vortex created in the system with higher depth allows oil phase entering the system more effectively. That means dispersion performance of PBTD impellers are more suitable for the production of Pickering emulsions. Also, the large impellers have larger impeller zone compared the small impellers. Since drop breakup occurs mostly in the

impeller zone, the large impellers form smaller drops. The best performance among PBT impellers is obtained with PBTD T/2 impeller when it is located at e/T=0.2.

4.2. Future Work

In this thesis the effect of hydrodynamics on the production of Pickering emulsions was investigated. The content of studies related to the effect of hydrodynamics on the production of Pickering emulsions is still scant. The topics that can be investigated can be summarized as the following:

- Scale-up studies are needed for application of the results of this thesis to industrial tanks.
- Different types of oil that have different viscosity values can also be tested to see the effect of viscosity on drop size of Pickering emulsions.
- In this study, the selected power/mass values were calculated by taking the power number values of the impellers for baffled case due to lack of information related to unbaffled case. There are a few studies about the impeller power numbers in unbaffled tanks where the shaft is located at the center and at the eccentric position. However, the results contradict. Therefore, studies should be done to remove contradictions.
- The effect of different off-bottom clearances on drop size can also be investigated for this study.
- The effect of different oil/water content can be tested. To clarify drop breakup process and to decrease drop coalescence lower oil/water content can be used.
- Elliptic particles which provide better surface coverage can be tested instead of spherical ones to investigate how the difference in coverage of the particles will affect drop size and drop size distribution at different hydrodynamic conditions.

REFERENCES

A Basic Guide to Particle Characterization. (2015). Retrieved from www.malvern.com/contact

Abdulrasaq, U. K., & Ayranci, I. (2019). The effect of hydrodynamic parameters on the production of Pickering emulsions in a baffled stirred tank. *AIChE Journal*, (May), 1–12. https://doi.org/10.1002/aic.16691

Adamson, A. W., & Gast, A. P. (1997). *Physical Chemistry of Surface* (6 th). John Wiley & Sons, Inc.

Aloi, L. E., & Cherry, R. S. (1996). *Cellular Response to Agitation Characterized by Energy Dissipation at the Impeller Tip*. *51*(9), 1523–1529.

Assirelli, M., Bujalski, W., Eaglesham, A., & Nienow, A. W. (2008). Macro- and micromixing studies in an unbaffled vessel agitated by a Rushton turbine. *Chemical Engineering Science*, *63*(1), 35–46. https://doi.org/10.1016/j.ces.2007.07.074

Aydın, E. (2015). Effect of Calculation Models on Particle Size Distribution Estimated by Laser Diffraction. *9th International Soil Science Congress on "The Soul of Soil and Civilization,"* (January). Retrieved from https://www.researchgate.net/publication/299263782%0AEffect

Bancroft, W. D. (1913). The Theory of Emulsification, V. *The Journal of Physical Chemistry*, *17*, 501–519. https://doi.org/10.1021/j150141a002

Bhattacharya, S., Hebert, D., & Kresta, S. M. (2007). Air entrainment in baffled stirred tanks. *Chemical Engineering Research and Design*, *85*(5 A), 654–664. https://doi.org/10.1205/cherd06184

Binks, B. P., & Fletcher, P. D. I. (2001). Particles Adsorbed at the Oil-Water Interface: A Theoretical Comparison between Spheres of Uniform Wettability and "Janus"

Particles. *Langmuir*, *17*(16), 4708–4710. https://doi.org/10.1021/la0103315

Binks, B. P., & Lumsdon, S. O. (2001). Pickering Emulsions Stabilized by Monodisperse Latex Particles: Effects of Particle Size. *Langmuir*, *17*(15), 4540–4547. https://doi.org/10.1021/la0103822

Binks, B. P. (2002). Particles as surfactants - Similarities and differences. *Current Opinion in Colloid and Interface Science*, *7*(1–2), 21–41. https://doi.org/10.1016/S1359-0294(02)00008-0

Binks, B. P., Murakami, R., Armes, S. P., & Fujii, S. (2006). Effects of pH and Salt Concentration on Oil-in-Water Emulsions Stabilized Solely by Nanocomposite Microgel Particles. *Langmuir*, *22*(5), 2050–2057. https://doi.org/10.1021/la053017+

Binks, B. P, & Clint, J. H. (2002). *Solid Wettability from Surface Energy Components : Relevance to Pickering Emulsions*. (1), 1270–1273. https://doi.org/10.1021/la011420k

Busciglio, A., Scargiali, F., Grisafi, F., & Brucato, A. (2016). Oscillation Dynamics of Free Vortex Surface in Uncovered Unbaffled Stirred Vessels. *Chemical Engineering Journal*, *285*, 477–486. https://doi.org/10.1016/j.cej.2015.10.015

Cabaret, F., Bonnot, S., Fradette, L., & Tanguy, P. A. (2007). Mixing time analysis using colorimetric methods and image processing. *Industrial and Engineering Chemistry Research*, *46*(14), 5032–5042. https://doi.org/10.1021/ie0613265

Casagrande, C., Fabre, P., Raphaël, E., & Veyssié, M. (1989). "Janus Beads": Realization and Behaviour at Water/Oil Interfaces. *Epl*, *9*(3), 251–255. https://doi.org/10.1209/0295-5075/9/3/011

Chapple, D., Kresta, S. M., Wall, A., & Afacan, A. (2002). The effect of impeller and tank geometry on power number for a pitched blade turbine. *Chemical Engineering Research and Design*, *80*(4), 364–372. https://doi.org/10.1205/026387602317446407

Chesters, A. K. (1991). The Modelling of Coalescence Processes in Fluid-Liquid Dispersions : A Review of Current Understanding. *Chemical Engineering Research and Design*, *69*(4), 259–270.

Chevalier, Y., & Bolzinger, M. A. (2013). Emulsions Stabilized with Solid Nanoparticles: Pickering Emulsions. *Colloids and Surfaces A: Physicochemical and Engineering Aspects*, *439*, 23–34. https://doi.org/10.1016/j.colsurfa.2013.02.054

Choplin, L., Torandell, S., & Servoin, J. (1998). In Situ Rheological Monitoring in Semi-batch Emulsification Process for Cosmetic Lotion Production. *The Canadian Journal of Chemical Engineering*, *76*. https://doi.org/10.1002/cjce.5450760321

Comstock, J. M. (1992). *Emulsions Fundamentals and Applications in the Petroleum Industry* (L. L. Schramm, Ed.). https://doi.org/10.1021/ba-1992-0231.fw001

Coulaloglou, C. A., & Tavlarides, L. L. (1977). Description of interaction processes in agitated liquid-liquid dispersions. *Chemical Engineering Science*, *32*(11), 1289–1297. https://doi.org/10.1016/0009-2509(77)85023-9

Delaplace, G., Bouvier, L., Moreau, A., Guérin, R., & Leuliet, J. C. (2004). Determination of mixing time by colourimetric diagnosis - Application to a new mixing system. *Experiments in Fluids*, *36*(3), 437–443. https://doi.org/10.1007/s00348-003-0741-7

Devi, T., & Kumar, B. (2017). Vortex Depth Analysis in an Unbaffled Stirred Tank with Concave Blade Impeller. *Chemistry & Chemical Technology*, *11*(3), 301–307.

Drelich, A., Gomez, F., Clausse, D., & Pezron, I. (2010). Evolution of Water-in-Oil Emulsions Stabilized with Solid Particles Influence of Added Emulsifier. *Colloids and Surfaces A: Physicochemical and Engineering Aspects*, *365*(1–3), 171–177. https://doi.org/10.1016/j.colsurfa.2010.01.042

Galletti, C, Pintus, S., & Brunazzi, E. (2008). Effect of shaft eccentricity and impeller blade thickness on the vortices features in an unbaffled vessel. *Chemical Engineering Research and Design*, *7*(October), 391–400. https://doi.org/10.1016/j.cherd.2008.11.013

Galletti, Chiara, & Brunazzi, E. (2008). On the main flow features and instabilities in an unbaffled vessel agitated with an eccentrically located impeller. *63*, 4494–4505. https://doi.org/10.1016/j.ces.2008.06.007

Grenville, R. K., Giacomelli, J. J., Mixing, P., Brown, D. A. R., Padron, G. A., & Dispersions, L. L. (2017). Impeller Performance in Stirred Tanks. *Chemical Engineering*, (August). Retrieved from https://www.researchgate.net/publication/319042061%0AMixing:

Griffin, W. C. (1949). Classification of Surface-Active Agents by HLB. *Journal of the Society of Cosmetic Chemists*, *1*, 311–326. Retrieved from https://pdfs.semanticscholar.org/8f10/78fe0193580f16afac0e0cb14d2471b7e338.pdf

Haque, J. N., Mahmud, T., Roberts, K. J., & Rhodes, D. (2006). Modeling turbulent flows with free-surface in unbaffled agitated vessels. *Industrial and Engineering Chemistry Research*, *45*(8), 2881–2891. https://doi.org/10.1021/ie051021a

Hekmat, D., Hebel, D., & Schmid, H. (2007). Crystallization of Lysozyme : from Vapor Diffusion Experiments to Batch Crystallization in Agitated ml-scale Vessels. *Process Biochemistry*, *42*, 1649–1654. https://doi.org/10.1016/j.procbio.2007.10.001

Hemrajani, R. R., & Tatterson, G. B. (2004). Mechanically Stirred Vessels. In E. L. Paul (Ed.), *Handbook of Industrial Mixing: Science and Practice*. https://doi.org/10.1002/0471451452.ch6

Jaworski, Z., Dyster, K. N., & Nienow, A. W. (2001). The Effect of Size, Location and Pumping Direction of Pitched Blade Turbine Impellers on Flow Patterns:

LDA Measurement and CFD Predictions. *Institution of Chemical Engineers*, *79*(November), 4–11.

Kaptay, G. (2006). On the Equation of the Maximum Capillary Pressure Induced by Solid Particles to Stabilize Emulsions and Foams and on the Emulsion Stability Diagrams. *Colloids and Surfaces A: Physicochemical and Engineering Aspects*, *282–283*, 387–401. https://doi.org/10.1016/j.colsurfa.2005.12.021

Karcz, J., & Szoplik, J. (2004). An effect of the eccentric position of the propeller agitator on the mixing time. *Chemical Papers*, *58*(1), 9–14.

Khan, B. A., Akhtar, N., Khan, H. M. S., Waseem, K., Mahmood, T., Rasul, A., Khan, H. (2012). Basics of pharmaceutical emulsions: A review. *African Journal of Pharmacy and Pharmacology*, *5*(25), 2715–2725. https://doi.org/10.5897/AJPP11.698

Leng, D. E., & Calabrese, R. V. (2004). Immiscible Liquid-Liquid Systems. In E. L. Paul (Ed.), *Handbook of Industrial Mixing: Science and Practice* (pp. 639–753). John Wiley & Sons, Inc.

Levine, S., Bowen, B. D., & Partridge, S. J. (1989). *Stabilization of Emulsions by Fine Particles II . Capillary and van der Waals Forces Between Particles*. *38*, 345–364.

Lipin, A. G., Lipin, A. A., & Wojtowicz, R. (2017). The Performance of the Rushton Turbine Eccentrically Positioned in a Mixing Vessel. Part I: The Qualitative CFD Analysis. *Technical Transactions*, 191–196. https://doi.org/10.4467/2353737XCT.17.100.6576

Madivala, B., Vandebril, S., Fransaer, J., & Vermant, J. (2009). Exploiting Particle Shape in Solid Stabilized Emulsions. *Soft Matter*, *5*(8), 1717–1727. https://doi.org/10.1039/b816680c

Malvern, I. L. (2017). Mastersizer 3000 User Manual.

Mastersizer 3000.

Retrieved from https://www.malvernpanalytical.com/en/products/product-range/mastersizer-range/mastersizer-3000

McClements, D. J. (2016). *Food Emulsions Principles, Practices and Techniques* (Third). https://doi.org/10.1016/S0376-7361(09)70018-4

McClements, D. J., & Gumus, C. E. (2016). Natural emulsifiers — Biosurfactants, phospholipids, biopolymers, and colloidal particles: Molecular and physicochemical basis of functional performance. *Advances in Colloid and Interface Science*, *234*, 3–26. https://doi.org/10.1016/j.cis.2016.03.002

Montante, G., Bakker, A., Paglianti, A., & Magelli, F. (2006). *Effect of the shaft eccentricity on the hydrodynamics of unbaffled stirred tanks*. *61*, 2807–2814. https://doi.org/10.1016/j.ces.2005.09.021

Musik, M., & Talaga, J. (2016). *Investigation of Fluid Dynamics in an Unbaffled Stirred Vessel with an Eccentrically Located Rushton Turbine*.

Niknafs, N. (2011). *Mechanistic Understanding of Emulsion Formation During Processing*. The University of Birmingham.

Özcan-Taskin, G., & Wei, H. (2011). The Effect of Impeller-to-Tank Diameter Ratio on Draw Down of Solids. *Chemical Engineering Science*, *58*(2003), 2011–2022. https://doi.org/10.1016/S0009-2509(03)00024-1

Pacek, A. W., Chamsart, S., Nienow, A. W., & Bakker, A. (1999). The Influence of Impeller Type on Mean Drop Size and Drop Size Distribution in an Agitated Vessel. *Chemical Engineering Science*, *54*, 4211–4222.

Pickering, S. U. (1907). CXCVI. - Emulsions. *Journal of Chemical Society*, *91*, 2001–2021.

Ramsden, W. (1903). Separation of Solids in the Surface-Layers of Solutions and "Suspensions" (Observations on Surface-Membranes, Bubbles, Emulsions, and

Mechanical Coagulation)-Preliminary Account. *Proceedings of the Royal Society of London*, *72*, 156–164. Retrieved from https://www.researchgate.net/publication/260210690

Rawle, A. (2003). Basic Principles of Particle Size Analysis. *Surface Coatings International Part A: Coatings Journal*, *86*(2), 58–65.

Rigg, R. T., & York, N. (1985). United States patent. *Geothermics*, *14*(4), 595–599. https://doi.org/10.1016/0375-6505(85)90011-2

Roscoe, R. (1952). The viscosity of suspensions of rigid spheres. *British Journal of Applied Physics*, *3*(8), 267–269. https://doi.org/10.1088/0508-3443/3/8/306

Rosen, M. J. (2004). *Surfactants and Interfacial Phenomena* (3 rd). John Wiley & Sons, Inc.

Rousseaux, J. M., Muhr, H., & Plasari, E. (2001). Mixing and Micromixing Times in the Forced Vortex Region of Unbaffled Mixing Devices. *Canadian Journal of Chemical Engineering*, *79*(5), 697–707. https://doi.org/10.1002/cjce.5450790501

Scargiali, F, Tamburini, A., Caputo, G., & Micale, G. (2017). Chemical Engineering Research and Design On the assessment of power consumption and critical impeller speed in vortexing unbaffled stirred tanks. *Chemical Engineering Research and Design*, *123*(Diid), 99–110. https://doi.org/10.1016/j.cherd.2017.04.035

Scargiali, F., Busciglio, A., Grisafi, F., & Brucato, A. (2012). Oxygen Transfer Performance of Unbaffled Stirred Vessels in View of Their Use as Biochemical Reactors for Animal Cell Growth. *Chemical Engineering Transactions*, *27*, 205–210. https://doi.org/10.3303/CET1227035

Scargiali, F., Busciglio, A., Grisafi, F., Tamburini, A., Micale, G., & Brucato, A. (2013). Power consumption in uncovered unbaffled stirred tanks: Influence of the viscosity and flow regime. *Industrial and Engineering Chemistry Research*,

52(42), 14998–15005. https://doi.org/10.1021/ie402466w

Schrade, A., Landfester, K., & Ziener, U. (2013). Pickering-type stabilized nanoparticles by heterophase polymerization. *Chemical Society Reviews*, *42*(16), 6823–6839. https://doi.org/10.1039/c3cs60100e

Soto, E., Zenit, R., & Ascanio, G. (2011). *Effect of Eccentricity on the Pumping Capacity in an Unbaffled Vessel*. *89*(October), 1051–1058. https://doi.org/10.1002/cjce.20604

Tadros, T. F. (2013). *Emulsion Formation and Stability*. https://doi.org/10.1002/9783527647941

Tang, J., Quinlan, P. J., & Tam, K. C. (2015). Stimuli-responsive Pickering emulsions: Recent advances and potential applications. *Soft Matter*, *11*(18), 3512–3529. https://doi.org/10.1039/c5sm00247h

Tsabet, E. (2014). *De La Particule Au Procede: Modelisation de la Production D'Emulsions De Pickering*. Ecole Polytechnique De Montreal.

Tsabet, È., & Fradette, L. (2015a). Effect of processing parameters on the production of Pickering emulsions. *Industrial and Engineering Chemistry Research*, *54*(7), 2227–2236. https://doi.org/10.1021/ie504338d

Tsabet, È., & Fradette, L. (2015b). Effect of the properties of oil, particles, and water on the production of Pickering emulsions. *Chemical Engineering Research and Design*, *97*(1), 9–17. https://doi.org/10.1016/j.cherd.2015.02.016

Tsabet, È., & Fradette, L. (2015c). Semiempirical Approach for Predicting the Mean Size of Solid-Stabilized Emulsions. *Industrial and Engineering Chemistry Research*, *54*(46), 11661–11677. https://doi.org/10.1021/acs.iecr.5b02910

Tsabet, È., & Fradette, L. (2016). Study of the properties of oil, particles, and water on particle adsorption dynamics at an oil/water interface using the colloidal probe technique. *Chemical Engineering Research and Design*, *109*, 307–316.

https://doi.org/10.1016/j.cherd.2016.02.001

Virden, A. (2017). *Introduction to particle sizing and laser diffraction*.

Walstra, P. (1993). Principles of Emulsion Formation. *Chemical Engineering Science*, *48*(2), 333–349. https://doi.org/10.1016/0009-2509(93)80021-H

Wu, J., & Ma, G. H. (2016). Recent Studies of Pickering Emulsions: Particles Make the Difference. *Small (Weinheim an Der Bergstrasse, Germany)*, *12*(34), 4633–4648. https://doi.org/10.1002/smll.201600877

Ye, Z., Jiang, X., & Wang, Z. (2012). Measurements of particle size distribution based on Mie scattering theory and Markov chain inversion algorithm. *Journal of Software*, *7*(10), 2309–2316. https://doi.org/10.4304/jsw.7.10.2309-2316

APPENDICES

A. Mixing Time Code

```
%%%
```

```
green1 = frame1(:,:,2);        % Green channel
blue1 = frame1(:,:,3);         % Blue channel

frameLast = imread(x2);        %Read last image
redLast = frameLast(:,:,1);    % Red channel
greenLast = frameLast(:,:,2); % Green channel
blueLast = frameLast(:,:,3);  % Blue channel

%%%Threshold Calculation%%%%%%%%
X = 0.5;         % For Bromocresol Purple
thresh_g = green1 + X*(greenLast-green1); %GREEN
thresh_b = blue1 + X*(blueLast-blue1);    %BLUE
thresh_r = red1 + X*(redLast-red1);       %RED
%%%%%%%%%%%%%%%%%%%%%%%%%%%%%%%%%%%%%%%%%%%%%%%%%%%%%%%%%%%%%%%%%%%%%%%%%%%%
%%%%%%%

mixedg = zeros(size(frame1)); %Pre- allocated for mixed green array
mixedr = zeros(size(frame1)); %Pre-allocated for mixed red array
mixedb = zeros(size(frame1)); %Pre-allocated for mixed blue array

Mg = zeros(length(theFiles),1); %Pre-allocated for mixed green
pixels array
Mr = zeros(length(theFiles),1); %Pre-allocated for mixed red pixels
array
Mb = zeros(length(theFiles),1); %Pre-allocated for mixed blue pixels
array
t  = zeros(length(theFiles),1); %Pre-allocated for time array

%%%%%%%%%%%%%%%%%%%%%%%%%%%%%%%%%%%%%%%%%%%%%%%%%%%%%%%%%%%%%%%%%%%%%%%%%%%%
%%%%%%%
% Loading and reading of images

for k = 1 : length(theFiles)
  baseFileName = theFiles(k).name;
  fullFileName = fullfile(myFolder, baseFileName);
  fprintf(1, 'Now reading %s\n', fullFileName);

  frame = imread(fullFileName);  % Read the files
  red = frame(:,:,1);            % Red channel
  green = frame(:,:,2);          % Green channel
  blue = frame(:,:,3);           % Blue channel

  figure(1)
  imshow(frame)          %%%Show the images
% imshow(green)         %%%Show the green component images
  drawnow; % Force display to update immediately.
%%%%%%%%%%%%%%%%%%%%%%%%%%%%%%%%%%%%%%%%%%%%%%%%%%%%%%%%%%%%%%%%%%%%%%%%%%%%
%%%%%%%

%%%%%%%%% Comparison with threshold pixels %%%%%%%

  [m,n] = size(green);
```

```
  N = m*n;                    % total number of frames
for i =1:m
    for j = 1:n
        if green(i,j) > thresh_g(i,j)      %% green component
           mixedg(i,j) = 1;
        else mixedg(i,j)=0;
        end
%%% Uncomment this section if you want to calculate for blue and red
components%%%
%         if red(i,j) > thresh_r(i,j)      %% red component
%            mixedr(i,j) = 1;
%         else mixedr(i,j)=0;
%         end
%         if blue(i,j) > thresh_b(i,j)     %% blue component
%            mixedb(i,j) = 1;
%         else mixedb(i,j)=0;
%         end
    end
end

N_mixedg =nnz(mixedg);
Mg(k) = N_mixedg/N;
% N_mixedr =nnz(mixedr);
% Mr(k) = N_mixedr/N;
% N_mixedb =nnz(mixedb);
% Mb(k) = N_mixedb/N;

t(k)= 0.04*k;     %%%convert to seconds because frames are each 0.04
sec
end

%%%%%%%%%%%%%%%%%%%%%%%%%%%%%%%%%%%%%%%%%%%%%%%%%%%%%%%%%%%%%%%%%%%%%%%%%%%%
%%%%%%
%%%%%%%% Post processing %%%%%%%%%%

figure(2)
plot(t,Mg,'g')           %%Plot green component mixing curve
hold on
% plot(Mb,'b')           %%Plot blue component mixing curve
% plot(Mr,'r')           %%Plot red component mixing curve

title('Mixedness vs Time')
xlabel('Time(s)') % x-axis label
ylabel('Mixedness') % y-axis label
%%%%%%%%%%%%%%%%%%%%%%%%%%%%%%%%%%%%%%%%%%%%%%%%%%%%%%%%%%%%%%%%%%%%%%%%%%%%
%%%%%%
```